AARHUS
UNIVERSITET
DCE - NATIONALT CENTER FOR MILJØ OG ENERGI

NIRAS

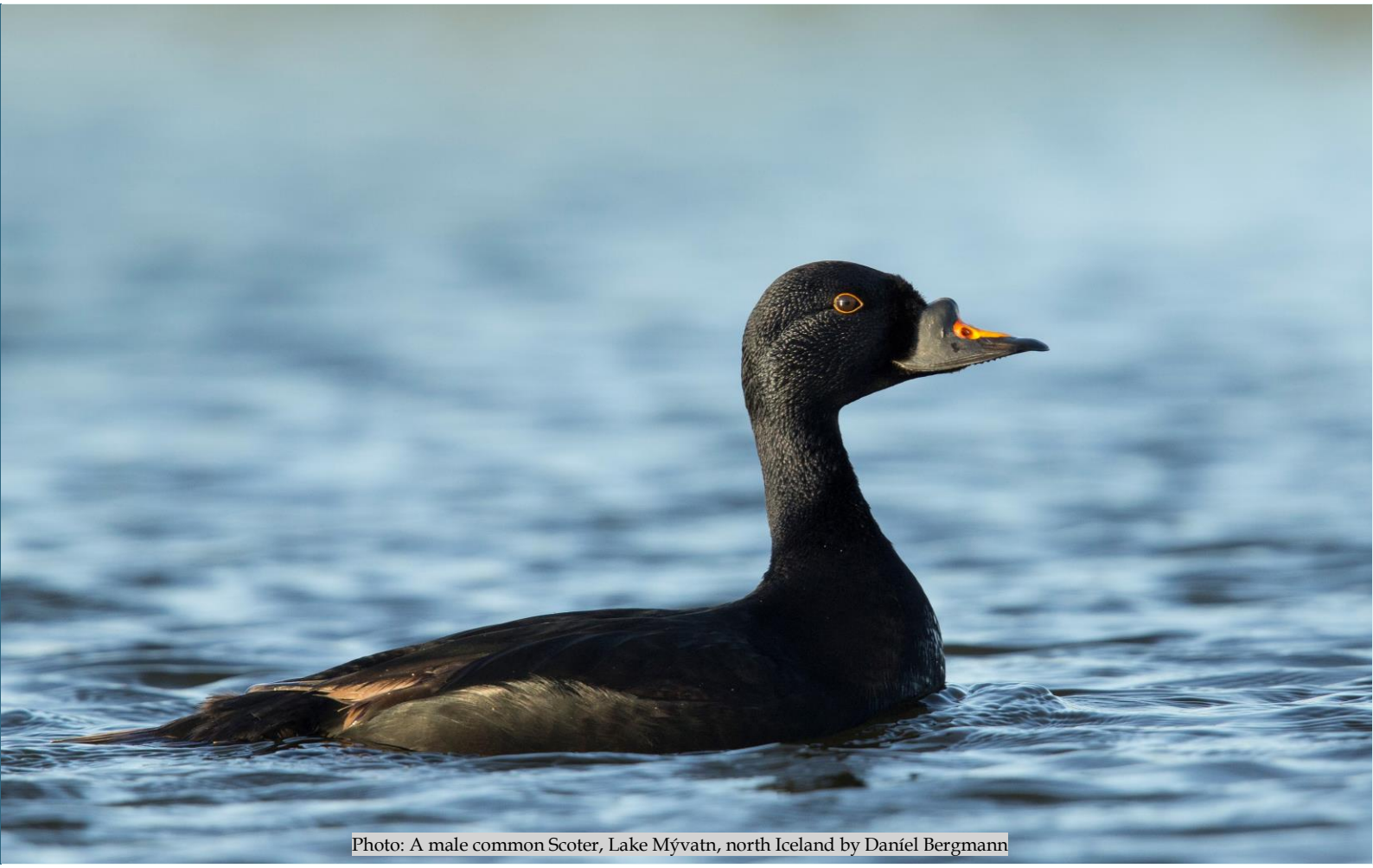

Photo: A male common Scoter, Lake Mývatn, north Iceland by Daníel Bergmann

Changes in the distribution and abundance of common scoter and diver species in the Horns Rev I, II and III offshore windfarm areas, Denmark, 2025

Bird distribution responses to wind farms, Horns Rev

Energinet Eltransmission A/S

Date: 28. Oktober 2025

Rev. no.	Date	Description	Done by	Verified by	Approved by
2.0	28th October 2025	Horns Rev. Analyses of the distribution of common scoter and divers, 2025	Lindesay Scott-Hayward (CREEM) Ib Krag Petersen (DCE) Monique MacKenzie (CREEM) Claus Lunde Pedersen (DCE) Saana Isojunno (CREEM) Rasmus Due Nielsen (DCE) Jacob Sterup (DCE) Heidi Maria Thomsen (DCE) Rune Sø Neergaard (NIRAS)	Tony Fox (DCE) Rune Sø Neergaard (NIRAS)	Søren Granskov (NIRAS) Camilla Uldal (DCE)

Contents

Preface

This report was commissioned by Energinet. It describes results obtained from the bird survey program in connection with the planned construction of the offshore wind farms (OWF's) in the North Sea 1 area, and specifically addresses the distributional behaviour of divers (red-throated diver/black-throated diver) and common scoter within and around the Horns Rev I, the Horns Rev II and Horns Rev III offshore wind farms.

The report builds upon data collected under this project in combination with bird survey data from other previous projects within that same area between 2000 and 2012. The present report is the continuation of a similar analyses conducted in 2024, but containing data from six more surveys, conducted between November 2024 and April 2025.

The report has eight main chapters. Chapter 1 is Introduction and objectives of the report. Chapter 2 details the methods used. Chapter 3 describes the results of the work. In Chapter 4 the results are discussed. Chapter 5 provides conclusions from the work. Chapter 6 contains suggestions for future studies, while Chapter 7 is a list of references. Chapter 8 contains three Appendices.

Front page illustration: An adult male common scoter at Lake Mývatn, north Iceland, photographed by Daníel Bergmann, Iceland.

Declaration

This report was prepared in close collaboration between CREEM, Univ. of St. Andrews, Aarhus University (DCE) and NIRAS. Aarhus University has been responsible for the data collection and data collation from survey data from 2000 to 2025 in the survey area. CREEM was responsible for statistical analyses of the data, encompassing Distance Sampling detection functions, spatial modelling of the survey data and for the comparison of changes in distribution between phases of the OWF development in the survey area. The text associated with the presentation of the modelling results is primarily written by CREEM, with input from AU. NIRAS was responsible for project coordination.

The report was peer-reviewed by Tony Fox, Aarhus University, and quality assured by Camilla Uldal at DCE, Aarhus University and Rune Sø Neergaard, NIRAS. Søren Granskov, NIRAS gave final approval for publication of the report by NIRAS.

Energinet commented on a first and second draft of the report before the final version was published, the comments and author replies can be found here:

https://dce.au.dk/udgivelser/oevrige-dce-udgivelser/eksterne-udgivelser/2025.

The report is published by the Danish Energy Agency as part of the tender for OWF's in the North Sea I area.

The report and associated investigations were financed by Energinet. Energinet wrote the initial section of the Introduction chapter.

List of key terms

A list of terms (in English and Danish) and their explanations in relation to the Horns Rev study.

English (abbreviation)	Danish	Explanation
HR I	Horns Rev I havvindmøllepark	The Horns Rev I OWF
HR II	Horns Rev II havvindmøllepark	The Horns Rev II OWF
HR III	Horns Rev III havvindmøllepark	The Horns Rev III OWF
Phase 0	Før opførelse af HR I, HR II og HR III	The pre-construction phase of both the HR I, the HR II and the HR III OWF's
Phase 1	Efter opførelse af HR I, men før opførelse af HR II og HR III	The post-construction phase of HR I and pre-construction phase of both the HR II and the HR III OWF's
Phase 1*	Efter opførelse af HR I, og før opførelse af HR II og HR III, begrænset til optællinger foretaget senere end 1. november 2005, der blev gennemført i sammenlignelige undersøgelsesområder.	The post-construction phase of HR I and pre-construction phase of both the HR II and the HR III OWF's with temporal restriction to post 1st November 2005, a time span with comparable survey areas.
Phase 2	Efter opførelse af HR I og HR II, men før opførelse af HR III	The post-construction phase of HR I and HR II, and pre-construction phase of the HR III OWF
Phase 3	Efter opførelse af HR I, HR II og HR III	Post-construction of all three OWF's

Summary

Between February 2000 and April 2025, 62 observer-based aerial surveys of birds were conducted at Horns Rev, an area of the North Sea off central Jutland, using a Distance Sampling line transect survey design. The survey area covered the offshore wind farm (OWF) areas of Horns Rev I (HR I), Horns Rev II (HR II) and Horns Rev III (HR III). The surveys were classified into four main phases according to the construction and operation of the three wind farms developed within the area. Phase 0 included 15 surveys prior to any wind farm construction, Phase 1 included 25 surveys post-construction HR I and pre-construction HR II and HR III, Phase 2 included 10 surveys post-construction HR I and HR II, but pre-construction HR III, while Phase 3 included 12 surveys post-construction of all three OWF's. Owing to changes in survey coverage and expansion in geographic ranges during Phase 1, which could bias the results, Phase 1* was created to represent the latter surveys from November 2005 to late spring 2007. The combined data set collected between 2000 and 2025 offers a unique opportunity to address the potential change in the displacement of birds over time, based on empirical data.

This report describes the changes in abundance and distribution of common scoter *Melanitta nigra* and divers (predominantly red-throated diver *Gavia stellata* but potentially including some black-throated divers *Gavia arctica*) over the period, based on the statistical analysis of visual aerial survey data in the Danish North Sea Horns Rev area gathered during the surveys described above. Species-specific Distance Sampling analyses were undertaken to correct for various aspects of avian detection probabilities, pooled across surveys. This was since followed by survey-specific spatial analyses with covariates including water depth (bathymetry), distance from the coast and/or a geographical covariate to model the distributions of common scoters and divers at a fine geographical scale for each survey.

The number of common scoters in the entire survey area increased markedly from Phase 0 to Phase 2 due to the distributional expansion west and northward from the coastal area and not necessarily an increase in overall abundance. The density of birds declined in Phase 3, which was dominated by the decline in the 2024/2025 winter surveys compared with previous survey years. Because of a general shift in the distribution of common scoter in the survey area over the first years of the survey period, it was difficult to assess the impact of the installation of the HR I. Common scoters showed significant displacement from the footprint of HR II within a distance of 3 km between Phase 1* and 2 and within a distance of 6 km between Phase 1* and 3. The displacement effect was also be analysed in direction-specific sectors around HR II. The longest displacement distances occur in the western sector in both phase differences (5 km and 8 km respectively). Within the HR II footprint (the area within the outer perimetry of the Horns Rev II offshore wind farm) common scoter densities decline by 50% between Phase 1* and 2 and a further 65% in Phase 3. Common scoter densities significantly increased in the HR III footprint between Phase 1* and 2, when HR III was not constructed. Between Phase 2 and 3, after the construction of HR III, significant declines of common scoters were observed. These declines were in keeping with a general density decline in much of the survey area and therefore not necessarily directly related to the construction of HR III.

While common scoters occurred in the Horns Rev survey area in high densities, diver densities were much lower. Diver densities in the HR I area were found to be fairly stable between Phases 0 - 2, but significantly decreased between Phase 2 and 3, a decline that was in line with declines across much of the study area. HR II showed strong evidence for divers being significantly displaced around its footprint within 5.5 km between Phase 1* and 2 (pre- and post-construction) and within 8.5 km between Phase 1* and 3. The largest displacement distances were observed in the northeast, Phase 1*-2, and the southeast, Phase 1*-3. Initially post construction, Diver densities declined by 75% within the footprint of the wind farm (100% grid cells significantly decreasing) and then by a further 24% between Phase 2 and 3 (30% cells significantly decreasing).

We evaluated the long-term distribution of common scoter and diver species, bird species classified as sensitive to human disturbances, in and around the HR I, II and III OWF's at Horns Rev. Due to low and variable numbers of divers and common scoters in the HR I area this wind farm did not allow for definite conclusions of the displacement effect of that wind farm. We found that divers and common scoters decreased in and around the HR II wind farm after its construction. Both divers and common scoter continued to be found in decreased densities in the HR II area between Phase 2 and 3. Within the HR III area, with larger and more widely spaced turbines, declines in the density of common scoter or divers was observed in the post-construction phase, though not as pronounced as in the HR II area and at least in part owing to survey area wide declines observed in the 2024/2025 surveys.

1 Introduction and project objectives

Human activities have been shown to have effects on bird distributions at sea, for instance, by showing displacement activity caused by ship traffic (Schwemmer et al. 2011; Fliessbach et al. 2019; Petersen et al. 2017). A method of assessing the vulnerability of different bird species to disturbance from approaching ships developed in Germany ranked divers (red-throated diver, *Gavia stellata,* and black-throated diver *G. arctica*) as being the most vulnerable of all species to such disturbance, with 95% of the observed birds reacting to approaching ships. Common scoter, *Melanitta nigra,* ranked number six on that list, with 83% of the observed birds responding to ships (Fliessbach et al. 2019). These two species have also shown avoidance behaviour in response to newly constructed OWF's. In the German North Sea, comparisons of 14 years of pre-construction data and ten post-construction surveys over two years showed marked displacements of divers, discernible by reduced densities within ca. 16 km from the wind farms (Mendel et al. 2019). Another study from the same German North Sea area using a combination of aerial digital surveys and satellite telemetry data from 33 satellite telemetry-tagged red-throated divers showed 90 % reductions in density within the footprint of the OWF's and within a distance of 5 km from the wind farm periphery, with significant displacement detectable within a distance of 10-15 km (Heinänen et al. 2020).

Both red-throated diver (a specially protected species listed on Annex I of the Birds Directive) and common scoter (for which Denmark has special responsibility for the moulting and wintering distribution of the population) are numerous and relatively highly concentrated in Danish waters, especially in the North Sea. For this reason, and particularly for predicting the effects of future developments in offshore wind power, it is important to know if these major displacement responses are common to all types of OWF's. Furthermore, it is important to establish if there is any evidence for modification of these responses over time, i.e. whether birds have shown signs of moderating their responses as they have got used to the initially unfamiliar and highly disturbing stimuli of turbines and associated maintenance traffic.

In the period from 2023 to 2025, aerial surveys to determine avian distribution and abundance at sea were conducted as part of the baseline pre-investigations for the North Sea 1 OWF site, located in the eastern part of the Danish North Sea and partly north of the Horns Rev survey area, commissioned by Energinet. The aerial survey and subsequent data analyses were conducted in collaboration between Aarhus University/DCE, the University of St. Andrews, Scotland and NIRAS A/S. The purpose of these surveys and the results of the analyses was to gather baseline information to support future environmental impact assessments related to upcoming wind farm projects.

As a supplementary part of this project, Energinet commissioned NIRAS, in collaroration with Aarhus University and University of St. Andrews, to conduct twelve aerial surveys of birds in the Horns Rev area between November 2023 and 2025, to determine potential changes in displacement shown by two specific key bird species, common scoter *Melanitta nigra* and red-throated diver *Gavia stellata* (by far the most numerous of the two diver species in the study area) in relation to constructed windfarms, supplementing a similar analysis undertaken in 2014. The main objective of this study was to assess the degree to which displacement responses to the wind turbines shown by the two bird species had changed over time; for instance, to see if initial avoidance response distances had been reduced (sometimes interpreted as potential habituation to the stimulus of the constructed wind turbines).

At Horns Rev, a shallow sand bar extending ca. 40 km west of Blåvandshuk in west Jutland, the HR I OWF first became operational in 2002. In the autumn of 2009, the HR II OWF was completed and became operational, followed by the HR III OWF in the same general area in 2019.

In relation to environmental assessments of these specific wind farm developments, a series of aerial surveys of birds have been conducted covering the general Horns Rev area. These included 19 aerial surveys between February 2000 and April 2003, followed by seven additional surveys between September 2003 and September 2004 to monitor post-construction effects in relation to the construction of the HR I OWF. Fourteen further surveys were conducted from March 2005 to April 2007 in the Horns Rev area to contribute to Environmental Assessments prior to the construction of the HR II OWF. Between March 2011 and April 2012, a further ten aerial surveys were conducted in the Horns Rev area as post-construction surveys in relation to the HR II OWF. As part of this present project, 12 aerial surveys were conducted between November 2023 and April 2025. A total of 62 aerial surveys over 25 years provide the background data for assessing potential changes in bird distributions in relation to the presence of the turbines undertaken here. All aerial surveys were conducted by Aarhus University/DCE under a series of different contracts using the same survey protocol (see Table 1-1).

A previous analysis of changes in distributions of common scoter and red-throated diver from pre- and post-construction bird survey data was performed for the HR II OWF (Petersen et al. 2014). The conclusion was that common scoters were displaced around the HR II wind farm. This present report aims to assess whether there have been changes in common scoter and red-throated diver distributions in relation to all three wind farms over time, including data from twelve additional surveys conducted between November 2023 and April 2025. The following sections describe the surveys, the Distance Sampling methods applied and the spatial analysis framework, which comprises model selection, diagnostics, inference and outputs. The results are presented for each species, while the appendices contain an executive summary of the methods.

1.1 Study area

The overall survey area covers an area of 2,818 km^2. It extends from the west Jutland coastline westwards to ca. 50 km west of Blåvandshuk and a maximum of ca. 50 km northwards from an east-west line drawn from the southern point of Fanø (Figure 1-1).

The area contains three OWF's of different turbine configurations. The HR I wind farm consists of 80 turbines, spaced regularly 560 meters apart. HR II comprises 91 turbines in arcs spaced 693 meters apart in the inner arc and 905 meters in the outer arc. HR III has 49 turbines arranged in a more irregular design, generally comprising 1,105 meters between columns and 1,751 meters between rows (Figure 1-1).

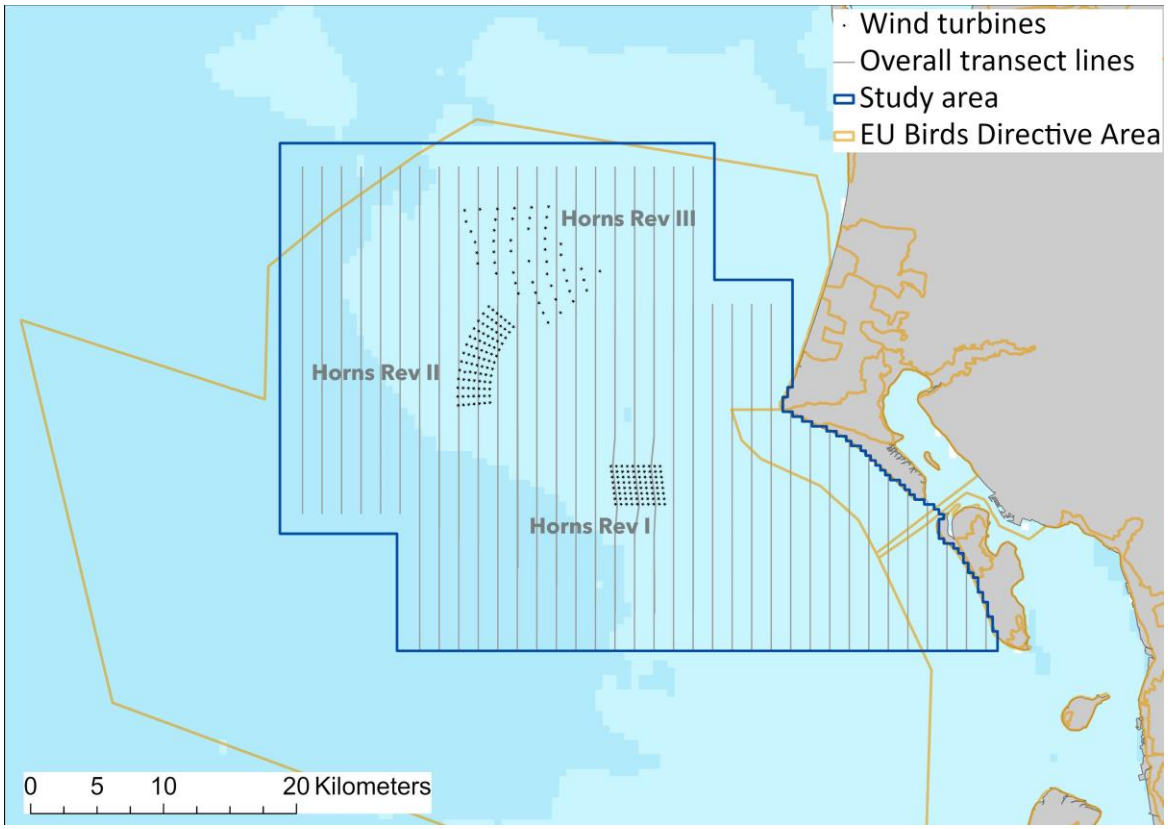

Figure 1-1. The Horns Rev OWF study area, showing the fullest extent of coverage over all surveys combined achieved for the species considered here (dark blue line). The general survey transect lines are shown (grey lines). The turbine positions of the three OWF's, Horns Rev I (southeast), Horns Rev II (southwest) and Horns Rev III (north), are indicated. The extent of the EU Birds Directive Special Protection Areas 57 and 113 within the study area is also shown (ochre lines).

The survey coverage changed over time between February 2000 and April 2025 in relation to differing survey needs and project objectives and so covered different sub-areas within the overall study area (Figure 1-2, Table 1-1). The survey coverage for each of the 62 aerial surveys can be found in Appendix 1 (Chapter 8.1 (Figure 8-1 to Figure 8-10 and Table 8-1)). One of the surveys was omitted from these analyses as neither of the target species were present in the area at that time of year.

Table 1-1. The number of aerial surveys performed, and the area covered (in square kilometers) for each of six survey campaigns in the Horns Rev area between 2000 and 2024. In total, 62 surveys were conducted, one of which was omitted from the analyses in this report as no birds of the two target species were observed.

Period	Number of surveys	Km²
February 2000 to August 2005	30	1,911
November 2005	1	2,697
February 2006 to May 2006	6	2,035
January 2007 to April 2007	4	1,873
March 2011 to April 2012	10	2,337
November 2023 to April 2025	12	2,122

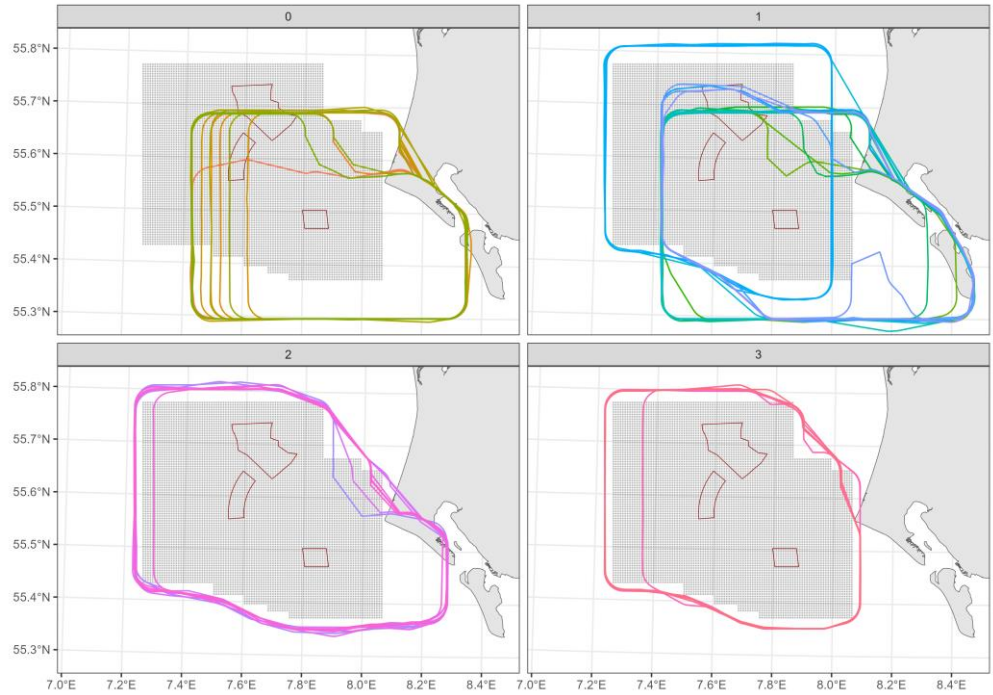

Figure 1-2. Maps showing the survey coverage (coloured polygons with multiple surveys in each phase) in relation to the spatial model prediction area (grey dotted areas). The wind farm footprints are outlined in red.

These surveys covered the time prior to any wind farm construction (Phase 0), post-construction of HR I (Phase 1), post-construction of HR II (Phase 2) and post-construction of HR III (Phase 3; Table 1-2). Phase 1* is a shortened Phase 1 to include only the latter 10 surveys when the survey coverage was broader.

Table 1-2. Table detailing the construction phases, time frame and survey effort. The number of surveys from which data was used for the present analysis is given (Number of surveys).

Phase	Phase number	Date range	Number of surveys
Pre-construction	0	Feb 2000 - Apr 2002	15
Post HR I	1	Aug 2002 - Apr 2007	25
Post HR I - shortened	1*	Nov 2005 - Apr 2007	10
Post HR I & II	2	Mar 2011 - Apr 2012	10
Post HR I, II & III	3	Nov 2023 - Mar 2025	12

The bathymetry of the study area extends from 0 to 35 meters depth. Horns Rev is a shallow sand bar extending into the sea from Blåvandshuk, to just west of the HR II OWF. Due to current and wave action, the sandy seabed is subject to turbulent movement and substrate instability.

Most of the study area falls within the "southern Danish North Sea" EU Bird Directive area (SPA113), which was enlarged from its original geographical extent by a revision in 2023. With the enlargement the list of bird species designated for the area was extended to include common scoter. The originally designated species, red-throated diver, black-throated diver and little gull remain on the list of designated species. The southeastern part of the study area also falls within the "Vadehavet" Bird Directive area (SPA57).

This report describes the distribution and abundance of birds in the four phases shown in Figure 1-2 and assess the results for significant changes in and around the three wind farm footprints. Phase 1 was divided into an early and a late phase, using the late part of that as Phase 1*. The objectives of the analyses in this report is to assess whether or not, and if so to what degree, a species might be showing distributional changes that suggest a return to areas within and around an OWF after a redistribution or decline post-construction. Therefore, to meet this objective, various outputs were produced, and a range of comparisons were made, including those that tested changes in density with distance from a wind farm footprint.

2 Methods

Visual aerial surveys were used to collect seabird data using line transect Distance Sampling methods (Buckland et al. 2001). During these surveys, trained observers searched for and recorded birds in distance bands in addition to environmental conditions at the time (e.g. sea state or sun glare).

2.1 Data collection

Data on bird abundance and distribution were collected using standard methods; human observers visually gathered data during aerial surveys, flying transects between designated GPS waypoints at a regular speed of 100 knots and an altitude of 76 meters (Figure 1-1). Twin-engine Partenavia P-68, Cessna 337 or Tecnam P2006T high-wing aircraft were used for the surveys. Observations were recorded within distance bands parallel to the aircraft to allow for the modelling of differential detectability at increasing distances from the observers (Petersen & Sterup 2019, NOVANA Technical Specification TA A188), following standard Distance Sampling line transect survey methods (Buckland et al. 2001, 2015).

Two trained observers recorded birds from either side of the aircraft. The bird species or species group was noted for each record, along with information on flock size, behaviour (sitting on the sea surface, flushing, flying or diving), perpendicular distance from the survey track and time. In addition, the environmental conditions at the time (e.g. sea state or sun intensity) were registered. The perpendicular distance was classified in predefined distance bands with increasing distance from the survey track line within 1.5 km on either side of the aircraft (Figure 2-1).

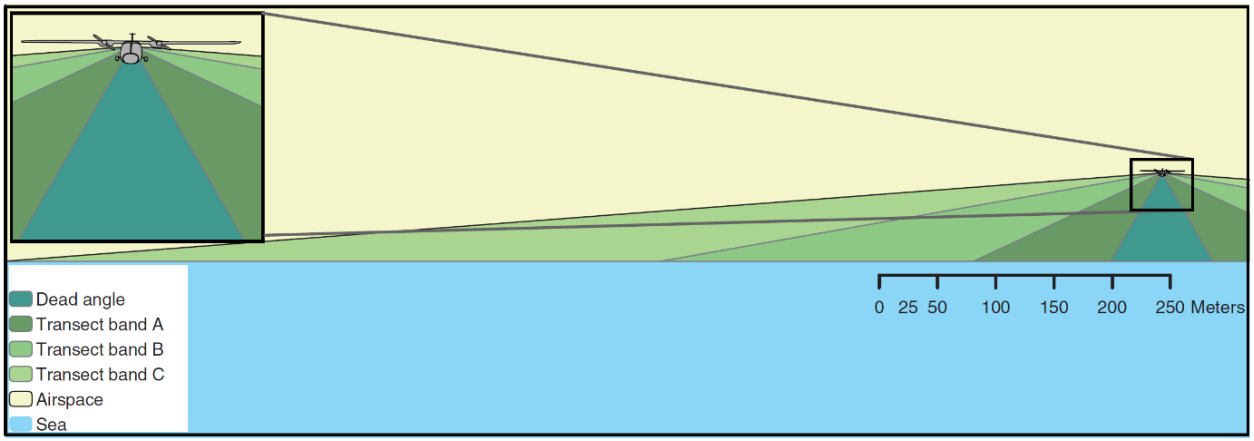

Figure 2-1. The transect band definitions for aerial line transect surveys. From the survey altitude of 76 m, there is a dead area extending to 44 m on each side of the survey track under the aircraft that the observers could not cover.

The survey transect lines were designed as parallel north-south oriented lines, covering the survey area. The transect lines were separated by 2 km for most transects, although in parts of the area, the distance between transects was 4 km.

Aerial surveys were conducted under good weather conditions, with a visibility of more than 3 km and wind speeds preferably less than 6 m/s. Higher wind speeds lead to more waves (measured as "sea state" during the surveys). Data collected under sea states 4 or higher was omitted from the data analysis.

At Horns Rev, a total of 62 aerial surveys of birds were conducted between 2000 and 2025. The precise survey coverage area differed slightly between the different projects and contracts. The coverage per survey is

presented in Appendix 8.1, showing the precise survey track lines covered during each survey and the numbers of both species encountered.

2.2 Survey data

The data used for this analysis consists of 62 surveys from February 2000 to April 2025. The transect lines for each survey were split into segments of approximately 500 m long up to 1000 m wide. Detected birds on both sides of the aircraft were assigned to four distance bins perpendicular to the flight direction (A-D) with categories 0 m-119 m (A), 119 m-388 m (B) and 388 m-956 m (C) as shown in Figure 2.1 plus an additional band 956 m-1456 m (D). Clinometers were used to aid designate observations to the appropriate distance bin. A band width of 44 m under both sides of the plane along the flight line was not visible to observers and, therefore, birds were not recorded from here and this area did not contribute to the dataset. Band D was removed from analysis for all species owing to very few or no observations.

All latitude/longitude locations were converted to UTMs using UTM Zone 32N. The transects for the surveys are shown in Figure 2-2. The number of segments per survey is presented under the column "Number of Segments" in the Table.

Table 2-1. Table detailing the survey effort (total area and number of segments) for each of the surveys and the number of segments in each of the wind farm footprints.

Survey Date	Phase	Area Covered (km^2)	Number of Segments	HRI Segments	HRII Segments	HRIII Segments
2000-02-17	0	1581	1688	24	30	6
2000-02-21	0	1098	1184	24	0	0
2000-03-19	0	1525	1680	24	32	6
2000-04-27	0	1377	1514	24	32	6
2000-08-21	0	1388	1539	24	34	6
2000-10-06	0	1307	1472	24	22	6
2000-12-22	0	1171	1251	24	0	6
2001-02-09	0	1443	1540	24	32	6
2001-03-20	0	1564	1687	24	33	6
2001-04-21	0	1319	1691	24	32	6
2001-08-22	0	1566	1677	24	32	6
2001-09-26	0	1456	1550	24	28	6
2002-01-07	0	1274	1401	24	7	6
2002-03-12	0	1393	1478	16	32	4
2002-04-09	0	1296	1402	24	33	6
2002-08-08	1	1310	1404	24	30	5
2003-02-13	1	1218	1433	24	15	6
2003-03-16	1	1622	1741	24	32	12
2003-04-23	1	1606	1758	24	31	12
2003-09-05	1	1440	1722	24	32	6
2003-12-04	1	1295	1440	24	16	3
2003-12-30	1	1162	1290	24	14	6
2004-02-29	1	1562	1784	24	33	6
2004-03-26	1	1607	1782	24	31	6
2004-05-10	1	1599	1779	24	32	6

Survey Date	Phase	Area Covered (km^2)	Number of Segments	HRI Segments	HRII Segments	HRIII Segments
2004-09-09	1	1503	1632	24	14	6
2005-03-08	1	1676	1788	24	23	6
2005-04-02	1	1177	1775	24	31	5
2005-05-14	1	1666	1781	24	35	6
2005-08-17	1	1660	1776	24	33	6
2005-11-18	1	2198	2454	24	30	84
2006-02-02	1	1621	1712	24	33	88
2006-02-25	1	1622	1713	24	29	87
2006-03-12	1	1433	1714	24	34	87
2006-04-15	1	1616	1708	24	32	88
2006-05-11	1	1484	1720	24	25	88
2007-01-25	1	1378	1470	24	30	31
2007-02-15	1	1190	1385	24	32	28
2007-03-03	1	1308	1399	24	32	35
2007-04-01	1	1464	1639	24	34	21
2011-03-01	2	1133	1216	24	37	81
2011-03-26	2	1200	1311	24	36	80
2011-04-11	2	1172	1305	24	46	79
2011-10-13	2	952	1297	24	35	81
2011-11-17	2	1184	1256	24	36	80
2012-01-15	2	1260	1336	24	36	81
2012-02-08	2	813	1294	24	36	80
2012-03-02	2	1155	1227	24	37	82
2012-03-22	2	1166	1271	24	37	81
2012-04-11	2	1171	1282	24	35	81
2023-11-17	3	1117	1213	24	36	81
2023-12-27	3	1017	1079	24	36	81
2024-01-09	3	1127	1194	24	36	81
2024-02-27	3	1127	1192	24	36	81
2024-04-08	3	1133	1201	24	36	81
2024-04-22	3	1099	1198	24	38	81
2024-11-05	3	1021	1157	24	34	82
2024-12-10	3	1125	1182	24	35	82
2025-02-15	3	1114	1207	24	36	81
2025-02-28	3	1150	1210	24	36	81

Survey Date	Phase	Area Covered (km^2)	Number of Segments	HRI Segments	HRII Segments	HRIII Segments
2025-03-20	3	1123	1181	24	40	81
2025-04-03	3	1125	1183	24	34	82

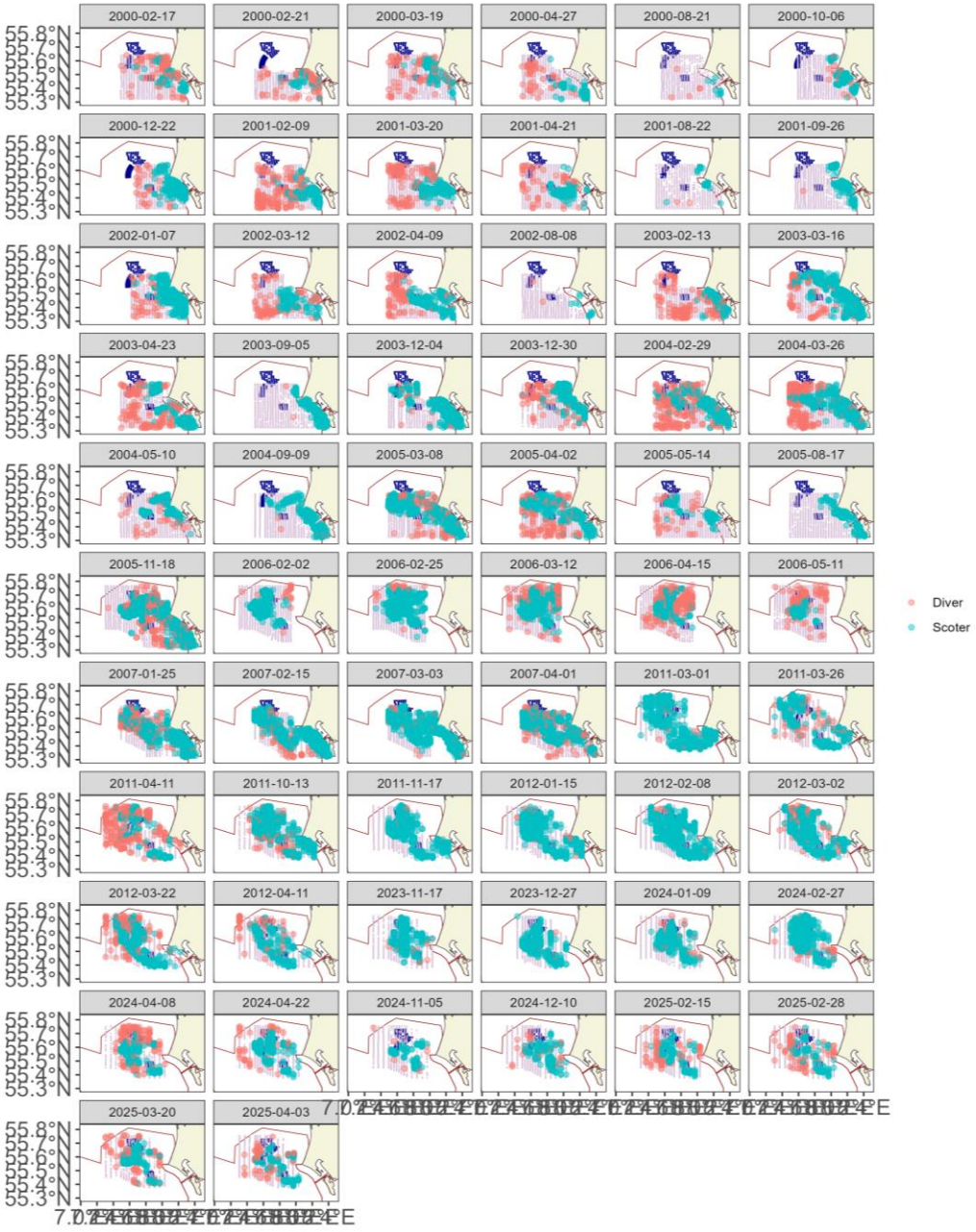

Figure 2-2. All survey data mapped by survey. The coloured circles represent non-zero segment counts for the two species groups. The pale purple represent segments with zero bird detections.

2.3 Distance Sampling Analysis

All survey data were collected using visual aerial methods and so correction for declining detectability with increasing distance from the plane was accounted for using Distance Sampling methodology (Multiple Co-variate Distance Sampling, MCDS) (Marques and Buckland 2004; Marques et al. 2007; Buckland et al. 2001). Analyses were conducted for each of the common scoter and divers datasets by pooling the information across all surveys. The Distance Sampling analysis models the decreased probability of detecting a bird or group of birds with increased distance away from the track line of the survey aircraft.

To allow for the detectability of birds varying due to external factors (not just distance from observer) other covariates were included in the distance model. The candidate variables trialled were bird group size, behaviour, observer and sea state (Table 2-2). For some observers there were too few observations so in those cases, the observers' observations were combined with the next smallest. Observations with sea states greater than four were removed. For scoters, which were occasionally seen in very large numbers (up to 20,000), any segments with birds were assumed to have perfect detection and omitted from the detection analysis. The observed values for these segments were used in the spatial analysis. Both half-normal and hazard rate detection functions were trialled (allowing different steepness/shape of the decline in detectability with distance) and the best of all competing models chosen using BIC. The effects of glare, and any mitigations as a result, was approached using a dedicated analysis. Further details on this and the distance analysis can be found in Appendix 8.2.

Table 2-2. Table detailing the covariates used in the detection function fitting.

Covariates	Values
Behaviour	S (sitting or diving) and F (flying or flushing)
Observer	17 Observers
Sea State	0, 0.5, 1, 1.5, 2, 2.5, 3, 3.5 (calm to rough)

2.4 Spatial Analysis

The following sections describe the modelling methods employed for this analysis and a description of the outputs which follow. Appendix 8.2 provides full details of the methods.

The outputs from the detection function analysis give a detectability corrected count (abundance) in a small area (estimated for areas along segment of approximately 500 m). Spatial models are then used to turn the distance corrected counts along transect lines into spatial distribution maps, whilst accounting for data characteristics and modelling assumptions. The spatial modelling process was undertaken using a spatially adaptive Generalised Additive Model framework (GAM) with an error family suitable for count per unit area response data, the Tweedie distribution (Miller, 2013). The effort associated with each observation varied depending on the associated segment length and width, and so segment area was included as a log-scale offset term in the model.

Additionally, survey coverage was not constant throughout, and particularly in the early years did not fully cover the prediction area used for this present analysis (the grey dotted area defined in Figure 1-2). Because this lack of data potentially causes extrapolation artefacts, the model framework was extended to use the principle of quadrature points (Berman and Turner 1992). These points were generated on a 1 x 1 km grid in the combined prediction-survey area for each survey to provide a data reference for the model in areas that have not been surveyed. The quadrature points/pseudo-absences were used only in the area within the predicted area of interest but outside the coverage area of a given survey. This approach meant that the model framework used was weighted Tweedie GAM.

As each survey was analysed separately, only spatially-referenced explanatory variables were considered (and not "time"). Specifically, the candidate variables for inclusion in the spatial model were a set of one-dimensional terms, water depth and distance to coast, which were permitted to change linearly or non-linearly with the response. A two-dimensional term using geographic coordinates to account for surface patterns was also considered for inclusion, to include unmodelled environmental variability (Scott-Hayward, Oedekoven, et al. 2014). The flexibility of these smooth functions (1D or 2D) was determined using the BIC criterion, whilst the

more computationally intensive 5-fold cross-validation was used to choose between competing models (with different numbers of variables).

The response data were collected along survey lines in sequence, and so consecutive observations were likely to be correlated in space and time. While a spatial term was also considered for inclusion, any resulting temporal auto-correlation in model residuals was also accounted for by using robust standard errors as part of the modelling process. These essentially inflate the standard errors in relation to the positive correlation observed within pre-specified blocks (here, transects) of residuals.

Uncertainty in the outputs, reflected in both the detection model and spatial model was captured using 'bootstrapping'. This process involves repeatedly sampling from the parameter distributions of each model and obtaining a new set of predicted abundances across the spatial grid. From this process, 500 sets of plausible predictions for every grid cell were generated, which may be used in a variety of ways to estimate uncertainty and answer questions such as "does the spatial distribution vary between two surveys or phases".

All models were fitted using the MRSea R package (Scott-Hayward et al., 2023; R Core Team, 2024) and subjected to various diagnostic checks (e.g. assessment of the assumed mean-variance relationship, a key assumption check).

Further methodological details on model specification, fitting, and diagnostics are available in Appendix 8.2.

2.4.1 Model Framework

The response variable for the spatial models under analysis here, are bird counts in a small area (segment) which have been corrected for detectability. This response was modelled using a Tweedie framework, which includes an estimated dispersion parameter (ϕ) and Poisson-Gamma mixing parameter (ξ) to return an appropriate mean-variance relationship in each case. The mixing parameter takes on values from 1 (equivalent to quasi-Poisson) and 2 (equivalent to Gamma). If the estimated parameter was close to 1, the models were considered quasi-Poisson. A set of candidate explanatory variables were associated with each segment to model the signal, and in this study each of the 62 surveys was analysed separately, including covariate selection, for each species. The candidate environmental covariate was water depth (bathymetry) while distance from coast (as a one-dimensional term) was also considered in each model, in the unlikely case there was compelling evidence for consistent spatial patterns with distance from coast which were the same in all directions. Additionally, to account for more realistic (and localised) surface patterns (due to perhaps unmeasured covariates) a spatial surface was also fitted to each model. Specifically, a two-dimensional CReSS-based surface using a Gaussian radial basis function was included in the model (Scott-Hayward, Oedekoven, et al. 2014).

As an illustration, the following equation represents an example of a Tweedie model with log link function and fitted with a one-dimensional smooth term (e.g., bathymetry) alongside a two-dimensional spatial smooth:

$$y_{ij} \sim Tw(\mu_{ij}, \phi, \xi)$$

$$\mu_{ij} = e^{\left(\beta_0 + s_1\left(\text{Bathymetry}_{ij}\right) + s_2\left(\text{XPos}_{ij}, \text{YPos}_{ij}\right)\right)}$$

where y_{ij} is the estimated count for transect i segment j and s_1 represents either a quadratic B-spline or natural cubic spline smooth of depth. Here, s_2 is a two dimensional smooth of space (with coordinates XPos and YPos in UTMs). Implicit in this model are also coefficients for the intercept (β_0) and any spline-based coefficients associated with the smooth terms. The effort associated with each observation varied depending on the associated segment area and so segment area was included as an offset term (on the log scale).

A globally applicable depth or distance to coast term and a more flexible spatial term were trialled for inclusion in each model, to indicate how best to model spatial patterns in each case. In particular, this quantifies if any spatial patterns are sufficiently described by the one-dimensional covariates (which applies the same across the surface) or if a more considered approach to spatial patterns was required for each survey and for each species. For example, if depth was selected and a two-dimensional spatial element was not deemed necessary (as determined by the model selection procedure governed by objective fit criteria) then this signals that any

spatial patterns are primarily a function of the depth, regardless of the geographical location of this depth in the survey area.

If the two-dimensional spatial term was selected for inclusion in a model, then the spatial density patterns (over and above any environment-related terms) were accommodated using a spatially adaptive term which permits different amounts of flexibility across the surface in a targeted and yet parsimonious way (hence, relatively complex spatial patterns can be accommodated with very few parameters).

Selection between competing models was undertaken using an information criterion metric, BIC, which has a penalty related to the extent of the data supporting the model.

2.5 Model specifics

More specifically, the MRSea package CReSS-SALSA based spatially adaptive generalized additive models, with targeted flexibility, were fitted to data from each survey to allow for non-linear relationships between the one-dimensional and two-dimensional covariates and the response (Scott-Hayward, Mackenzie, et al. 2014, 2014; Scott-Hayward et al. 2023; Walker et al. 2010).

CReSS is a complex-region spatial smoother, whilst SALSA is a Spatially Adaptive Local Smoothing Algorithm both developed to examine animal survey data for signs of changes in animal abundance and distribution following marine renewables development. However, the methods are suitable for a wide range of applications.

The degrees of freedom for these terms determine the flexibility of these smooth (and nonlinear) relationships the more degrees of freedom, the more flexible the relationship can be.

The spatial patterns in each analysis were based on a two-dimensional Gaussian radial basis function (df = [2,100]). The flexibility of both the spatial and 1D elements constituted part of the model selection procedure and, for each survey, was determined using SALSA and the BIC measure of fit.

Uncertainty about model parameter estimates proceeded via robust standard errors due to the nature of the survey procedure. These essentially work by inflating the standard errors (normally obtained under traditional approaches) in relation to the positive correlation observed within pre-specified blocks of residuals. In cases where this residual correlation is minimal, the adjustments are small, and when the correlation is more extreme, the inflation is larger.

A transect-based blocking structure was used to reflect potential correlation within blocks while independence (i.e., no correlation) between blocks was assumed. To ensure this assumption was realistic, the decay of any residual correlation to zero (i.e., independence) with the distance between points (within blocks along transects) was assessed visually. Specifically, transects in each survey were used as the blocking structure. An Auto Correlation Function (ACF) plot was used to check the suitability of this blocking structure via a 'decay to zero' trend within blocks.

2.5.1 Modelling diagnostics

All modelling approaches are based on assumptions, and the violation of these can lead to spurious results to a greater or lesser extent. To assess the adequacy of model fit and assumptions a range of diagnostic measures were used.

- ACF plot: A blocking structure was used to account for potential residual non-independence for each model and a robust standard error approach was based on unique transects. Figure 2-3 shows an

example ACF plot with the temporal correlation within each transect shown in grey and the average in red. The plot shows a mean lag one correlation of approximately 0.25 followed by a reassuring decay to zero. This indicates that the robust standard errors were necessary for this model (no residual correlation is indicated by a lag 1 correlation of near zero) and that the blocking structure is appropriate.

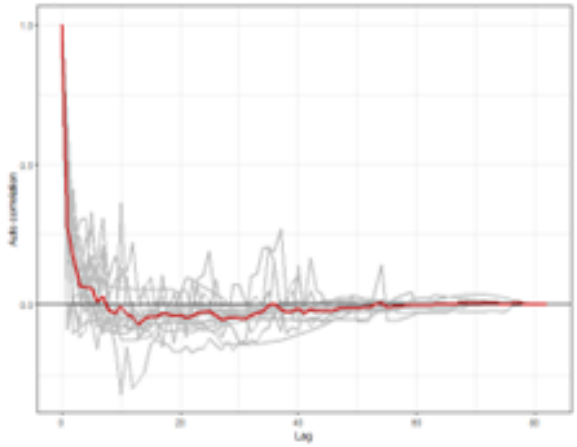

Figure 2-3. Example ACF plot: the grey lines represent the residual correlation observed in each transect and the red line the average of these values across transect.

- Mean-Variance plot: The assumed mean-variance relationship under the model was assessed visually using plots of the model's fitted values against the residuals' variance. In this analysis, Tweedie models were employed, which assume a nonlinear mean-variance relationship. Figure 2-4 shows an example plot. The observed residual variance is calculated in bins relating to quantiles of the fitted values (hence the irregular spacing). These are plotted as the black points and agreement between these, and the assumed relationship (Tweedie, dotted blue line) indicates the mean-variance assumption is appropriate. As the Quasi-Poisson and Poisson families are special cases of the Tweedie, these are included on the plot for comparison.

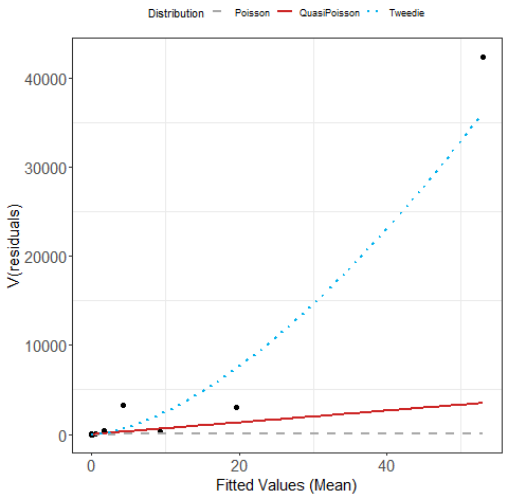

Figure 2-4. Plot showing the estimated Tweedie mean-variance relationship (blue dashed line). The red line shows the $V(\mu) = \Phi\mu$ relationship and the grey line the 1:1 relationship. The black points are the observed residual variances.

- DHARMa diagnostic plots: QQ plots and residuals against predicted values plots were assessed to ascertain the level of agreement between the data and the model (*Figure* **2-5**). These plots were created using the ***DHARMa R*** package and using simulated residuals. Given these outputs, we would expect that a correctly specified model shows:

  a) a straight 1-1 line, and no compelling evidence against the null hypothesis of a correct overall residual distribution, as indicated by the *p*-values for the associated tests in the QQ-plot.

b) visual homogeneity of residuals in both the vertical and horizontal directions, in the residuals against predictor plot.

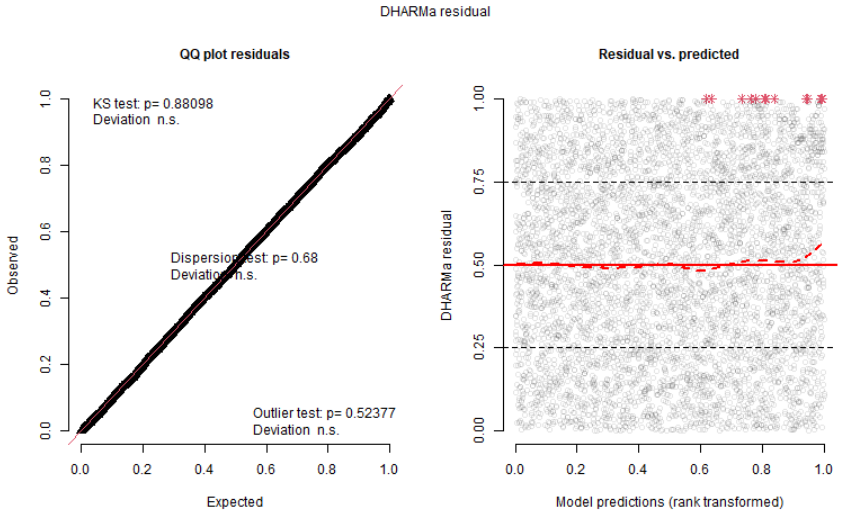

Figure 2-5. Example DHARMa plots: QQplot (left) and residuals against predicted values (right). The red asterisks are outliers, and the red line is a smooth spline around the mean of the residuals.

- Pearson residuals for each model were also spatially visualised to ensure no areas of consistent bias across the survey area. This would be indicated by clusters of negative or positive residuals in spatially similar locations.

Diagnostic outputs are not shown in the results chapter, but a full set (all 62 models for both species) is available on request.

2.5.2 Model Predictions and estimates of uncertainty

Based on each selected model, predictions of counts were made to a grid of points (each point representing a 1 km^2 grid cell) across the study area. Additionally, abundances within the survey-based prediction area were obtained by summing the grid cell counts across the relevant areas. A key output of any statistical modelling process is the incorporation of uncertainty from all steps and the presentation of this uncertainty alongside estimates (e.g. an abundance estimate with 95% confidence interval).

The uncertainty in the detection function was reflected using a parametric bootstrap ($n = 500$) of the fitted Distance Sampling model to obtain new estimated counts for each segment. The selected spatial model was then re-fitted to each of the new datasets to obtain a new set of parameter estimates for the model. The final output of this process was a parametric bootstrap procedure using the robust variance-covariance matrix from each parametric bootstrap model. These were used to calculate 500 sets of plausible model predictions, for every grid cell in the study area. To obtain 95% percentile-based confidence intervals and a coefficient of variation for each grid cell, the 2.5% and 97.5% quantiles of the 500 bootstrap predictions were taken along with the standard deviation. Using the bootstrap predictions, we can create a number of other outputs to assist in assessing consistency of distributional patterns (persistence) and distributional changes over time.

A calculation of 'persistence' was also undertaken across surveys within phases and across all surveys considered together, within species, using the geo-referenced estimates of density (abundance/associated area) across the survey area. Distributional persistence allows the reader to get a measure of intra/inter-annual

variability across multiple surveys. For example, there may be areas of consistent usage, despite survey-to-survey variability, which can provide context to the ability to detect post-construction changes. A persistence score of 1 indicates that the density in that grid cell was estimated to be above average in every bootstrap replicate in every survey (so uniformly above the mean; high persistence), while a value of 0.1 indicates that just 10% of the estimates were above the estimated mean, and thus indicates low persistence in that location.

Persistence scores were calculated for every grid cell in the following way: Each bootstrap replicate was allocated a binary value based on whether or not the estimate in each location was above the mean estimated density (1) throughout the survey area or below this mean estimated density (0). This was performed for all sets of plausible predictions in each grid cell (based on the bootstrap replicates), and the proportion of these bootstrap predictions over the mean (indicated by the value of 1) was calculated for each grid cell to give a persistence score for that location. A zero would result from the density in every survey and every bootstrap being below average.

Distributional changes over time were evaluated by comparing the estimated distributions from the four phases. Any changes during this time in and around the three wind farm footprints could also be observed. Difference plots were used to visualise any spatially explicit changes in the distribution of birds. The bootstraps from the modelling process described above were used to generate a 95% interval for the difference in abundance in each grid cell. If the interval contained zero, it was deemed not to indicate a statistically significant difference in abundance between the two comparison years, which is a conservative approach to determining change. If the range of plausible values for the difference (indicated by the 95% confidence interval) did not include zero, then the change was deemed significantly positive or negative. These bootstrap-based cell-wise differences between phases were also viewed in concentric rings that were within distance of the HR II footprint.

3 Results

3.1 Common Scoter – Observations

First, data from the last two arial survey campaigns (November 2023 to April 2024 respectively November 2024 to April 2025) are presented here. Common scoters were observed within the study area during all surveys conducted in the seasons 2023/2024 (Figure 3-1) and 2024/2025 (Figure 3-2). The majority of the birds were observed at Horns Rev on water depths less than 20 meters. Although the general distribution of common scoters within the survey area was similar between the two seasons, the total number of observed individuals was very different. During the six surveys conducted in 2023/2024 a total of 151,400 birds were observed (Table 8-2), while the corresponding number for the six surveys conducted in the 2024/2025 season was 18,052 birds (Table 8-3), an over eightfold reduction in observed numbers. During the 2023/2024 season common scoters were observed in high numbers in the Horns Rev III offshore wind farm area, while much fewer birds were observed there in the 2024/2025 season. For comparison, aerial survey coverage and common scoter distributions from the earlier surveys are provided in Appendix 8.1 (Figures 8.1-8.10 and Table 8-1).

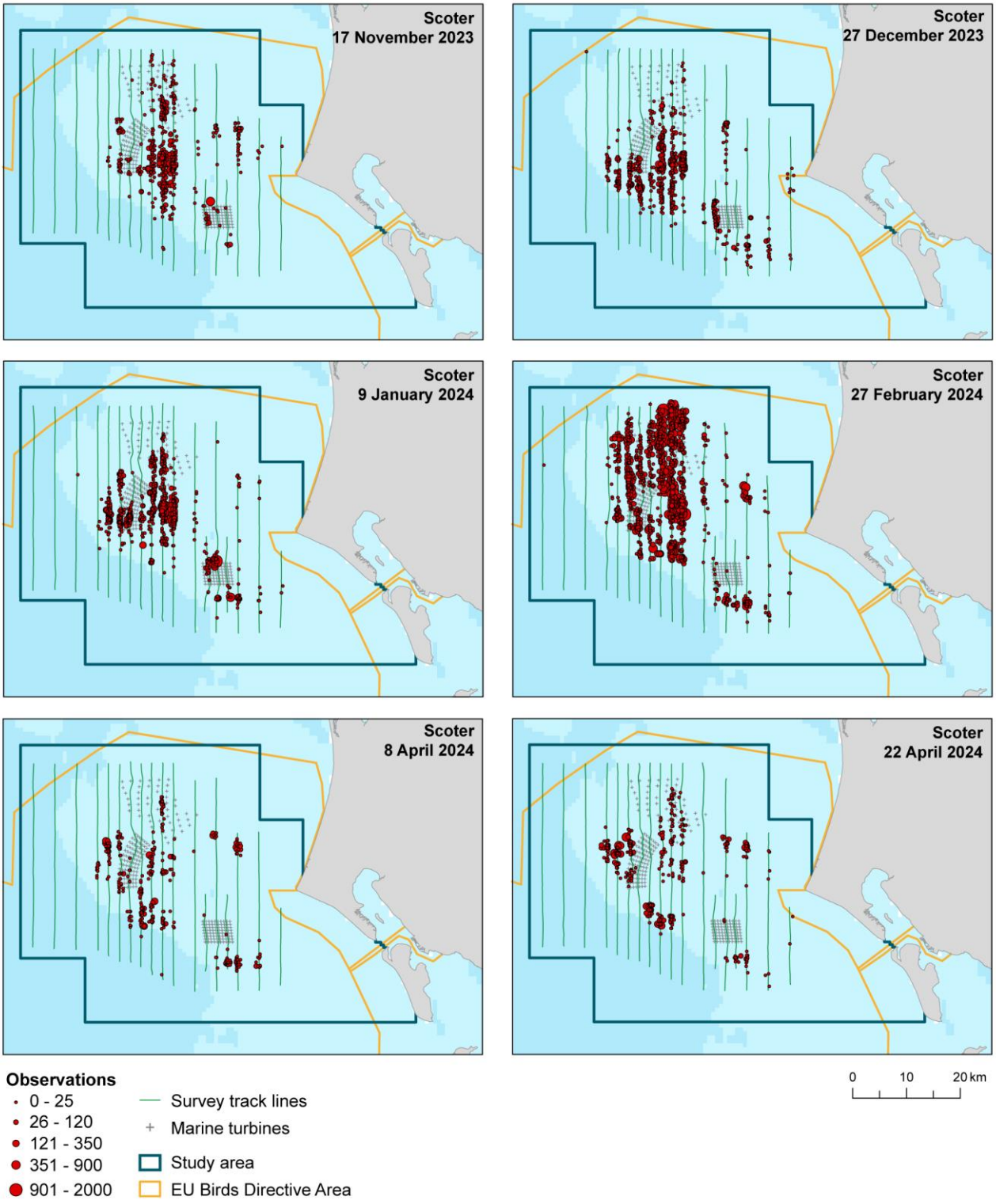

Figure 3-1. The number of common scoters observed and their distribution within the survey area for six aerial surveys conducted in the winter season of 2023/2024.

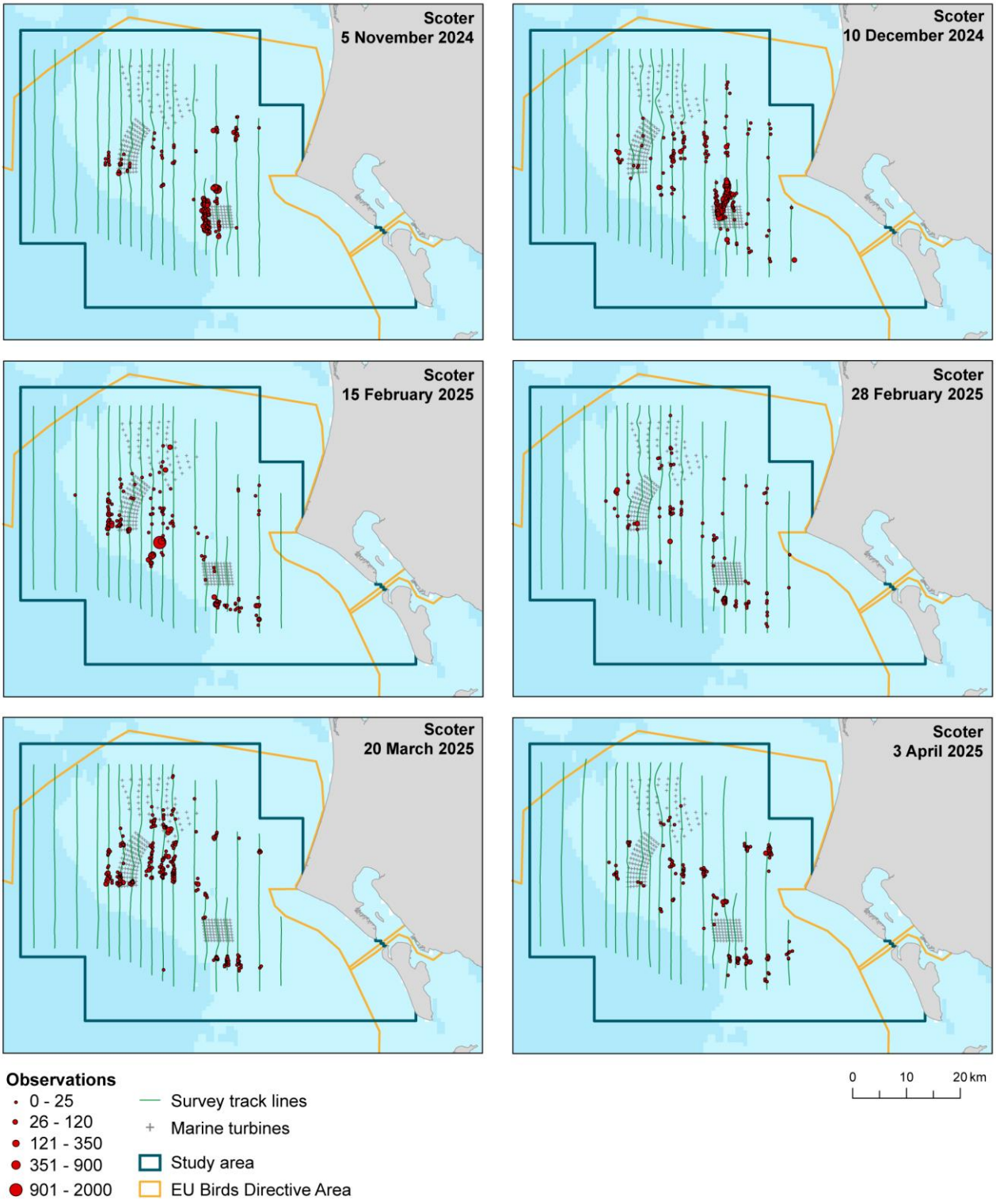

Figure 3-2. The number of common scoters observed and their distribution within the survey area for six aerial surveys conducted in the winter season of 2024/2025.

3.2 Common scoter - Distance Analysis

The average probability of sighting common scoter was estimated to be 0.29 (CoV=0.01). This probability was estimated using a hazard rate detection function and group size as a covariate for the combined data set (Figure 3-3). As might be expected, the larger the group size, the higher the probability of detection.

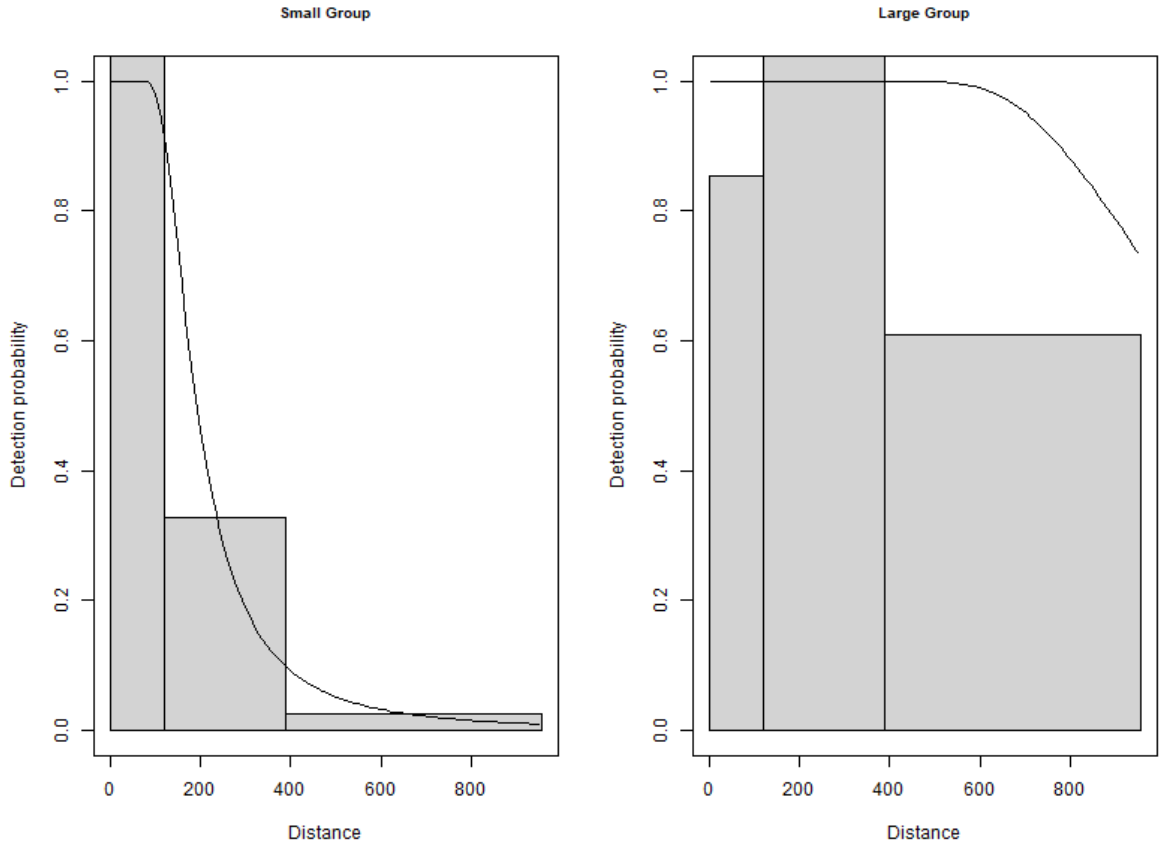

Figure 3-3. Graphs showing the estimated detection function of common scoter in small (1 bird) and large groups (200 birds). The histograms represent the distances (m) of the observed sightings across observers.

3.3 Common scoter Spatial Results by Survey

Figure 3-4 shows the distribution of the distance corrected counts for each of 62 surveys.

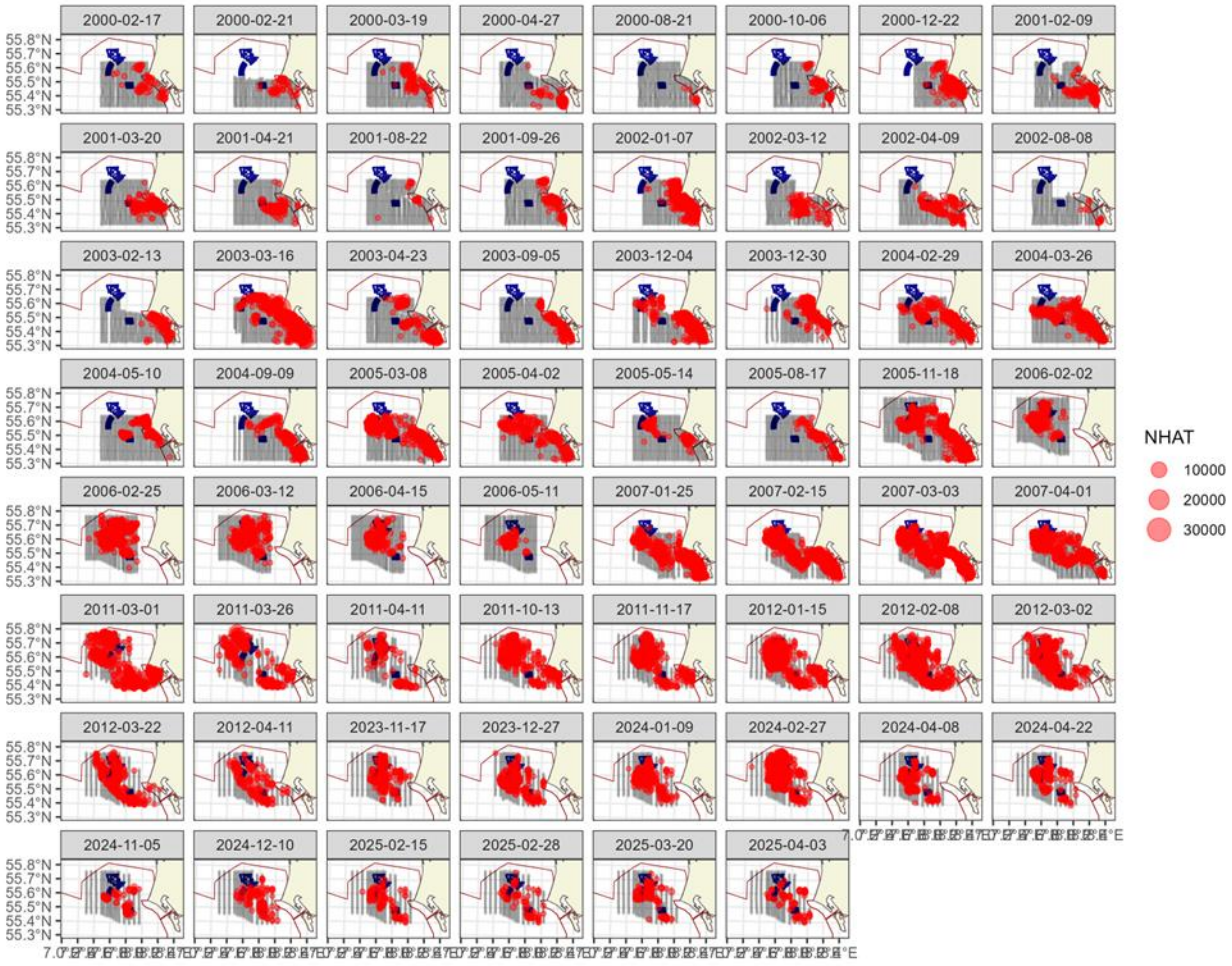

Figure 3-4. Distance-corrected counts for the common scoters across the 62 surveys. The red circles indicate the distance-corrected counts (NHAT) along the transect lines. The grey dots are segments with a count of zero.

3.3.1 Model Selection

For 47 of the 62 surveys, the models selected included a spatial term (of varying complexity) while the depth covariate (as a non-linear term) was selected for 15 of the surveys – in 11 of these models however, the spatial term was also included. The distance to coast covariate was selected as a non-linear term in 18 of the 62 models, and linear in three. All but eight also included a spatial term showing compelling evidence for non-uniform spatial patterns. The spatial surfaces selected ranged from two to 13 parameters for the spatial term (Table 3-1). The estimated abundances and associated 95 percentile confidence intervals for each survey are given in Table 3-2, illustrated in Figure 3-5 for all surveys combined and Figure 3-6 combined for each of the phases.

Table 3-1. Model selection results for common scoter for each survey. The model column represents the terms in the model.

Name	Model	Distribution	Variable 1D	Variable 2D	Number of Parameters	Dispersion parameter	Tweedie parameter
2000-02-17	Best 1D2D	Tweedie	s(distcoast, df=2)	s(x,y, df=8)	11	23.1	1.61
2000-02-21	2D Only	Tweedie	NA	s(x,y, df=3)	4	29.8	1.57
2000-03-19	Best 1D2D	Tweedie	s(distcoast, df=2)	s(x,y, df=6)	9	11.5	1.60

Name	Model	Distribution	Variable 1D	Variable 2D	Number of Parameters	Dispersion parameter	Tweedie parameter
2000-04-27	2D Only	Tweedie	NA	s(x,y, df=3)	4	134.3	1.49
2000-08-21	Intercept only	Tweedie	NA	NA	1	187.0	1.30
2000-10-06	Distance to coast	Tweedie	s(distcoast, df=2)	NA	3	25.4	1.49
2000-12-22	2D Only	Tweedie	NA	s(x,y, df=9)	10	28.7	1.49
2001-02-09	2D Only	Tweedie	NA	s(x,y, df=2)	3	74.4	1.55
2001-03-20	Best 1D2D	Tweedie	s(depth, df=2)	s(x,y, df=4)	7	20.3	1.61
2001-04-21	Best 1D2D	Tweedie	s(distcoast, df=2)	s(x,y, df=8)	11	11.0	1.61
2001-08-22	Depth	Tweedie	s(depth, df=2)	NA	3	197.5	1.41
2001-09-26	Best 1D2D	Tweedie	s(distcoast, df=2)	s(x,y, df=10)	13	3.5	1.54
2002-01-07	Best 1D2D	Tweedie	s(depth, df=2)	s(x,y, df=9)	12	25.1	1.52
2002-03-12	Distance to coast	Tweedie	s(distcoast, df=2)	NA	3	67.3	1.61
2002-04-09	2D Only	Tweedie	NA	s(x,y, df=5)	6	14.1	1.49
2002-08-08	Distance to coast	Tweedie	s(distcoast, df=2)	NA	3	14.4	1.39
2003-02-13	2D Only	Tweedie	NA	s(x,y, df=2)	3	134.9	1.61
2003-03-16	Best 1D2D	Tweedie	s(distcoast, df=2)	s(x,y, df=13)	16	45.6	1.58
2003-04-23	Distance to coast	Tweedie	s(distcoast, df=2)	NA	3	86.1	1.54
2003-09-05	Distance to coast	Tweedie	s(distcoast, df=2)	NA	3	8.6	1.46
2003-12-04	Best 1D2D	Tweedie	s(distcoast, df=2)	s(x,y, df=7)	10	30.3	1.49
2003-12-30	Distance to coast	Tweedie	distcoast, df=1	NA	2	450.3	1.55
2004-02-29	Best 1D2D	Tweedie	distcoast, df=1	s(x,y, df=6)	8	83.7	1.57
2004-03-26	2D Only	Tweedie	NA	s(x,y, df=8)	9	27.3	1.54
2004-05-10	2D Only	Tweedie	NA	s(x,y, df=9)	10	7.0	1.56
2004-09-09	Distance to coast	Tweedie	s(distcoast, df=2)	NA	3	92.9	1.48
2005-03-08	Best 1D2D	Tweedie	s(depth, df=2)	s(x,y, df=7)	10	30.7	1.54
2005-04-02	Best 1D2D	Tweedie	s(depth, df=2)	s(x,y, df=6)	9	29.3	1.50
2005-05-14	2D Only	Tweedie	NA	s(x,y, df=6)	7	16.3	1.60
2005-08-17	2D Only	Tweedie	NA	s(x,y, df=8)	9	7.1	1.55
2005-11-18	Depth	Tweedie	s(depth, df=2)	NA	3	294.5	1.61
2006-02-02	Best 1D2D	Tweedie	s(distcoast, df=2)	s(x,y, df=6)	9	26.6	1.58
2006-02-25	2D Only	Tweedie	NA	s(x,y, df=7)	8	51.5	1.55
2006-03-12	Best 1D2D	Tweedie	s(distcoast, df=4)	s(x,y, df=10)	15	18.7	1.51
2006-04-15	2D Only	Tweedie	NA	s(x,y, df=8)	9	28.5	1.54
2006-05-11	2D Only	Tweedie	NA	s(x,y, df=3)	4	12.8	1.50

Name	Model	Distribution	Variable 1D	Variable 2D	Number of Parameters	Dispersion parameter	Tweedie parameter
2007-01-25	Best 1D2D	Tweedie	distcoast, df=1	s(x,y, df=8)	10	33.7	1.55
2007-02-15	2D Only	Tweedie	NA	s(x,y, df=11)	12	33.3	1.54
2007-03-03	Best 1D2D	Tweedie	s(depth, df=2)	s(x,y, df=10)	13	23.9	1.54
2007-04-01	Best 1D2D	Tweedie	s(depth, df=2)	s(x,y, df=7)	10	33.0	1.57
2011-03-01	2D Only	Tweedie	NA	s(x,y, df=5)	6	79.3	1.61
2011-03-26	2D Only	Tweedie	NA	s(x,y, df=6)	7	108.4	1.61
2011-04-11	Depth	Tweedie	s(depth, df=2)	NA	3	160.2	1.61
2011-10-13	2D Only	Tweedie	NA	s(x,y, df=5)	6	55.1	1.52
2011-11-17	2D Only	Tweedie	NA	s(x,y, df=7)	8	42.8	1.58
2012-01-15	Best 1D2D	Tweedie	s(depth, df=2)	s(x,y, df=7)	10	22.6	1.58
2012-02-08	2D Only	Tweedie	NA	s(x,y, df=10)	11	36.1	1.59
2012-03-02	Best 1D2D	Tweedie	s(distcoast, df=2)	s(x,y, df=8)	11	32.0	1.60
2012-03-22	2D Only	Tweedie	NA	s(x,y, df=9)	10	21.1	1.59
2012-04-11	2D Only	Tweedie	NA	s(x,y, df=7)	8	28.4	1.57
2023-11-17	2D Only	Tweedie	NA	s(x,y, df=8)	9	16.7	1.60
2023-12-27	Best 1D2D	Tweedie	s(depth, df=2)	s(x,y, df=9)	12	13.7	1.56
2024-01-09	Depth	Tweedie	s(depth, df=2)	NA	3	82.0	1.61
2024-02-27	Distance to coast	Tweedie	s(distcoast, df=2)	NA	3	61.0	1.57
2024-04-08	Best 1D2D	Tweedie	s(depth, df=2)	s(x,y, df=7)	10	68.2	1.54
2024-04-22	Best 1D2D	Tweedie	s(depth, df=2)	s(x,y, df=5)	8	25.2	1.61
2024-11-05	Intercept only	Tweedie	NA	NA	1	194.2	1.59
2024-12-10	2D Only	Tweedie	NA	s(x,y, df=5)	6	19.1	1.60
2025-02-15	Distance to coast	Tweedie	s(distcoast, df=2)	NA	3	79.7	1.54
2025-02-28	2D Only	Tweedie	NA	s(x,y, df=6)	7	31.3	1.54
2025-03-20	Best 1D2D	Tweedie	s(depth, df=2)	s(x,y, df=8)	11	18.8	1.42
2025-04-03	Best 1D2D	Tweedie	s(distcoast, df=2)	s(x,y, df=8)	11	11.3	1.50

3.3.2 Abundance Estimates by Survey

The estimated abundances, densities and associated 95 percentile confidence intervals for each survey are given in Table 3-2, and illustrated in Figure 3-5 for all surveys combined and in Figure 3-6 combined for each of the phases. It is important to note that the six additional surveys undertaken from November 2024 to April 2025 (Phase 3) observed low numbers of common scoters compared with recent years.

Table 3-2. Estimated abundance and density of common scoter for each survey. The 95% CI are percentile-based confidence intervals.

Month	Area (Km^2)	Estimated Count	95% CI Count	Estimated Density	95% CI Density
2000-02-17	2019	5997	(2732, 15366)	3.0	(1.4, 7.6)
2000-02-21	2019	4078	(1859, 9155)	2.0	(0.9, 4.5)
2000-03-19	2019	13398	(6216, 28431)	6.6	(3.1, 14.1)
2000-04-27	2019	1377	(511, 3588)	0.7	(0.3, 1.8)
2000-08-21	2019	468	(120, 2286)	0.2	(0.1, 1.1)
2000-10-06	2019	3001	(1640, 5605)	1.5	(0.8, 2.8)
2000-12-22	2019	1868	(782, 4599)	0.9	(0.4, 2.3)
2001-02-09	2019	2492	(1015, 5797)	1.2	(0.5, 2.9)
2001-03-20	2019	9207	(4742, 18014)	4.6	(2.3, 8.9)
2001-04-21	2019	20336	(11821, 36862)	10.1	(5.9, 18.3)
2001-08-22	2019	757	(185, 4305)	0.4	(0.1, 2.1)
2001-09-26	2019	2546	(1748, 3855)	1.3	(0.9, 1.9)
2002-01-07	2019	18767	(11778, 32167)	9.3	(5.8, 15.9)
2002-03-12	2019	10610	(3768, 29232)	5.3	(1.9, 14.5)
2002-04-09	2019	8902	(5395, 14592)	4.4	(2.7, 7.2)
2002-08-08	2019	354	(112, 1155)	0.2	(0.1, 0.6)
2003-02-13	2019	42	(15, 151)	0.0	(0, 0.1)
2003-03-16	2019	104422	(62052, 183408)	51.7	(30.7, 90.8)
2003-04-23	2019	21414	(11890, 39735)	10.6	(5.9, 19.7)
2003-09-05	2019	3999	(2257, 7058)	2.0	(1.1, 3.5)
2003-12-04	2019	14338	(6339, 36943)	7.1	(3.1, 18.3)
2003-12-30	2019	20978	(8974, 46495)	10.4	(4.4, 23)
2004-02-29	2019	23162	(12387, 44540)	11.5	(6.1, 22.1)
2004-03-26	2019	40232	(26247, 64912)	19.9	(13, 32.1)
2004-05-10	2019	16651	(7529, 41263)	8.2	(3.7, 20.4)
2004-09-09	2019	4566	(2646, 8599)	2.3	(1.3, 4.3)
2005-03-08	2019	55929	(34885, 91342)	27.7	(17.3, 45.2)
2005-04-02	2019	16473	(10076, 28470)	8.2	(5, 14.1)
2005-05-14	2019	15491	(10258, 23587)	7.7	(5.1, 11.7)
2005-08-17	2019	3221	(1717, 6191)	1.6	(0.9, 3.1)
2005-11-18	2019	70405	(36492, 133176)	34.9	(18.1, 66)
2006-02-02	2019	59231	(32642, 114806)	29.3	(16.2, 56.9)
2006-02-25	2019	62617	(38427, 109140)	31.0	(19, 54)
2006-03-12	2019	54106	(28944, 106792)	26.8	(14.3, 52.9)
2006-04-15	2019	37208	(19024, 78505)	18.4	(9.4, 38.9)
2006-05-11	2019	9221	(5453, 16502)	4.6	(2.7, 8.2)
2007-01-25	2019	54290	(32613, 94019)	26.9	(16.2, 46.6)
2007-02-15	2019	131825	(79561, 239386)	65.3	(39.4, 118.6)

Month	Area (Km^2)	Estimated Count	95% CI Count	Estimated Density	95% CI Density
2007-03-03	2019	119043	(66633, 218244)	59.0	(33, 108.1)
2007-04-01	2019	69057	(39325, 126461)	34.2	(19.5, 62.6)
2011-03-01	2019	231729	(131460, 414315)	114.8	(65.1, 205.2)
2011-03-26	2019	119000	(70039, 212615)	58.9	(34.7, 105.3)
2011-04-11	2019	47650	(25578, 96676)	23.6	(12.7, 47.9)
2011-10-13	2019	37576	(22172, 64681)	18.6	(11, 32)
2011-11-17	2019	54665	(28343, 105888)	27.1	(14, 52.4)
2012-01-15	2019	190533	(123839, 311282)	94.4	(61.3, 154.2)
2012-02-08	2019	168321	(95322, 312948)	83.4	(47.2, 155)
2012-03-02	2019	106113	(59398, 197761)	52.6	(29.4, 97.9)
2012-03-22	2019	69827	(37677, 141434)	34.6	(18.7, 70)
2012-04-11	2019	24812	(13066, 49300)	12.3	(6.5, 24.4)
2023-11-17	2019	32672	(14596, 77835)	16.2	(7.2, 38.5)
2023-12-27	2019	51479	(25831, 125220)	25.5	(12.8, 62)
2024-01-09	2019	62009	(31044, 114742)	30.7	(15.4, 56.8)
2024-02-27	2019	146243	(85396, 255391)	72.4	(42.3, 126.5)
2024-04-08	2019	21536	(12411, 38447)	10.7	(6.1, 19)
2024-04-22	2019	28798	(11558, 70208)	14.3	(5.7, 34.8)
2024-11-05	2019	9661	(2935, 35469)	4.8	(1.5, 17.6)
2024-12-10	2019	15017	(6535, 34353)	7.4	(3.2, 17)
2025-02-15	2019	8915	(4490, 18206)	4.4	(2.2, 9)
2025-02-28	2019	4507	(1576, 14326)	2.2	(0.8, 7.1)
2025-03-20	2019	9848	(5151, 19744)	4.9	(2.6, 9.8)
2025-04-03	2019	9762	(5740, 18353)	4.8	(2.8, 9.1)

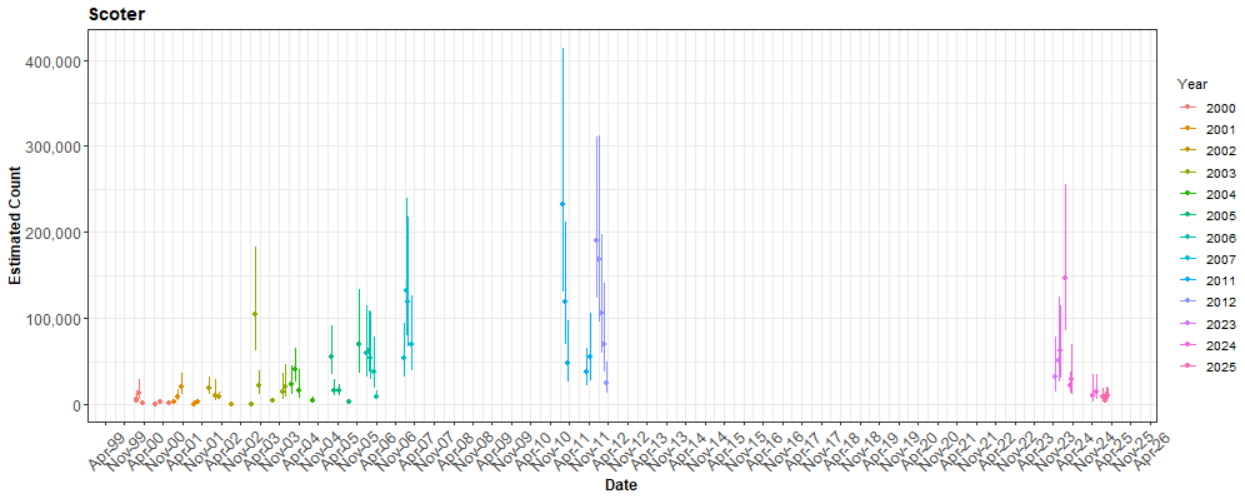

Figure 3-5. The estimated count of common scoter for each survey. The 95% CI are percentile-based confidence intervals from a parametric bootstrap with 500 replicates. As the analysis area has the same extension between surveys, the estimated abundances are comparable.

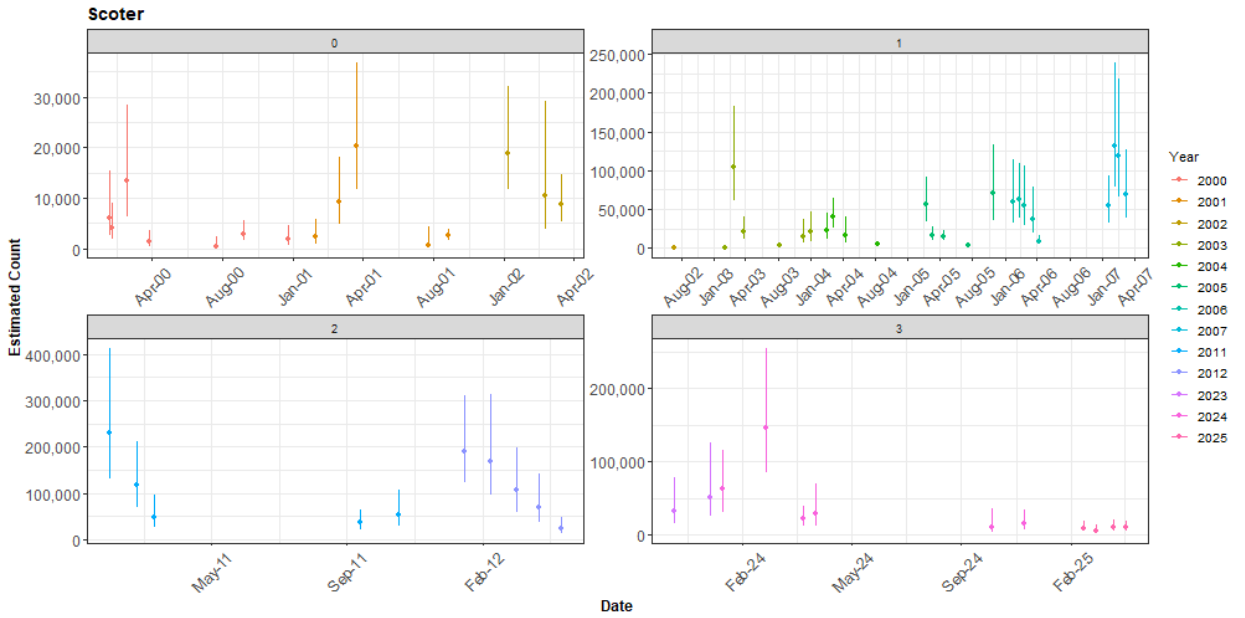

Figure 3-6. The estimated count of common scoter for each survey by phase. The 95% CI are percentile-based confidence intervals were derived from a parametric bootstrap with 500 replicates. To show more detail the y-axis is different for each phase.

3.3.3 Density Distributions

Figure 3-7 to Figure 3-10 show the estimated counts of common scoter in each 500 m x 500 m grid cells for each survey in each of the four phases. Generally, the estimated abundances fitted well to the raw data and there were no notable misalignments. In areas where the estimated counts were systematically higher, the abundances were also relatively high and there were no areas with large, estimated abundances unsupported by the data.

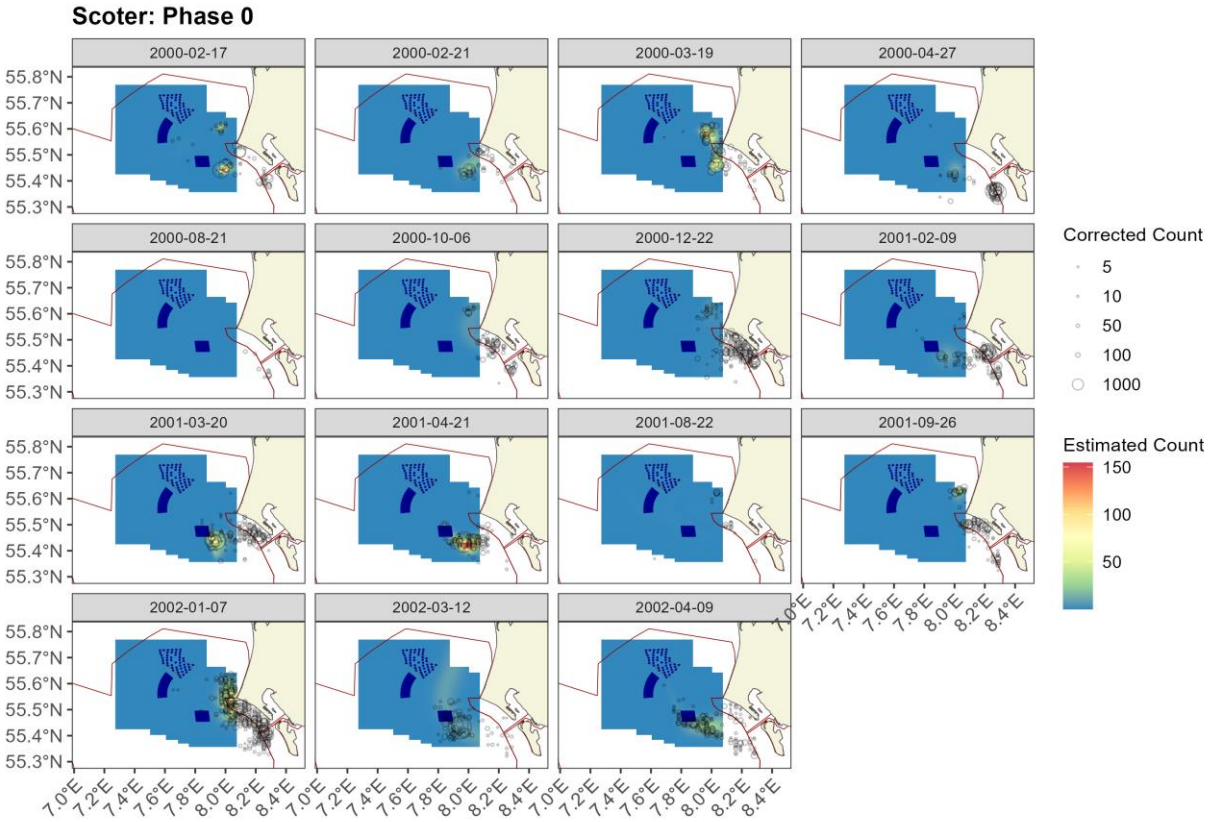

Figure 3-7. Maps showing the estimated common scoter abundance across the study site for each of the surveys in Phase 0. The estimated counts are per 500 m x 500 m grid cell. The open circles show the distance corrected counts. The coloured graphics represent the predicted counts in each location.

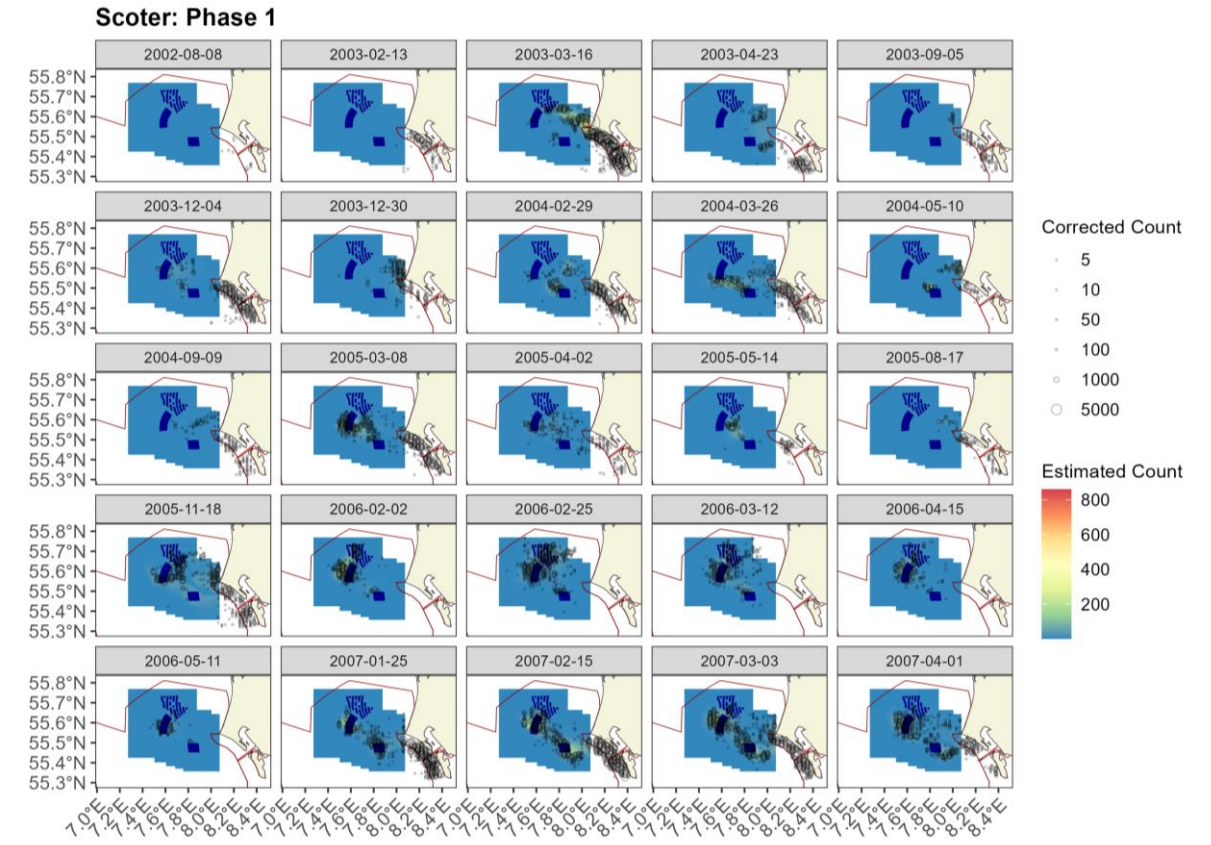

Figure 3-8. Maps showing the estimated common scoter abundance across the study site for each of the surveys in Phase 1. The estimated counts are per 500 m x 500 m grid cell. The open circles show the distance corrected counts. The coloured graphics represent the predicted counts in each location.

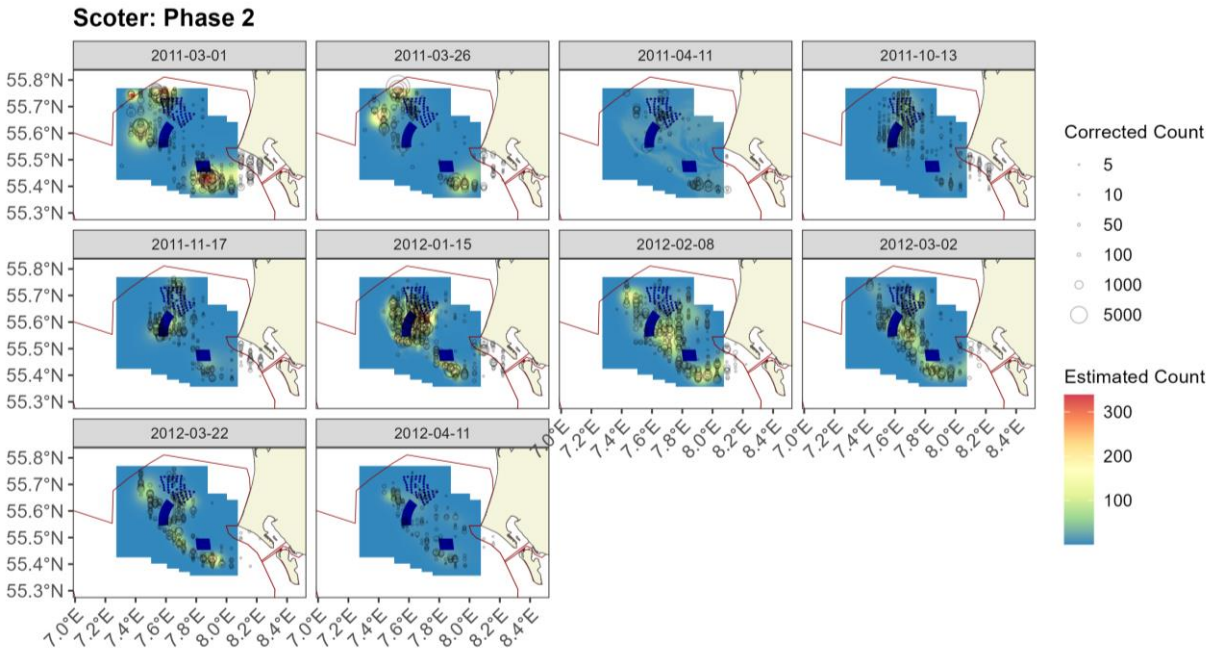

Figure 3-9. Maps showing the estimated common scoter abundance across the study site for each of the surveys in Phase 2. The estimated counts are per 500 m x 500 m grid cell. The open circles show the distance corrected counts. The coloured graphics represent the predicted counts in each location.

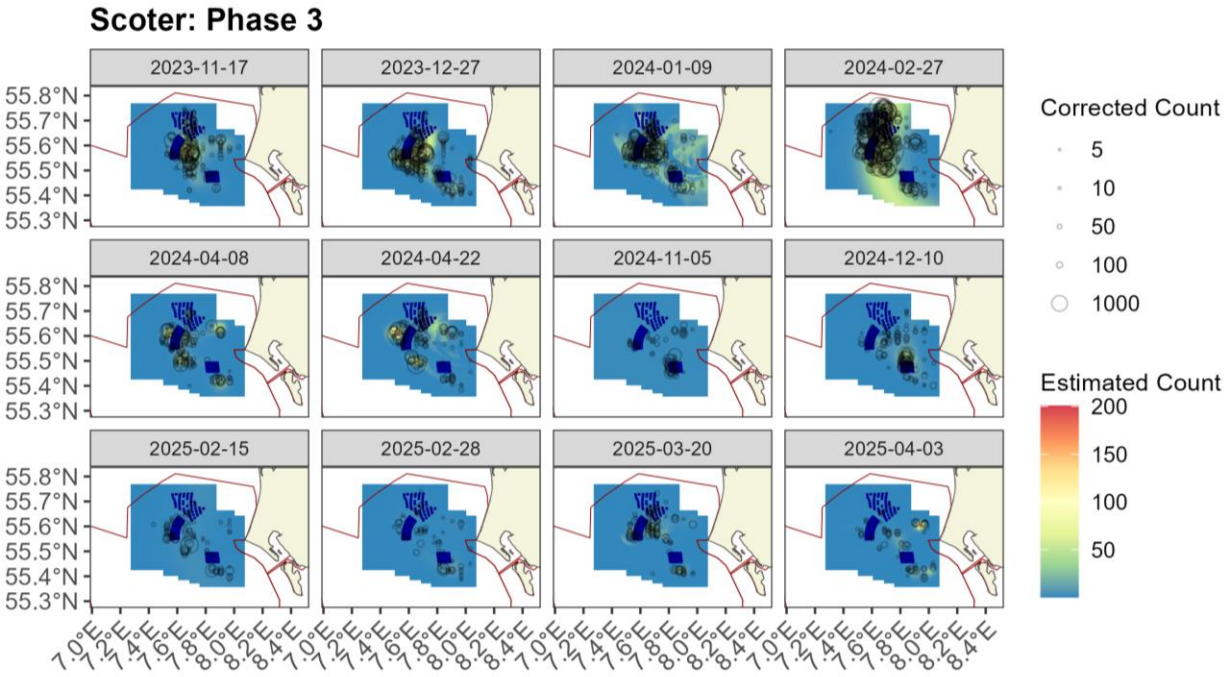

Figure 3-10. Maps showing the estimated common scoter abundance across the study site for each of the surveys in Phase 3. The estimated counts are per 500 m x 500 m grid cell. The open circles show the distance corrected counts. The coloured graphics represent the predicted counts in each location.

3.3.4 Uncertainty in spatial predictions

Broadly, the highest coefficient of variation (CoV) scores were associated with the `almost zero' predictions and it is known that the CoV metric is highly sensitive to any uncertainty for very small predictions. There was no material overlap between high values of the CoV metric and the transect lines/locations with non-zero counts. Therefore, results can be considered to be valid i.e. they do not compromise the model (Figure 3-11).

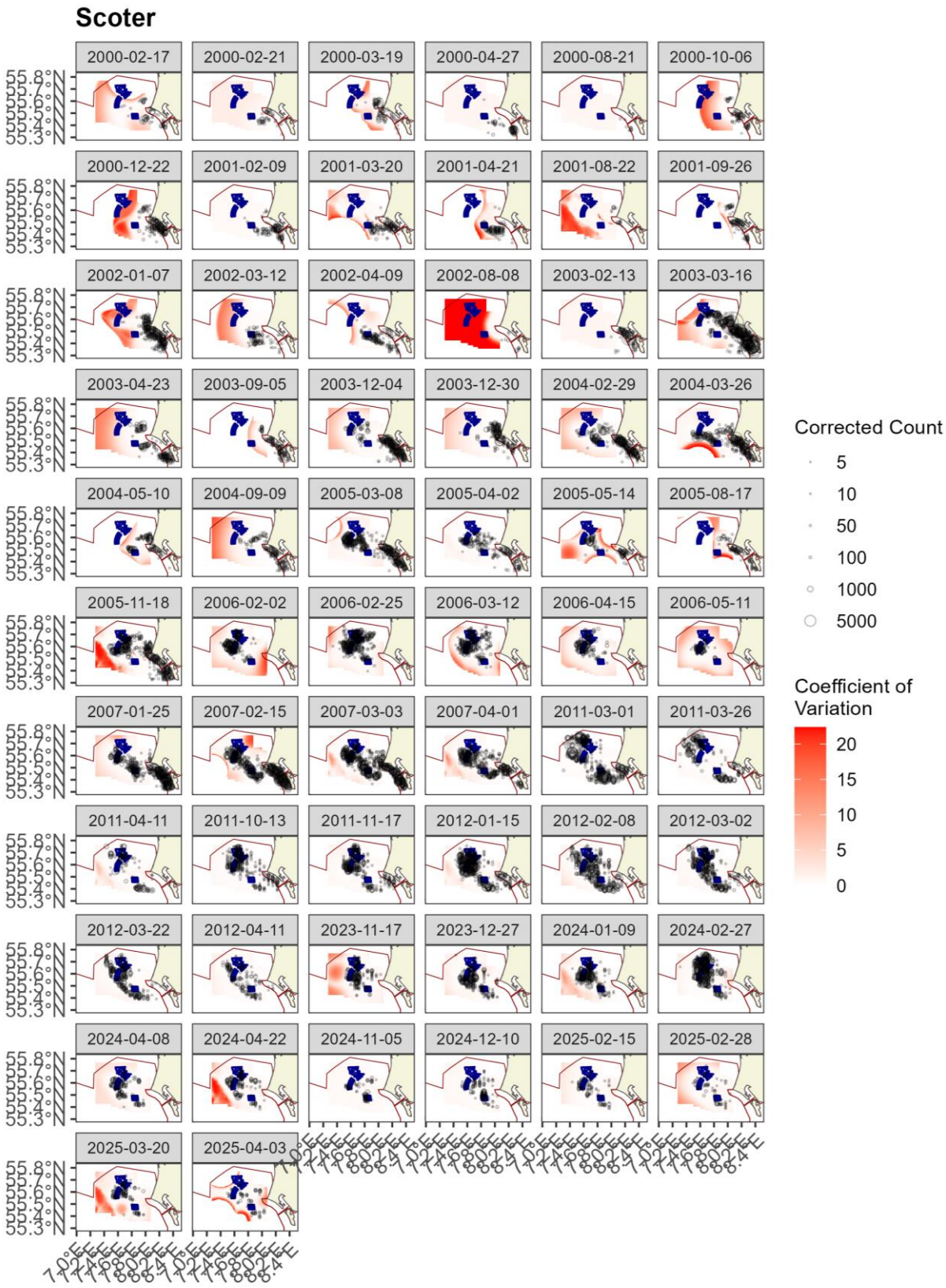

Figure 3-11. Maps showing the coefficient of variation across the study region for each of the surveys for common scoter. The open circles show the distance corrected counts. The presence of dark red CV scores in areas with virtually zero predictions are an artifact of the very small prediction rather than of any notable concern.

In the case, when the very small predicted values were excluded (Figure 3-12) there were some small red areas indicating high uncertainty but predominantly, these were in areas of very low predicted abundance.

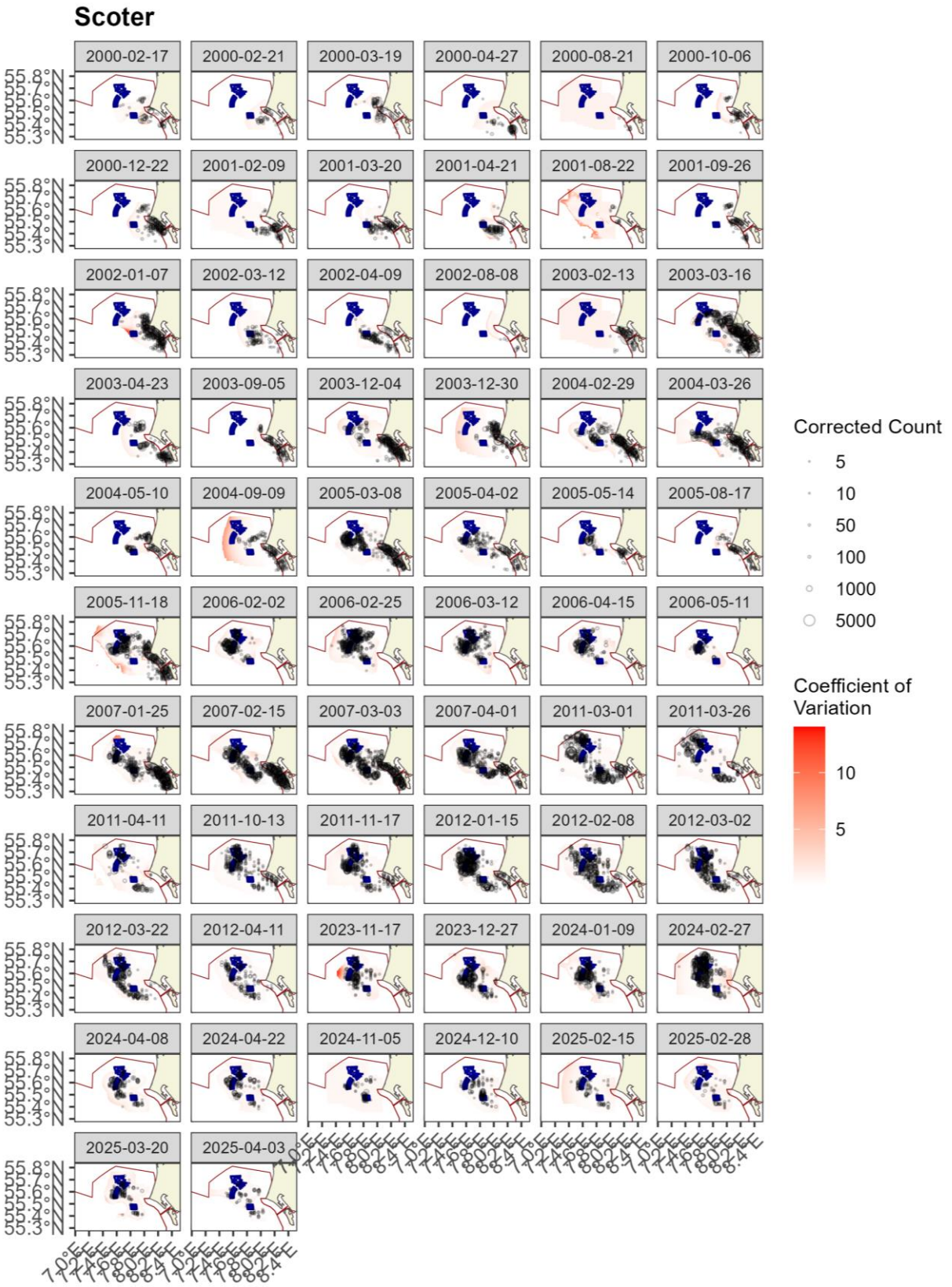

Figure 3-12. Maps showing the coefficient of variation across the study area for each of the surveys for common scoter after the removal of very small, predicted values. The open circles show the distance corrected counts.

3.4 Common scoter Spatial results by Phase

3.4.1 Phase-specific spatial patterns

The mean common scoter distribution map in Phase 0 (Figure 3-13) illustrates the lack of that species in the majority of the study area, with the highest density of birds to the south east of the area. The distribution for Phase I shows more birds in the area and concentrations around the HR I and HR II footprints. However, the majority of bird sightings in Phase 0 were to the east and so the change is not necessarily an indication of an increase in overall abundance of the species. The expansion in the distribution of the species from the coast into the offshore area to the west can be seen in more detail in Figure 3-14 which shows the distribution in the early years of Phase I and the latter years. Whilst there is some movement offshore pre November 2005, the main increase occurs after this (Phase 1*).

By Phase 2, common scoter were showing a more widespread distributional pattern with the highest concentrations to the south of the HR I footprint. During Phase 3, common scoter abundance was more concentrated in the centre of the survey area, covering the HR II footprint to some extent but with the greater concentration to the east of this footprint. Phase 3 also demonstrates a non-trivial concentration in the footprint of the HR III, even after its relatively recent construction.

Phase 3 showed a marked reduction of densities across the model area, with the highest abundances estimated in the area east of HRII, the central part of the model area. The densities previously found southeast of HRI and in the northwestern parts under Phase 2, declined. This decline was mainly caused by a pronounced reduction in common scoters in the survey area during the winter of 2024/2025 (Figure 3-2, Figure 3-5, Figure 3-10).

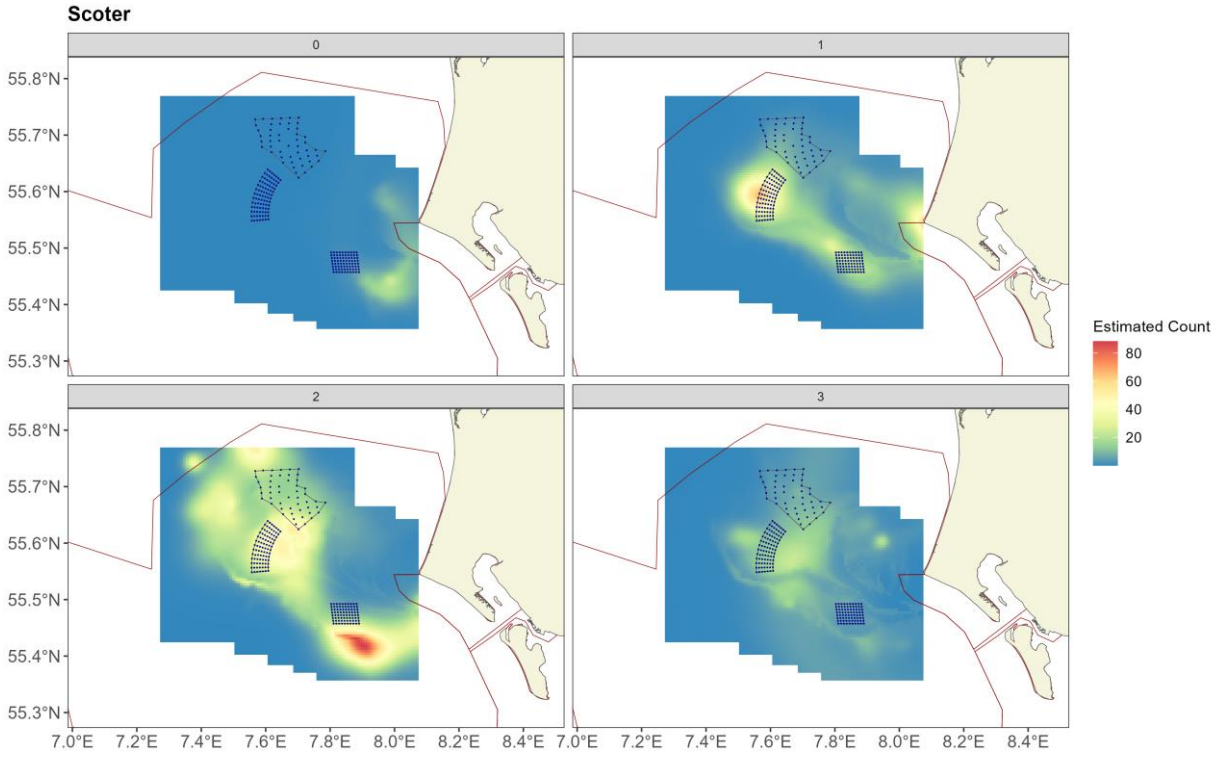

Figure 3-13. Distribution maps showing the estimated common scoter abundance across the study site for each of the surveys from Phase 0 to Phase 3. The estimated counts are per 500 m x 500 m grid cell. The open circles show the distance corrected counts. The coloured graphics represent the predicted counts in each location.

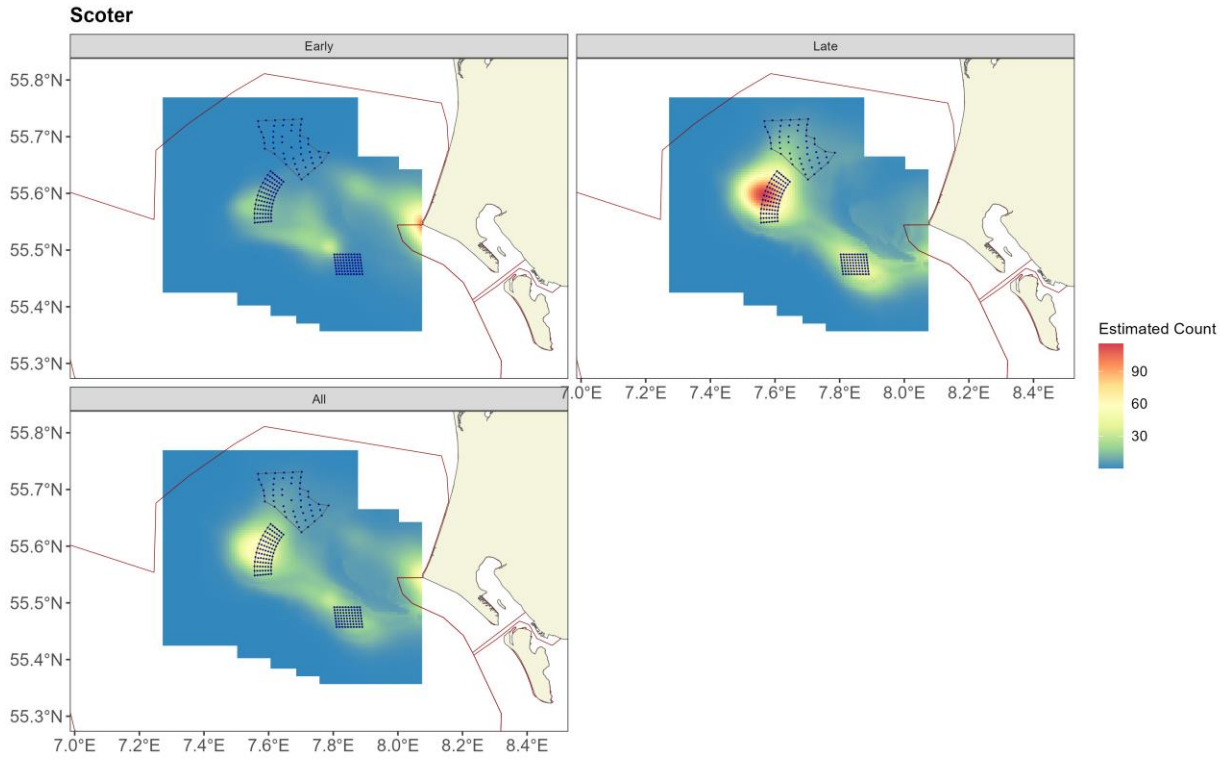

Figure 3-14. Distribution maps showing the estimated common scoter abundance across the study site within Phase 1 for "Early" surveys (pre November 2005), "Late" surveys (post November 2005) and for all combined. The estimated counts are per 500 m x 500 m grid cell. The coloured graphics represent the predicted counts in each location.

3.4.2 Overall Persistence

As well as looking at the mean distribution of birds in each phase, which may be influenced by a few surveys with large numbers of birds, we can assess the persistence of birds in each grid cell overall and by phase. The persistence analysis describes, at a fine geographical scale, areas of higher or lower usage by the species, evaluated over many surveys.

Across the 62 surveys (spanning 25 years) there is moderate to low persistence across the predicted area (Figure 3-15). The highest persistence (~ 50%) occurs in the central and south-eastern parts of the study area, along the extent of the Horns Rev sandbar.

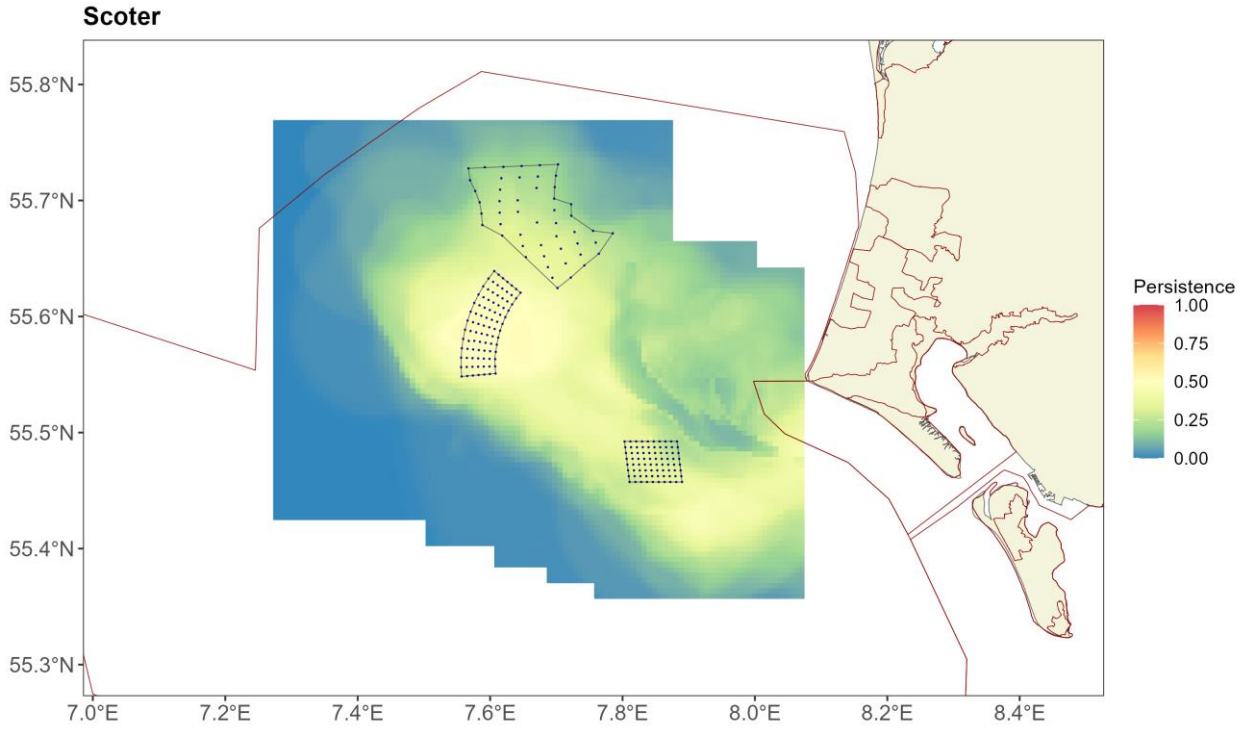

Figure 3-15. Persistence scores for common scoter across the 62 surveys. The polygons represent the windfarms Horns Rev I, II and III (black line).

Figure 3-16 to Figure 3-19 show the persistence of birds within each phase.

In Phase 0, prior to any construction, the birds show persistently high numbers to the east of the study area (Figure 3-16). After the construction of HR I (Phase 1), the birds became more prevalent offshore and more central in the study area, just to the northwest of the HR I footprint and into the area where HR II would be constructed (which occurred after that time).

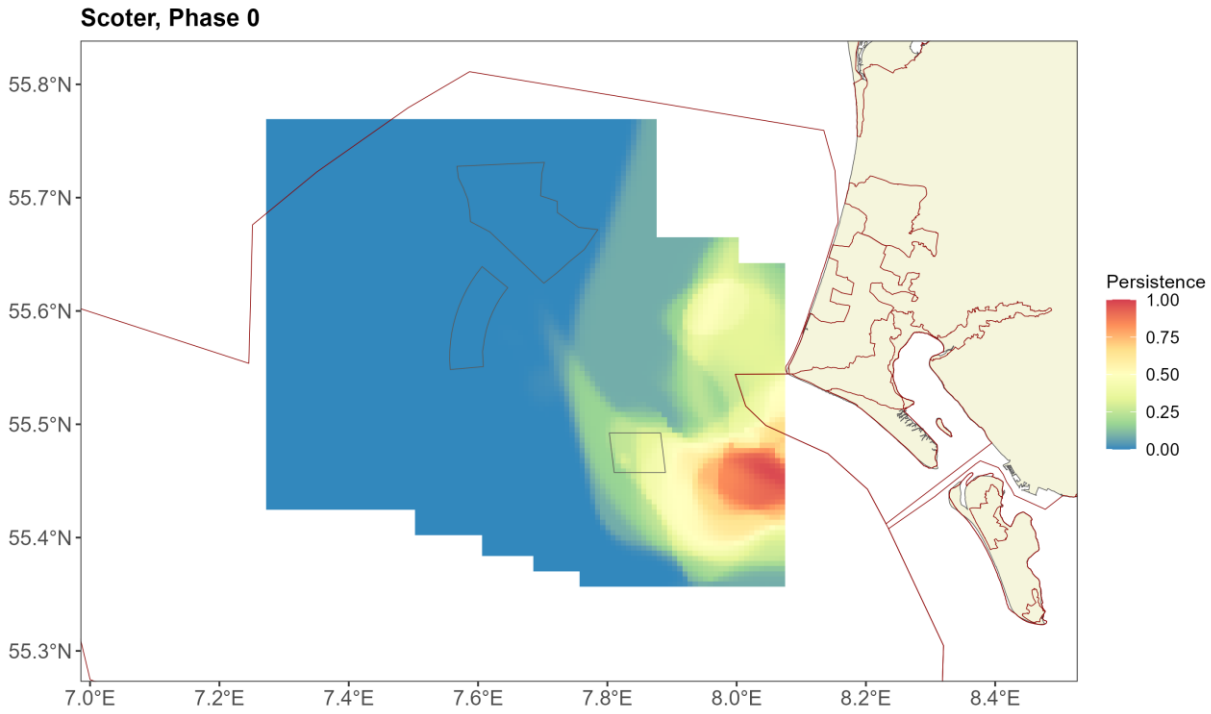

Figure 3-16. Persistence scores for common scoter across the 15 surveys in Phase 0. The polygons represent the windfarms Horns Rev I, II and III (black line).

The distribution of common scoters in Phase 1 is also more widespread compared with Phase 0 which has a more focused distribution, nearer to shore (Figure 3-17).

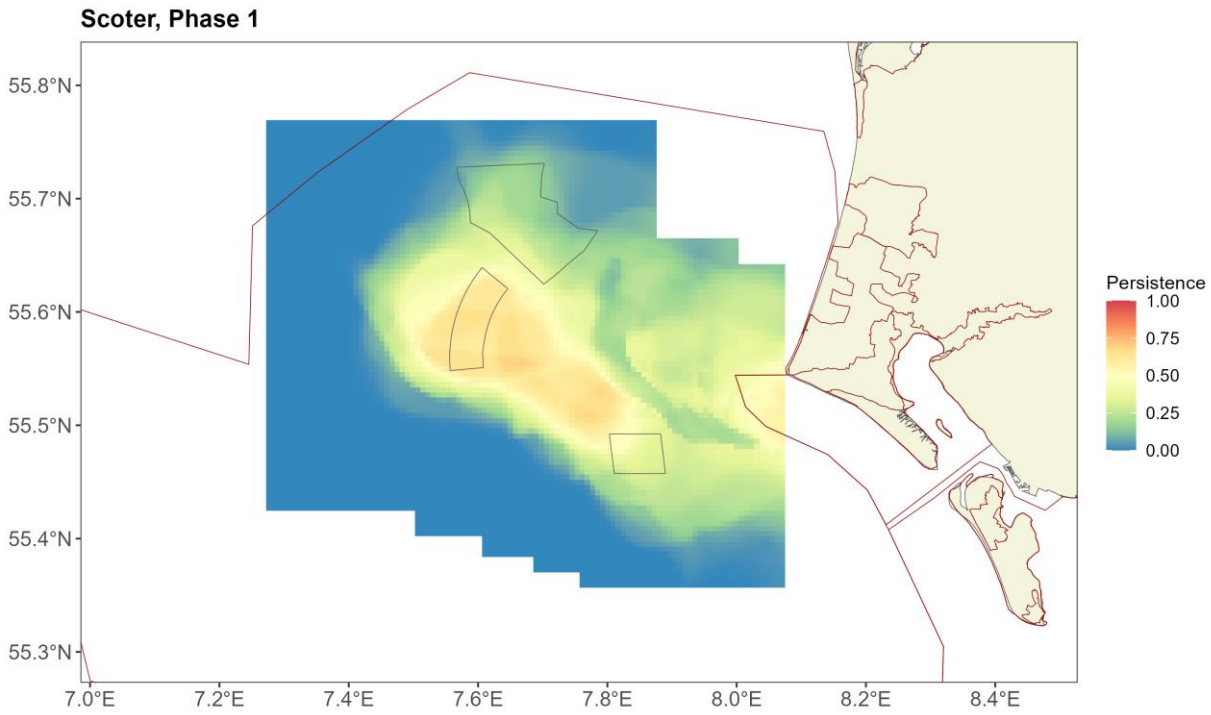

Figure 3-17. Persistence scores for common scoter across the 25 surveys in Phase 1. The polygons represent the windfarms Horns Rev I, II and III (black line).

Phase 2 is 2-5 years post-construction of HR II and 9-10 years post-construction of HR I. In this phase, the birds are persistently found to the south of HR I and on the eastern edge and north of HR II, and notably into the area where HR III was yet to be constructed (Figure 3-18).

The most recent surveys, in Phase 3, were carried out 5-7 years post-construction of HR III, 11-13 years post-construction of HR II and 21-23 years post-construction of HR I. During the Phase 3 surveys, the birds were persistently found in and around the HR II footprint. Additionally, while the persistence is relatively concentrated in and around HR II, some persistence was still seen to the south of HR I and in the southern part of HR III (Figure 3-19).

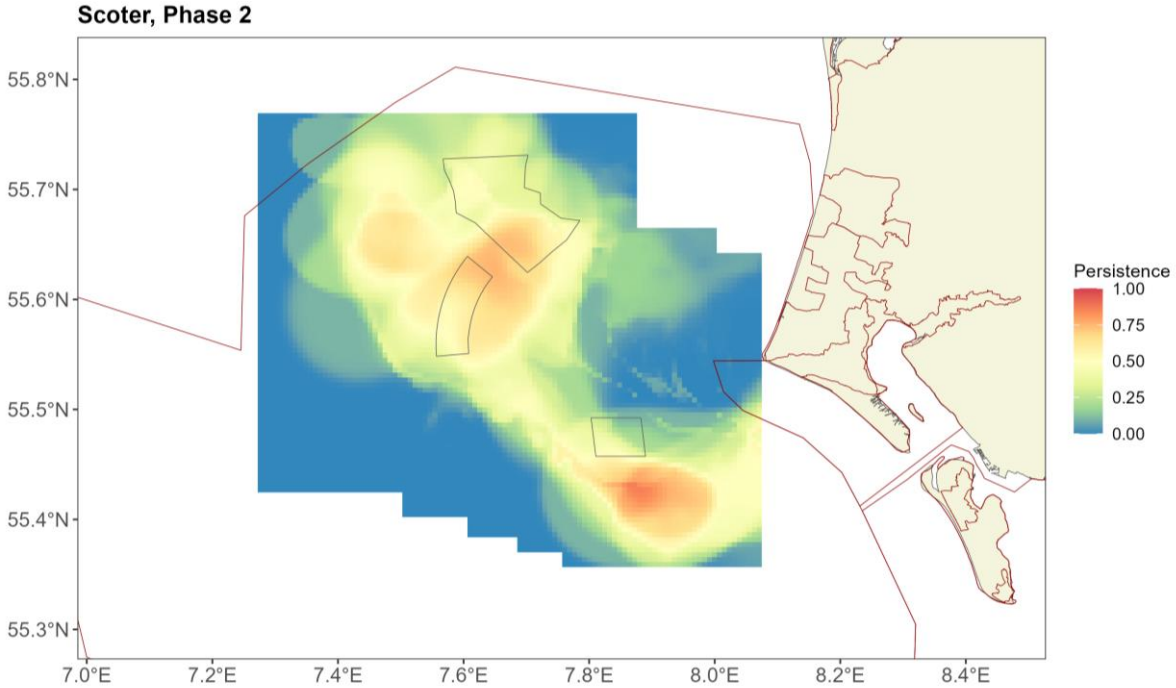

Figure 3-18. Persistence scores for common scoter across the 10 surveys in Phase 2. The polygons represent the windfarms Horns Rev I, II and III (black line).

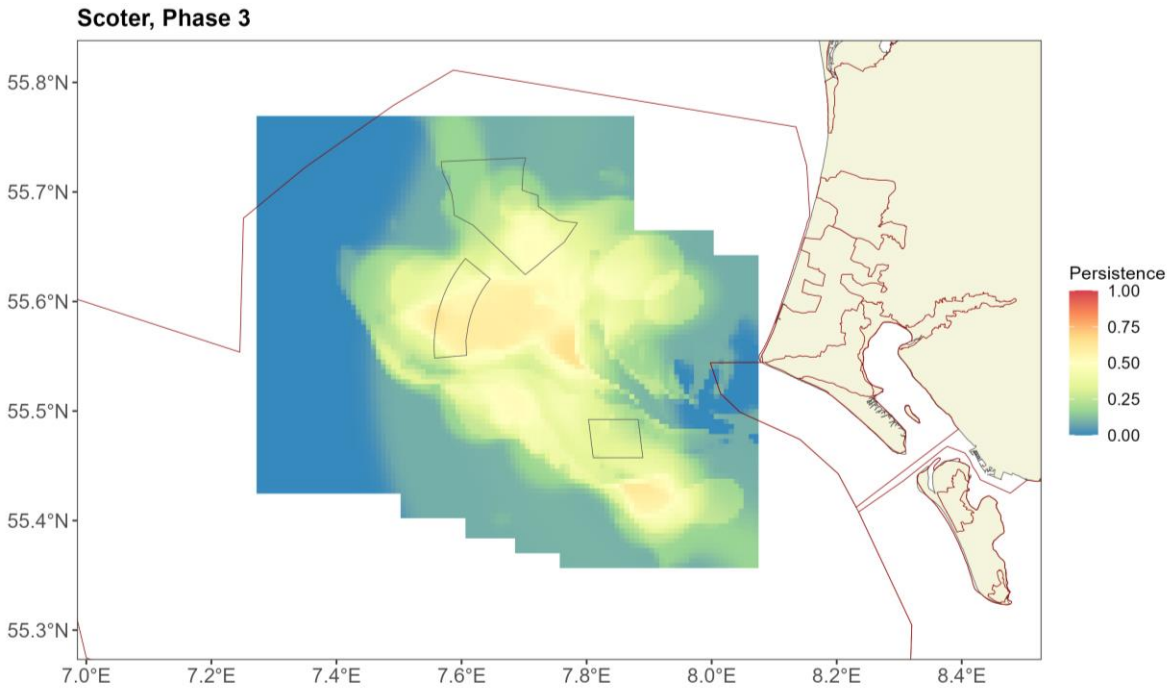

Figure 3-19. Persistence scores for common scoter across the 12 surveys in Phase 3. The polygons represent the windfarms Horns Rev I, II and III (black line).

3.4.3 Phase-specific windfarm footprint densities

The coincidence of the expansion west in the distribution of common scoter and the lack of birds seen in the HR I footprint does not lend it to a finer scale investigation of displacement. The data from the HR II wind farm is, on the other hand, ideal for making such a comparison, with sufficient pre- and post-construction data available to establish notable changes in density. The change in survey coverage across the span of years and the expansion of common scoters to the west during Phase 1 do however have the potential to lead to misleading results. Figure 3-20 shows that while early surveys captured the footprint of HR II, they provided limited coverage of HR III and the west of the study area at that time. Including all surveys in Phase 1 conflates the longer-term change across the five-year period, with any construction related changes we are aiming to detect. This leads to a dilution effect on the density surface, particularly around HR II, when including the early surveys in Phase 1. As there has been a clear distributional shift alongside a change in survey coverage, we have chosen to assess the data using only November 2005 data onwards (Phase 1*), in line with the analysis in the 2014 report (Petersen et al. 2014).

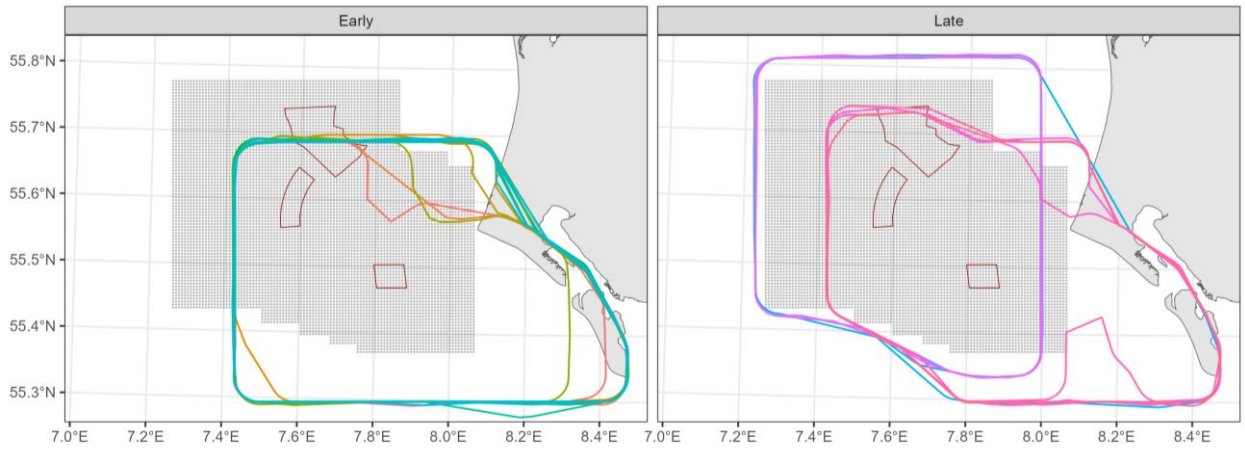

Figure 3-20. Maps showing the survey coverage within Phase 1 for "Early" surveys (pre November 2005) and "Late" surveys (post November 2005). The grey dotted areas show the prediction grid coverage.

Closer inspection of the estimated density of common scoters within and around the windfarm footprints at various spatial scales was carried out to better understand any windfarm related changes (Figure 3-21 and Table 3-3). If there were no changes in common scoter density across the 20 years in this figure, either inside the footprint or up to 1 km or 2 km from the footprint then we would expect to see horizontal lines for all four colours in Figure 3-21. However, the likelihood of changes in bird density across this time frame is incredibly high, regardless of windfarm construction, and so any changes must be examined from several perspectives.

In the study area, there has been a general increase in common scoter density from Phase 1 to 2 followed by a decrease in Phase 3 (indicated by the black lines in Figure 3-21), providing a backdrop of variable abundances during the 20 years across the survey area.

Inside the footprint of each of the three windfarms (HR I, HR II and HR III) we see different patterns as each windfarm is constructed. Post-construction of HR I (Phase 1) we see an initial large mean decrease in common scoter density with each phase. It is difficult to associate this change with the wind farm construction owing to the co-incident expansion of the geographic range of common scoter. By Phase 3, the mean density is similar to that of the study area as a whole.

In the case of HR II, there was a sharp decline in density (~50%; Table 3-3) inside the footprint after its construction (compared to prior-construction) with a further decrease of ~ 65% in Phase 3 (after HR III was constructed). Overall, from Phase 1-3 there was ~ 80% decrease in density in the HR II footprint.

Regarding HR III, densities increased from Phases 1 to 2, reflecting the pattern of increasing density in the study area as a whole. From Phase 2 to 3 (pre- to post-construction of HR III) there was a sharp decline in footprint densities, in keeping with the study wide decline.

There were very similar patterns within one and two kilometers of each windfarm footprint to those observed inside the footprint in each case.

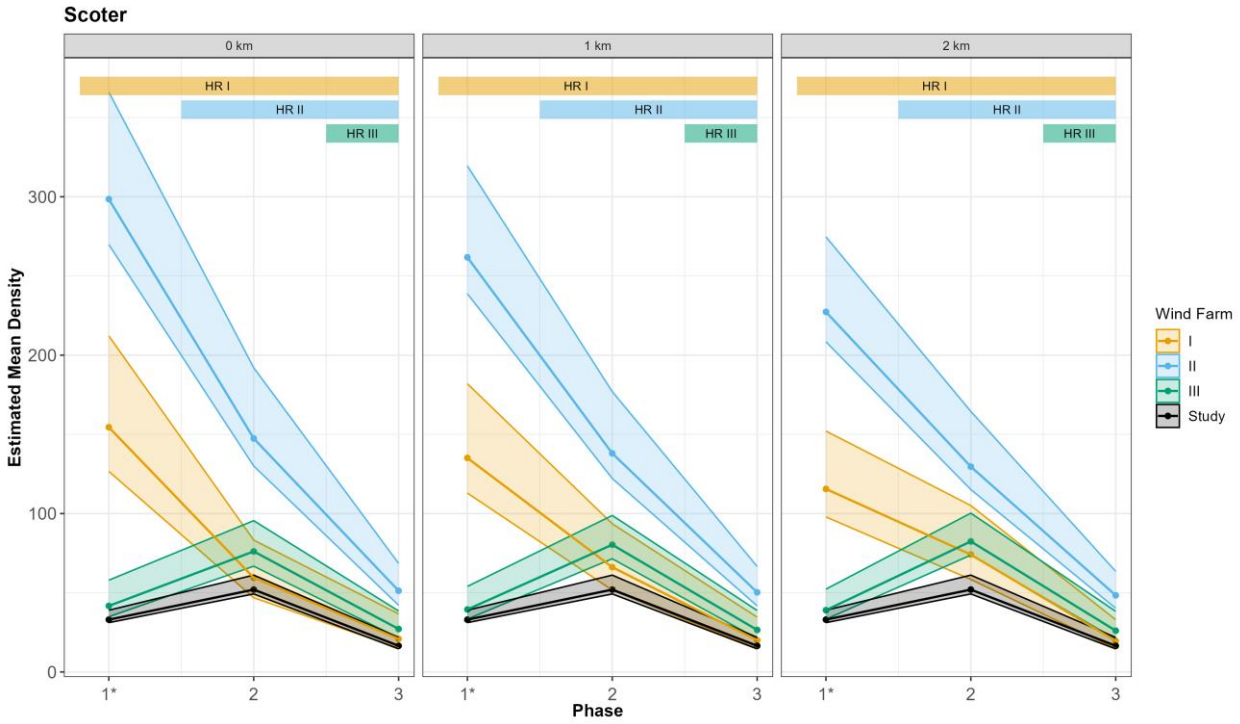

Figure 3-21. Graphs showing the estimated mean density of common scoter inside the footprint (indicated by 0 km from the footprint), footprint including a 1 km buffer (indicated by 1 km from the footprint) and footprint including a 2 km buffer (indicated by 2 km) of each windfarm for Phases 1 to 3. The bars at the top show the post-construction periods for each wind farm.*

Table 3-3. Table of common scoter abundance estimates and 95 percentile-based confidence intervals for each wind farm footprint and phase (1 to 3).*

Phase	I	II	III
1*	3130 (2570, 4300)	9110 (8230, 11200)	3570 (2980, 4960)
2	1210 (950, 1690)	4500 (3970, 5860)	6510 (5710, 8170)
3	424 (305, 744)	1560 (1290, 2090)	2320 (1840, 3300)

3.4.4 Phase-specific spatial differences

Having looked at general trends in density across the three footprints and three phases we can also assess changing spatial patterns using spatial difference plots. The shift in spatial patterns from Phase 0 to Phase 1 can be seen in Figure 3-22, which clearly illustrates a shift in common scoter numbers from the southeastern edge of the area of interest into the centre in Phase 1 and towards the HR II footprint before its construction. The increase in bird numbers in Phase 1, compared to Phase 0, is also evident here with significant increases in most locations in Phase 1 compared with Phase 0, and some higher than 20 birds/km^2 in many locations. While there is an abundance shift into the centre of the study area in Phase 1 (compared with Phase 0), there is also an increase on the eastern edge of the survey area in Phase 1, evidencing higher numbers than in Phase

0. There is a small, yet statistically significant, decrease in the south-eastern edge of the survey area, too, in Phase 1 compared with Phase 0.

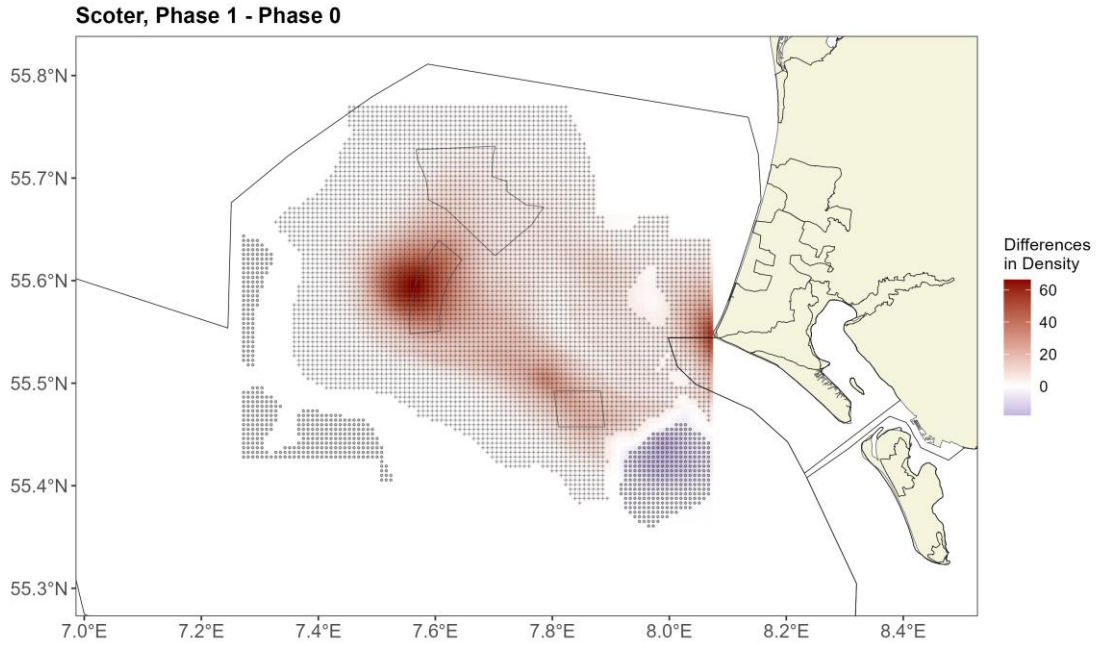

Figure 3-22. Map showing the estimated differences in the common scoter distribution between Phase 1 and Phase 0. Positive differences indicate more birds in Phase 1. A "+" sign in the reddish background colours indicates a significant positive difference and a "o" in bluish background colours a significant negative difference.

Figure 3-23 shows a significant decline over the HR II footprint between Phase 1* and 2, which is centered just to the western edge. Significant increases occur in the northwest and a concentration of common scoter numbers into the area south of the HR I footprint. The diminution in the previously relative abundant eastern edge of the survey area, is also signalled by the significant and relatively substantial decreases in this area.

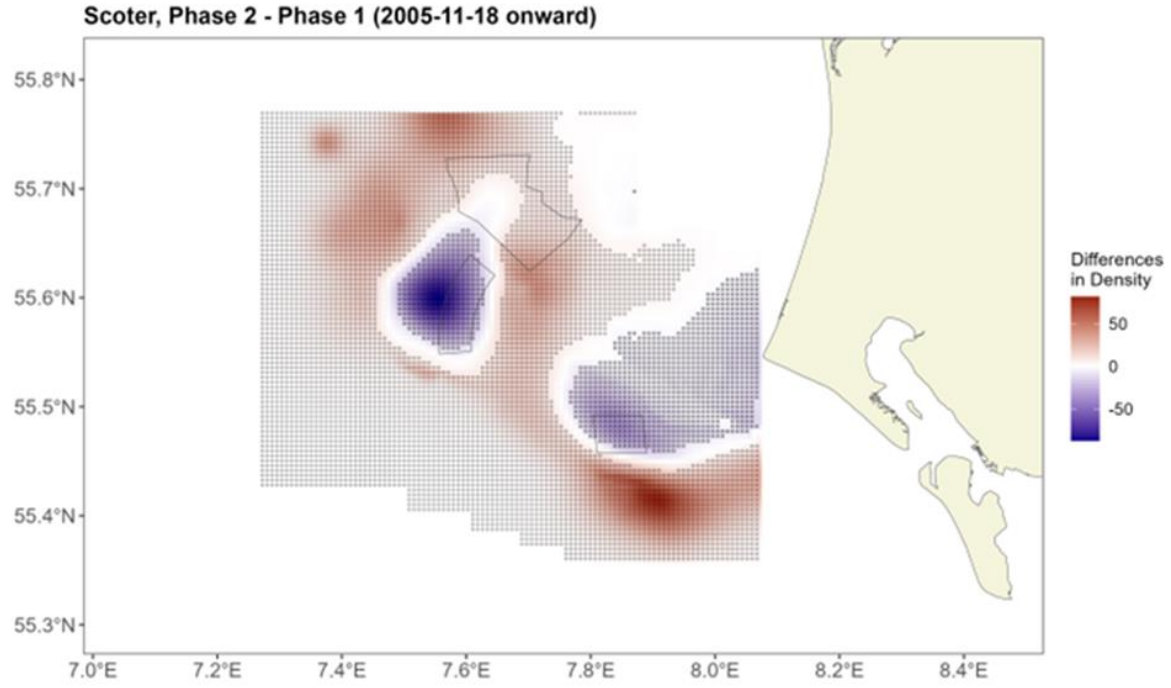

Figure 3-23. Map showing the estimated differences in the common scoter distribution between Phase 2 and Phase 1. Positive differences indicate more birds in Phase 2. A "+" sign in the bluish background colours indicates a significant positive difference and a "o" in reddish background colours a significant negative difference.*

The differences in common scoter density between Phases 2 and 3 show an overall decline in density across the majority of the study area (Figure 3-24). The main declines took place in the previously high-density area to the south of the HR I footprint and stretching north and west from there. There are some areas of significant increases in density, however the values are very small compared to the declines. This is different to the result of the data analysis for the 2023/2024 surveys and driven by the fact that all six of the 2024/2025 surveys observed very few common scoters.

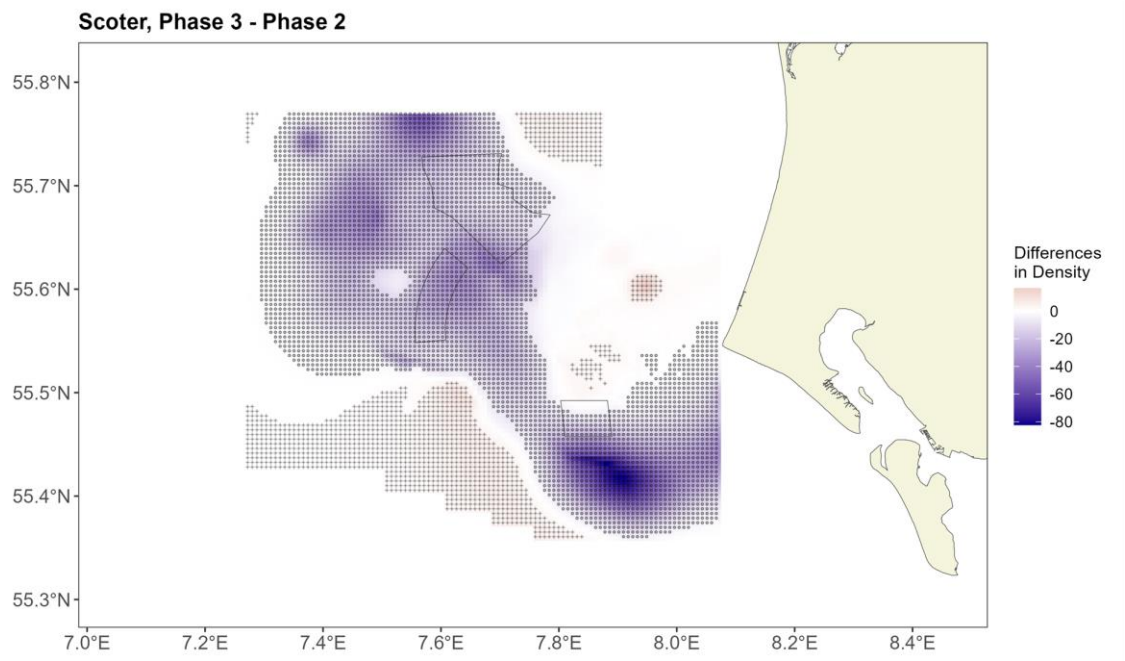

Figure 3-24. Map showing the estimated differences in the common scoter distribution between Phase 3 and Phase 2. Positive differences indicate more birds in Phase 3. A "+" sign in the reddish background colours indicates a significant positive difference and a "o" in bluish background colours a significant negative difference.

In Phase 3, compared with Phase 1*, common scoter show evidence of shifting away from the HR I and HR II footprints (Figure 3-25). The HR III area also showed significant declines in the southwestern parts of the wind farm and no detectable changes in the eastern and northern parts. The significant and notable decreases are in the areas within and surrounding these footprints, whereas the significant increases in density are lower in value and less concentrated across much of the rest of the study area.

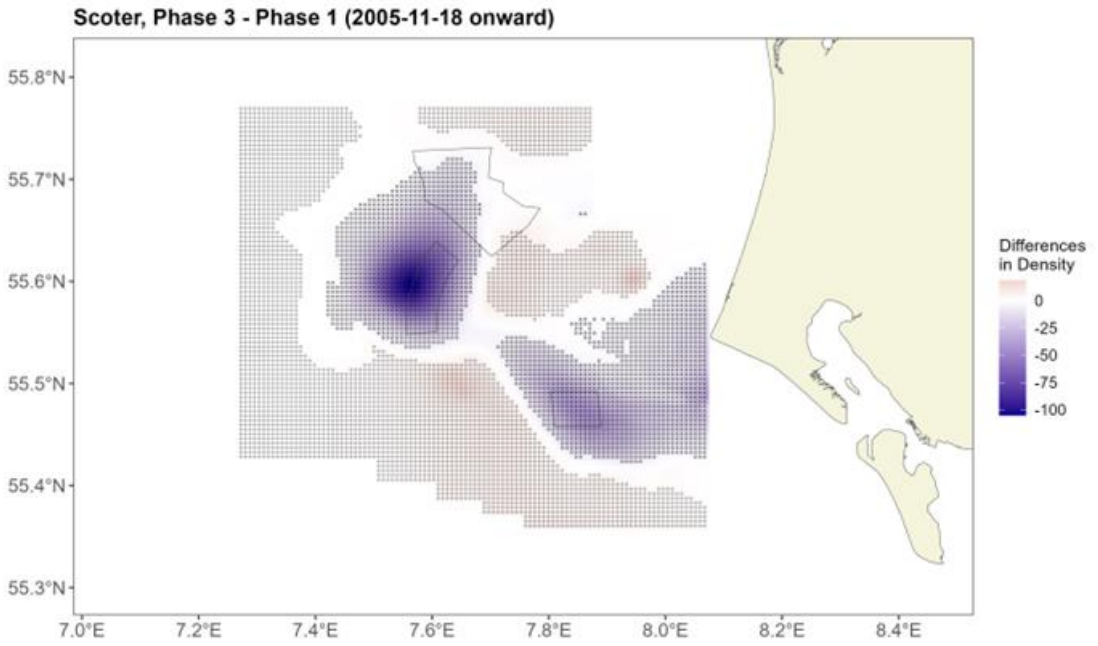

Figure 3-25. Map showing the estimated differences in the common scoter distribution between Phase 3 and Phase 1. Positive differences indicate more birds in Phase 3. A "+" sign in the reddish background colours indicates a significant positive difference and a "o" in bluish background colours a significant negative difference.*

In general, these difference maps show that the area in and around HR I supported few common scoters pre-construction and showed decreases in densities from Phase 1* to 2 and from Phase 1* to 3, while relatively stable densities between Phase 2 and 3. It is hard to know if the birds showed low levels of displacement response to this wind farm and have always been present at low density in the area, or if the construction has kept numbers low within and around HR I. The common scoter densities around HR II increased prior to construction (from Phase 0 to 1), reflecting the expansion of their distribution westward at this time, particularly increasing on and to the west of HR II. A marked decrease in common scoter densities within and around the HR II wind farm was seen between Phase 1* and 2, which was also observed between Phase 1* and 3. Between Phase 2 and 3 the decrease in densities was less pronounced.

From these results, it is possible to speculate that there was slightly less of an effect of the installation of HR III on bird density as compared to HR I and HR II. This less pronounced impact may be attributed to the wider spacing of the turbines in the footprint for this farm. To confirm these observations, additional data on common scoter responses from other offshore windfarms with different/larger spacings in different locations is needed for analysis.

3.5 Common scoter Horns Rev II (HR II) specific results

In addition to the above difference plots, we can look in more detail at the HR II footprint. Table 3-4 shows that 91% of the cells in the HR II are estimated to have significantly decreased density post-construction (Phases 1* to 2) and 100% of the cells in the HR II are estimated to have significantly decreased over the Phases 2-3 and 1*-3. No cells in the footprint were estimated to have increased in any of the Phases 1*, 2, or 3.

*Table 3-4. Table showing the percentage of cells in the Horns Rev II wind farm footprint that estimate an increase or a decrease in abundance and also the percentage of cells that showed significant increase or decrease (calculated from the bootstrap predictions) between phases. The * for Phase 1 indicates the shortened Phase 1.*

Horns Rev II	Pre-con. to 2-3 yrs post-con.	2-3yrs post-con. to 11-12 yrs post-con.	Pre-con. to 11-12 yrs post con.
	(Phase 1*-2)	**(Phase 2-3)**	**Phase (1*-3)**
% of cells in footprint increasing	0	0	0
% of those cells significantly increasing	0	0	0
% of cells in footprint decreasing	100	100	100
% of those cells significantly decreasing	91	100	100

3.5.1 HR II related changes across phases in all directions

We can also assess how the density changes between phases varied with distance from the footprint. To do this we collapse the spatial patterns down into one dimension using concentric rings of increasing distance from the footprint. Figure 3-26 illustrates a displacement effect (reduction in density) post-construction (Phase 2 – 1*) within approximately 3 km from the footprint (where the change rises to zero (indicating no difference)).

Comparing Phase 3 to Phase 1* however, we see compelling evidence for a displacement effect in the HR II footprint to approximately 6 km, after HR II and III are both constructed. This comment considers both the proximity of the difference in density estimates at each distance from the HR II footprint and the associated uncertainty of each estimate (indicated by the grey envelope in Figure 3-26).

The Phase 3-2 comparison shows a decline in density within a distance of more than 15 km. The largest decreases in density can be found within approximately 5 km of the footprint of HR II and the changes plateauing after that. This is in line with the overall decrease in abundance site-wide during Phase 3.

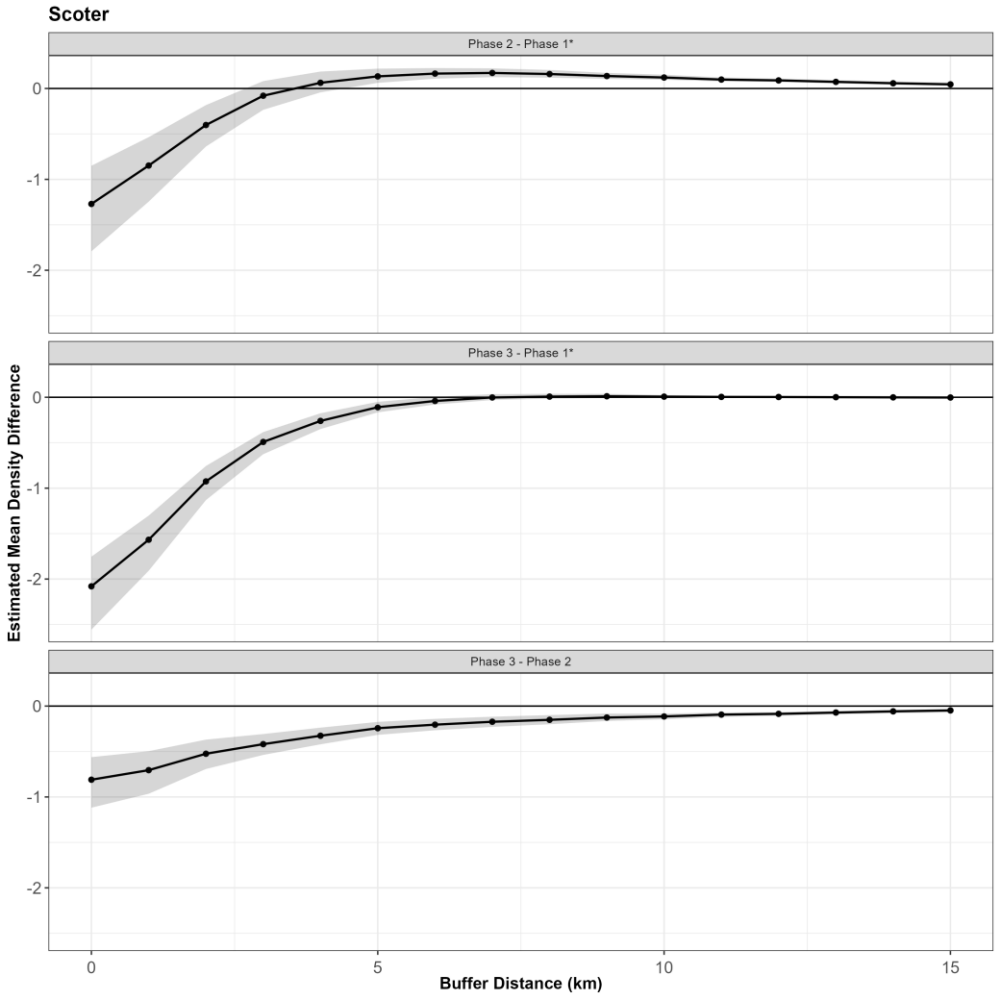

Figure 3-26. Graphs showing the change in the estimated mean common scoter density difference between Phases 2-1, 3-1* and 3-2, with increasing distance to the HR II footprint.*

3.5.2 HR II related changes across phases, direction specific

The results of the analyses presented in Figure 3.26 amalgamates all distance related displacement effects in all directions out from the HR II footprint however, differing environments and the construction of the other OWF within the Horns Rev area may also affect the displacements. For example, it is possible that significant decreases in density to the west of HR II may be cancelled out or masked by increases in density to the east and make displacement distances appear to be less significant than they might otherwise be. For this reason, we also narrow the directional scope to concentrate on assessing displacement effects in three specific orientations, Figure 3-27. The three sectors chosen are West (W), which is generally the offshore side of HR II, South-East (SE) which is more the onshore side including the area towards HR I and North-East (NE) which contains HR III, the first turbine of which is approximately 3 km from the edge of HR II.

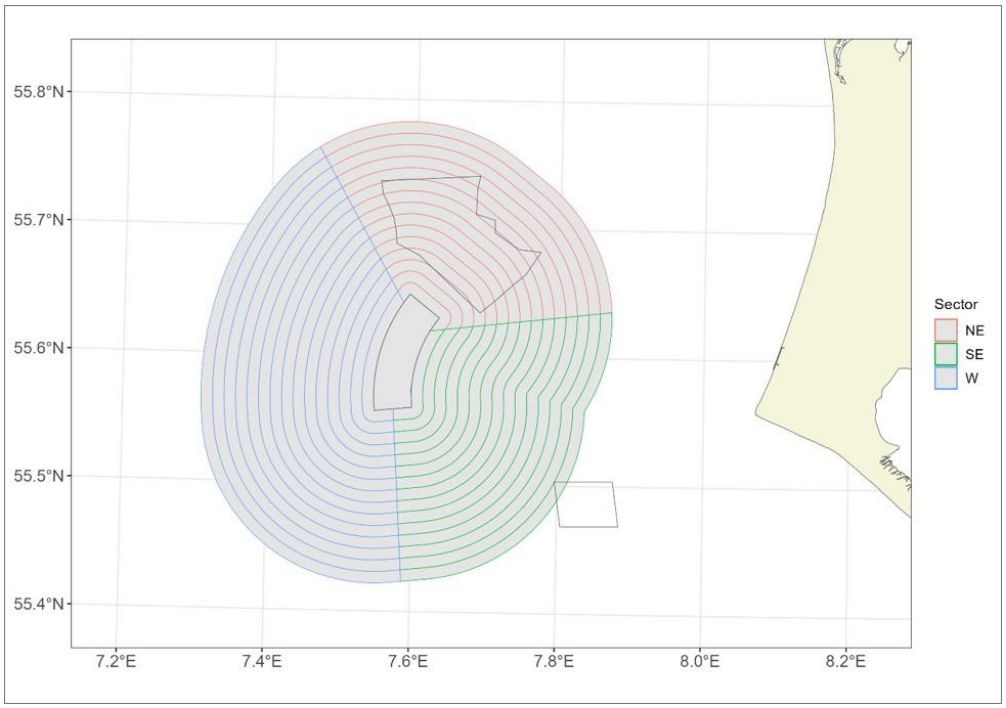

Figure 3-27. Map of the sectors used for the displacement analysis with 1 km buffers from the footprint of HR II, up to 15 km.

Figure 3-28 shows that NE of the HR II footprint, post construction of HR II, we see displacement of common scoter evident to 1 km of the footprint and an increase in density 3 - 15 km away in the area of the yet to be constructed HR III. The patterns are very similar in the SE sector, with displacement here also evident to 1 km of the footprint and an increase in density 3.5-11 km away. The western sector shows a stronger set of effects. Post construction shows a displacement effect to approximately 4.5 km and a longer-term displacement effect of up to 8 km.

Over the longer time span (pre to post construction of HR II and III; Phase 3-1*), there is evidence of a larger decrease within 6 km from the HR II footprint in the NE sector and 4 km away in the SE sector. The western sector shows the largest longer-term displacement effect of 8 km.

For Phase 3-2, despite the construction of HR III in the NE sector, all sectors show the general trend of decreasing density, regardless of distance from the footprint.

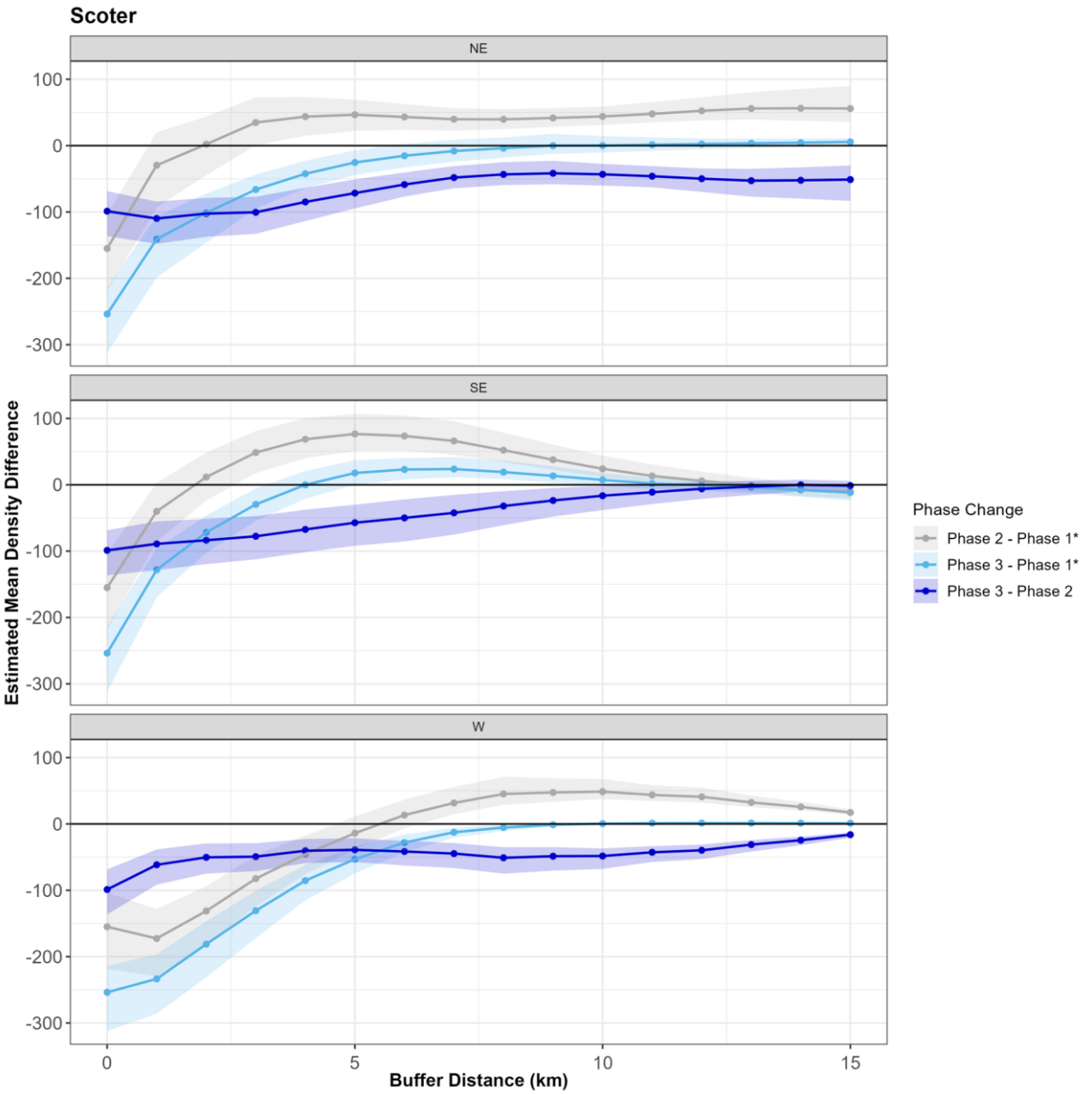

Figure 3-28. Graphs showing the differences in common scoter densities with distance to footprint by phase change and by sector. Any differences in underlying mean densities related to the HR II footprint would be indicated by a change near to the footprint with a decay thereafter.

3.6 Diver – Observations

Data from aerial surveys undertaken during the last two annual aerial survey campaigns showed that red-throated divers/black-throated divers were observed within the study area during all surveys conducted in the seasons 2023/2024 (Figure 3-29) and 2024/2025 (Figure 3-30). The majority of the birds were observed in the northern, western and southern parts of Horns Rev. The spatial distribution of observations was similar between the two seasons. During the six surveys conducted in 2023/2024 in total 366 birds were observed, while the corresponding number for the six surveys conducted in the 2024/2025 season was 519 birds (Table 8-3). For comparison, aerial survey coverage and diver distributions from the earlier surveys are provided in Appendix 8.1 (Figure 8-11-Figure 8-20 and Table 8-1).

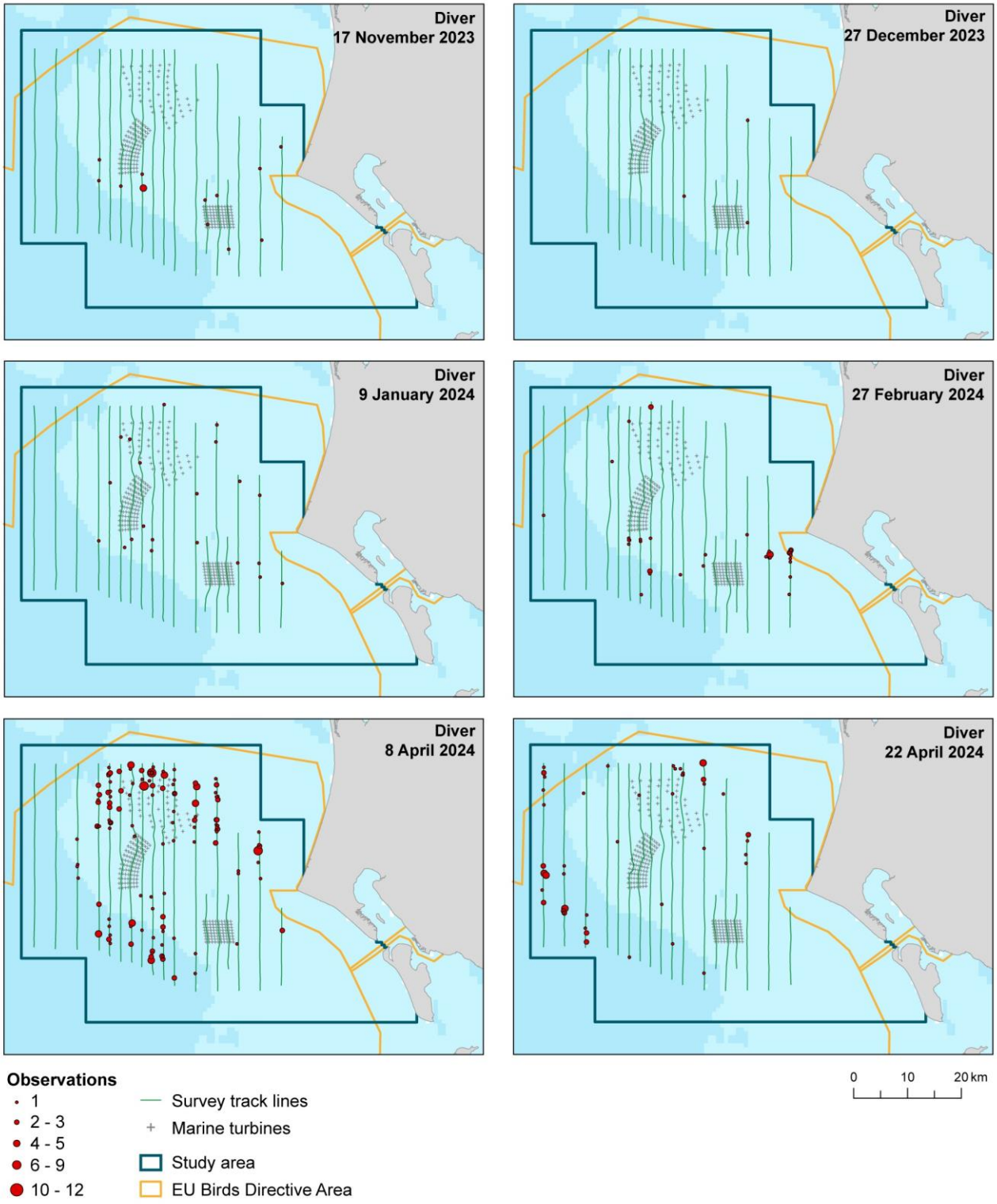

Figure 3-29. The number of diver species observed and their distribution within the survey area for six aerial surveys conducted in the winter season of 2023/2024.

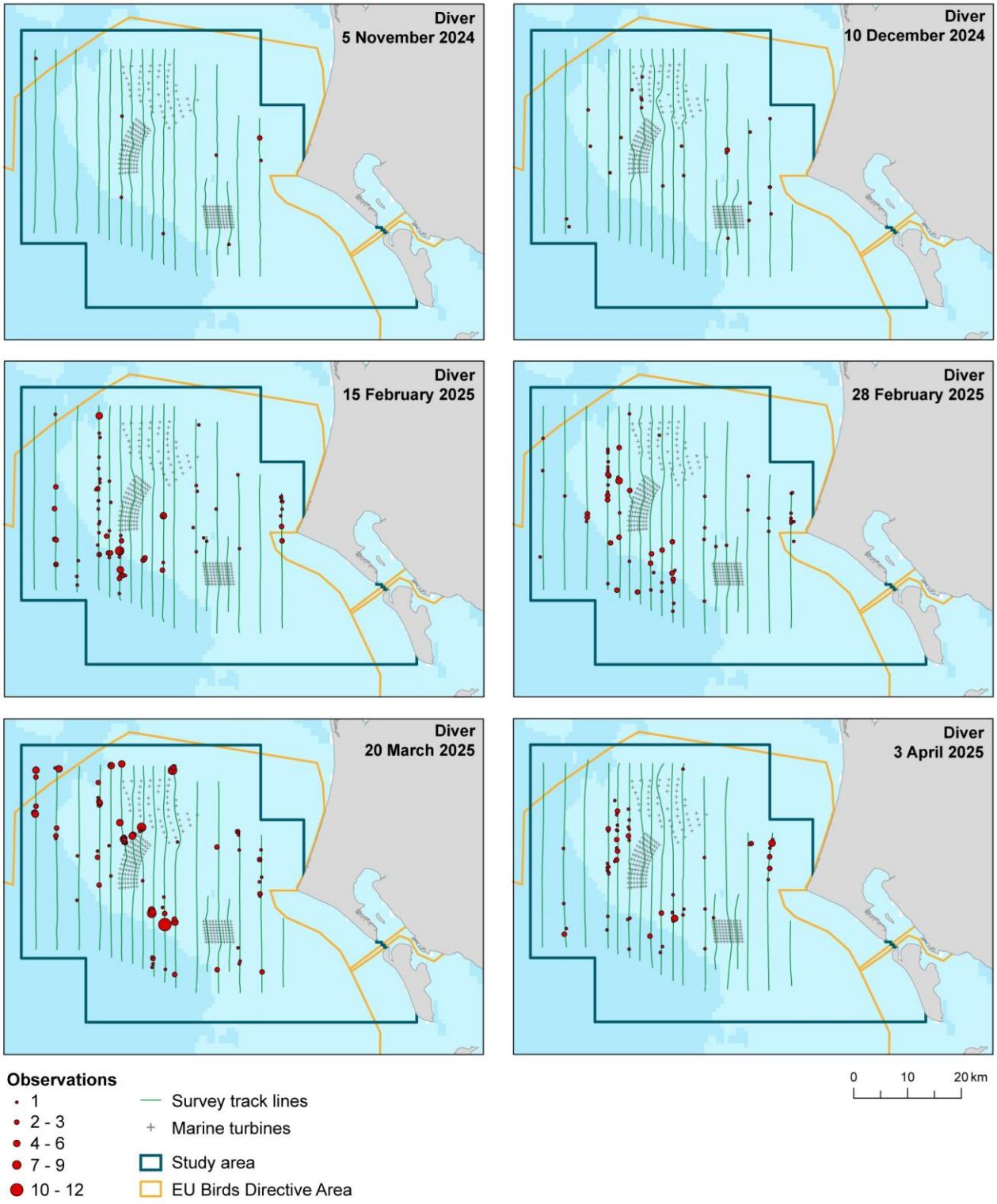

Figure 3-30. The number of diver species observed and their distribution within the survey area for six aerial surveys conducted in the winter season of 2024/2025.

3.7 Diver Distance Analysis

The average probability of sighting diver species was estimated to be 0.21 (CoV=0.02). This probability was estimated using a hazard rate detection function and observer and behaviour as covariates (Figure 3-31 and Figure 3-32). The results show, as might be expected, a higher detection probability of flying compared with sitting birds.

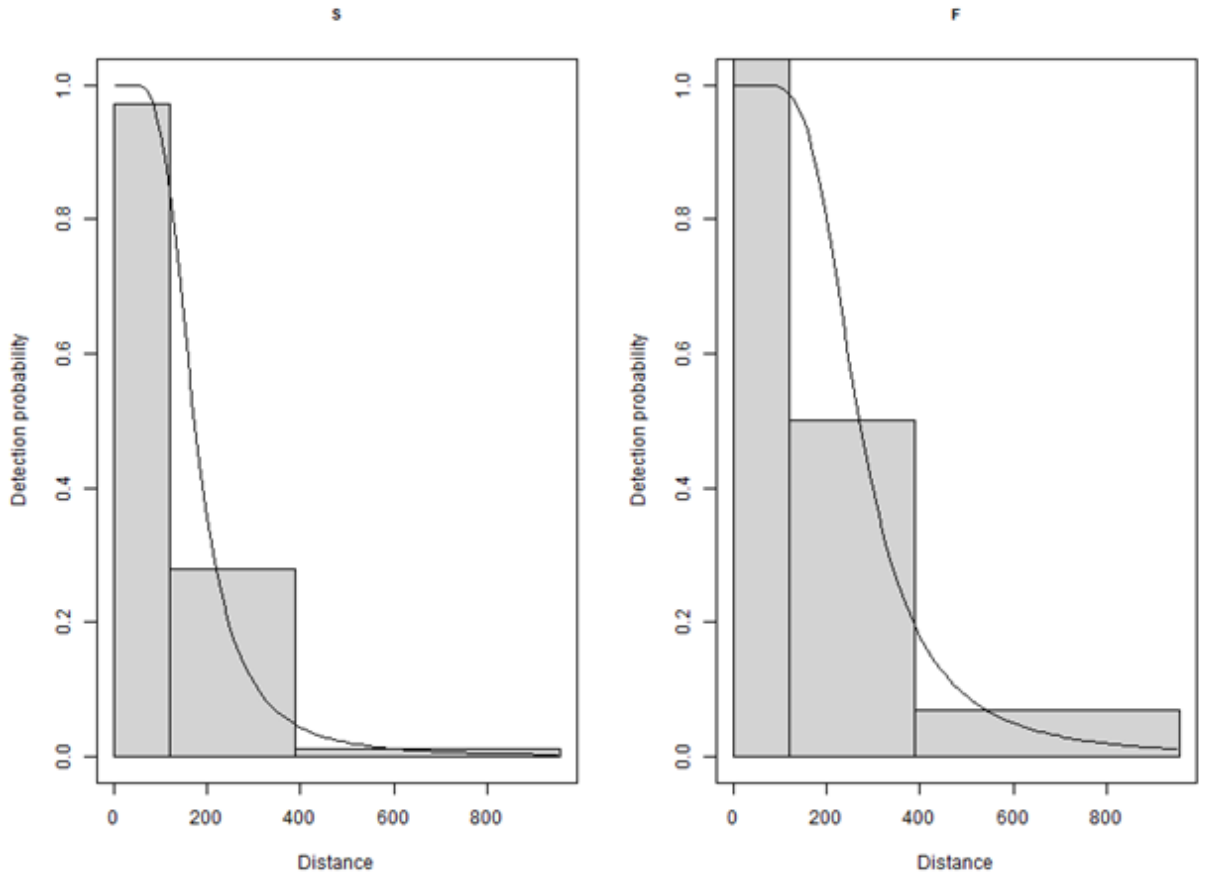

Figure 3-31. Graphs showing the estimated detection function. The histograms represent the distances of the observed sightings across behaviour types: sitting (S) and flying (F).

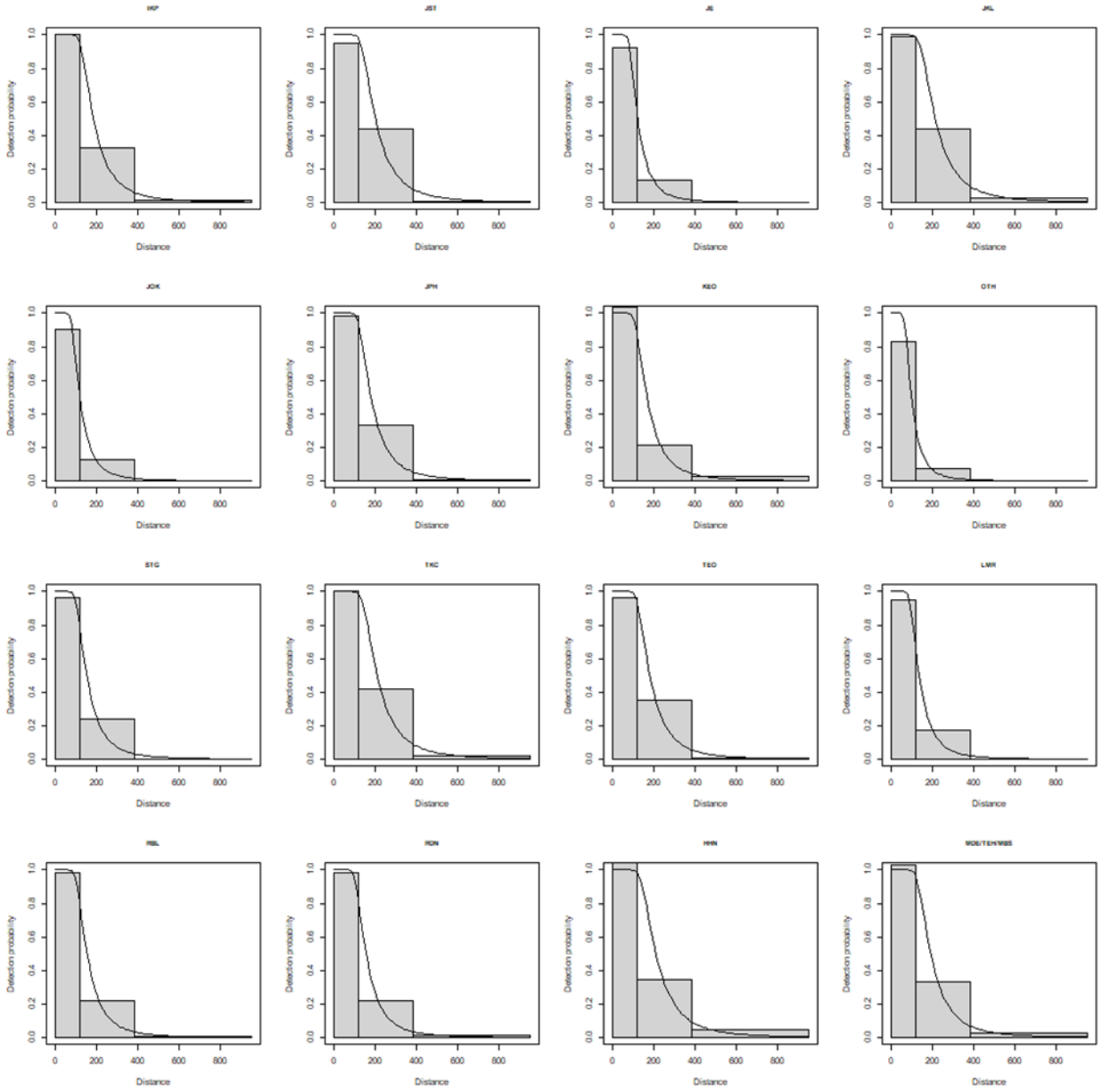

Figure 3-32. Graphs showing the estimated detection function. The histograms represent the distances of the observed sightings across different observers.

3.8 Diver Spatial Results by Survey

Figure 3-33 shows the distribution of the distance corrected counts for each of the 62 surveys.

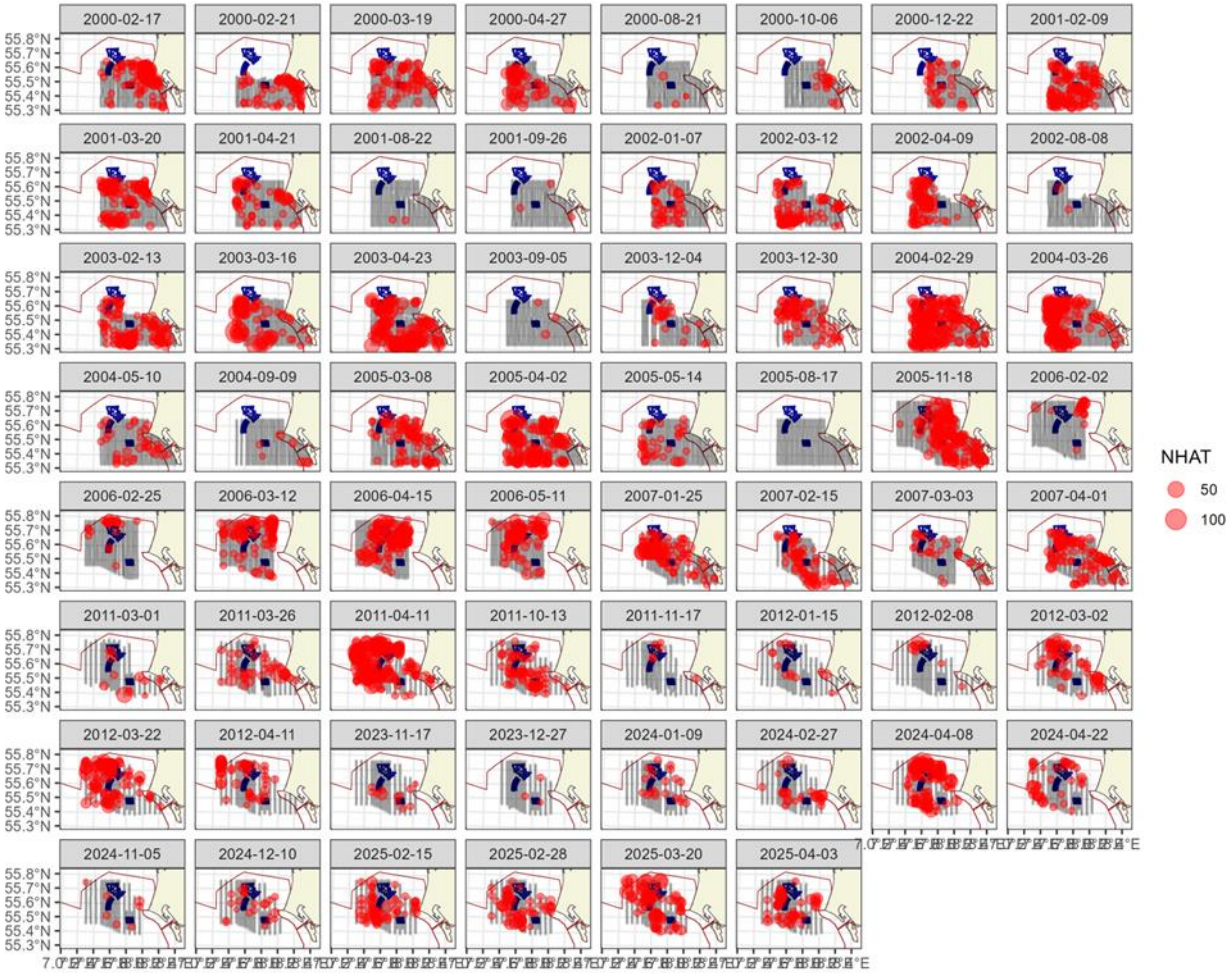

Figure 3-33. Distance-corrected counts for the diver species across the 62 surveys. The red circles indicate the distance-corrected counts along the transect lines. The pale grey dots are segments with a count of zero.

3.8.1 Model Selection

For seven of the 62 surveys, there were insufficient data to fit any model and further 12 models were selected as intercept only. This means a uniform distribution was estimated across the study area. However, for 40 of the 62 surveys, the models selected included a spatial term (of varying complexity) while the depth covariate was selected as a linear term for five of the surveys and non-linear for two surveys. In four of the linear term models, the spatial term was also included. The distance to coast covariate was selected as a non-linear term in five models, all of which also included a spatial term. The spatial surfaces selected ranged from two to ten parameters for the spatial term (Table 3-5). The estimated abundances and associated 95 percentile confidence intervals for each survey are given in Table 3-6 and Figure 3-34.

Table 3-5. Model selection results for diver species for each survey. The model column represents the terms in the model.

Name	Model	Distribution	Variable 1D	Variable 2D	Number of Parameters	Dispersion parameter	Tweedie parameter
2000-02-17	2D Only	Tweedie	NA	s(x,y, df=2)	3	20.5	1.32
2000-02-21	2D Only	quasipoisson	NA	s(x,y, df=8)	9	3.8	NA
2000-03-19	2D Only	Tweedie	NA	s(x,y, df=7)	8	13.5	1.28
2000-04-27	Intercept only	Tweedie	NA	NA	1	106.1	1.35
2000-08-21	No Model	NA	NA	NA	NA	NA	NA
2000-10-06	Intercept only	quasipoisson	NA	NA	1	10.4	NA
2000-12-22	Best 1D2D	quasipoisson	depth, df=1	NA	2	2.5	NA
2001-02-09	2D Only	quasipoisson	NA	s(x,y, df=8)	9	3.0	NA
2001-03-20	2D Only	quasipoisson	NA	s(x,y, df=6)	7	14.8	NA
2001-04-21	Best 1D2D	Tweedie	depth, df=1	s(x,y, df=2)	4	9.0	1.18
2001-08-22	No Model	NA	NA	NA	NA	NA	NA
2001-09-26	No Model	NA	NA	NA	NA	NA	NA
2002-01-07	Best 1D2D	Tweedie	s(distcoast, df=2)	s(x,y, df=2)	5	4.9	1.17
2002-03-12	2D Only	quasipoisson	NA	s(x,y, df=4)	5	7.3	NA
2002-04-09	2D Only	Tweedie	NA	s(x,y, df=3)	4	12.1	1.23
2002-08-08	No Model	NA	NA	NA	NA	NA	NA
2003-02-13	Intercept only	quasipoisson	NA	NA	1	8.2	NA
2003-03-16	2D Only	Tweedie	NA	s(x,y, df=7)	8	24.8	1.44
2003-04-23	2D Only	Tweedie	NA	s(x,y, df=7)	8	20.4	1.44
2003-09-05	No Model	NA	NA	NA	NA	NA	NA
2003-12-04	2D Only	Tweedie	NA	s(x,y, df=2)	3	12.3	1.28
2003-12-30	2D Only	quasipoisson	NA	s(x,y, df=2)	3	11.9	NA
2004-02-29	2D Only	Tweedie	NA	s(x,y, df=4)	5	12.5	1.23
2004-03-26	Best 1D2D	Tweedie	s(distcoast, df=3)	s(x,y, df=2)	6	30.7	1.25
2004-05-10	2D Only	Tweedie	NA	s(x,y, df=2)	3	8.9	1.12
2004-09-09	2D Only	quasipoisson	NA	s(x,y, df=2)	3	4.4	NA
2005-03-08	2D Only	Tweedie	NA	s(x,y, df=3)	4	10.9	1.18
2005-04-02	2D Only	Tweedie	NA	s(x,y, df=6)	7	14.6	1.30
2005-05-14	2D Only	Tweedie	NA	s(x,y, df=4)	5	4.6	1.12
2005-08-17	No Model	NA	NA	NA	NA	NA	NA
2005-11-18	Best 1D2D	Tweedie	s(distcoast, df=2)	s(x,y, df=2)	5	10.3	1.21
2006-02-02	Depth	quasipoisson	s(depth, df=2)	NA	3	7.0	NA
2006-02-25	2D Only	quasipoisson	NA	s(x,y, df=4)	5	4.3	NA
2006-03-12	2D Only	Tweedie	NA	s(x,y, df=3)	4	10.5	1.16
2006-04-15	2D Only	Tweedie	NA	s(x,y, df=8)	9	4.9	1.21
2006-05-11	2D Only	Tweedie	NA	s(x,y, df=2)	3	21.5	1.24
2007-01-25	Best 1D2D	Tweedie	s(distcoast, df=3)	s(x,y, df=3)	7	8.2	1.13

Name	Model	Distribution	Variable 1D	Variable 2D	Number of Parameters	Dispersion parameter	Tweedie parameter
2007-02-15	Best 1D2D	Tweedie	s(distcoast, df=2)	s(x,y, df=2)	5	6.1	1.17
2007-03-03	Best 1D2D	quasipoisson	depth, df=1	s(x,y, df=4)	6	1.8	NA
2007-04-01	2D Only	Tweedie	NA	s(x,y, df=4)	5	9.0	1.21
2011-03-01	Intercept only	Tweedie	NA	NA	1	89.8	1.38
2011-03-26	2D Only	Tweedie	NA	s(x,y, df=2)	3	14.4	1.22
2011-04-11	2D Only	Tweedie	NA	s(x,y, df=6)	7	20.5	1.29
2011-10-13	Best 1D2D	quasipoisson	depth, df=1	s(x,y, df=8)	10	5.6	NA
2011-11-17	Intercept only	quasipoisson	NA	NA	1	4.6	NA
2012-01-15	Best 1D2D	quasipoisson	depth, df=1	s(x,y, df=7)	9	1.0	NA
2012-02-08	Intercept only	Tweedie	NA	NA	1	99.0	1.38
2012-03-02	2D Only	Tweedie	NA	s(x,y, df=2)	3	12.4	1.19
2012-03-22	2D Only	Tweedie	NA	s(x,y, df=8)	9	16.7	1.27
2012-04-11	Intercept only	Tweedie	NA	NA	1	13.9	1.18
2023-11-17	2D Only	quasipoisson	NA	s(x,y, df=2)	3	2.4	NA
2023-12-27	No Model	NA	NA	NA	NA	NA	NA
2024-01-09	Intercept only	quasipoisson	NA	NA	1	2.7	NA
2024-02-27	2D Only	Tweedie	NA	s(x,y, df=2)	3	15.8	1.25
2024-04-08	2D Only	Tweedie	NA	s(x,y, df=10)	11	7.3	1.27
2024-04-22	2D Only	Tweedie	NA	s(x,y, df=2)	3	8.7	1.13
2024-11-05	Intercept only	quasipoisson	NA	NA	1	5.4	NA
2024-12-10	Intercept only	quasipoisson	NA	NA	1	4.6	NA
2025-02-15	Intercept only	Tweedie	NA	NA	1	18.8	1.28
2025-02-28	2D Only	Tweedie	NA	s(x,y, df=2)	3	9.2	1.16
2025-03-20	Depth	Tweedie	s(depth, df=2)	NA	3	23.8	1.38
2025-04-03	Intercept only	quasipoisson	NA	NA	1	9.1	NA

3.8.2 Abundance estimates by survey

The estimated abundances, densities and associated 95 percentile confidence intervals for each month are given in Table 3-6, and illustrated in Figure 3-32 for all surveys combined and in Figure 3-33 combined for each of the phases.

Table 3-6. Estimated abundance and density of diver species for each survey. The 95% CI are percentile-based confidence intervals.

Month	Area (Km^2)	Estimated Count	95% CI Count	Estimated Density	95% CI Density
2000-02-17	2019	920	(555, 1569)	0.5	(0.3, 0.8)
2000-02-21	2019	109	(41, 348)	0.1	(0, 0.2)
2000-03-19	2019	462	(196, 1195)	0.2	(0.1, 0.6)

Month	Area (Km^2)	Estimated Count	95% CI Count	Estimated Density	95% CI Density
2000-04-27	2019	565	(253, 1338)	0.3	(0.1, 0.7)
2000-08-21	2019	17	(15, 18)	0.0	(0, 0)
2000-10-06	2019	72	(32, 148)	0.0	(0, 0.1)
2000-12-22	2019	114	(63, 237)	0.1	(0, 0.1)
2001-02-09	2019	589	(354, 1098)	0.3	(0.2, 0.5)
2001-03-20	2019	620	(344, 1205)	0.3	(0.2, 0.6)
2001-04-21	2019	314	(151, 690)	0.2	(0.1, 0.3)
2001-08-22	2019	6	(5, 8)	0.0	(0, 0)
2001-09-26	2019	10	(9, 11)	0.0	(0, 0)
2002-01-07	2019	240	(118, 531)	0.1	(0.1, 0.3)
2002-03-12	2019	263	(150, 526)	0.1	(0.1, 0.3)
2002-04-09	2019	646	(379, 1139)	0.3	(0.2, 0.6)
2002-08-08	2019	10	(9, 10)	0.0	(0, 0)
2003-02-13	2019	569	(375, 818)	0.3	(0.2, 0.4)
2003-03-16	2019	913	(466, 1887)	0.5	(0.2, 0.9)
2003-04-23	2019	1130	(591, 2333)	0.6	(0.3, 1.2)
2003-09-05	2019	12	(11, 13)	0.0	(0, 0)
2003-12-04	2019	211	(112, 385)	0.1	(0.1, 0.2)
2003-12-30	2019	534	(353, 807)	0.3	(0.2, 0.4)
2004-02-29	2019	1392	(991, 2052)	0.7	(0.5, 1)
2004-03-26	2019	1485	(939, 3112)	0.7	(0.5, 1.5)
2004-05-10	2019	130	(73, 237)	0.1	(0, 0.1)
2004-09-09	2019	16	(5, 62)	0.0	(0, 0)
2005-03-08	2019	400	(207, 868)	0.2	(0.1, 0.4)
2005-04-02	2019	1663	(705, 4131)	0.8	(0.3, 2)
2005-05-14	2019	150	(81, 294)	0.1	(0, 0.1)
2005-08-17	2019	0	(0, 0)	0.0	(0, 0)
2005-11-18	2019	1145	(735, 1755)	0.6	(0.4, 0.9)
2006-02-02	2019	114	(33, 498)	0.1	(0, 0.2)
2006-02-25	2019	115	(43, 403)	0.1	(0, 0.2)
2006-03-12	2019	508	(287, 901)	0.3	(0.1, 0.4)
2006-04-15	2019	996	(600, 1696)	0.5	(0.3, 0.8)
2006-05-11	2019	952	(568, 1737)	0.5	(0.3, 0.9)
2007-01-25	2019	878	(599, 1352)	0.4	(0.3, 0.7)
2007-02-15	2019	403	(270, 647)	0.2	(0.1, 0.3)
2007-03-03	2019	91	(43, 219)	0.0	(0, 0.1)
2007-04-01	2019	621	(416, 1003)	0.3	(0.2, 0.5)
2011-03-01	2019	151	(71, 324)	0.1	(0, 0.2)
2011-03-26	2019	414	(246, 739)	0.2	(0.1, 0.4)

Month	Area (Km^2)	Estimated Count	95% CI Count	Estimated Density	95% CI Density
2011-04-11	2019	3197	(1804, 5716)	1.6	(0.9, 2.8)
2011-10-13	2019	703	(367, 1515)	0.3	(0.2, 0.8)
2011-11-17	2019	31	(13, 88)	0.0	(0, 0)
2012-01-15	2019	79	(30, 253)	0.0	(0, 0.1)
2012-02-08	2019	151	(54, 451)	0.1	(0, 0.2)
2012-03-02	2019	394	(242, 616)	0.2	(0.1, 0.3)
2012-03-22	2019	1398	(605, 3631)	0.7	(0.3, 1.8)
2012-04-11	2019	428	(179, 1084)	0.2	(0.1, 0.5)
2023-11-17	2019	74	(27, 240)	0.0	(0, 0.1)
2023-12-27	2019	12	(10, 14)	0.0	(0, 0)
2024-01-09	2019	118	(79, 175)	0.1	(0, 0.1)
2024-02-27	2019	245	(110, 587)	0.1	(0.1, 0.3)
2024-04-08	2019	1452	(836, 2699)	0.7	(0.4, 1.3)
2024-04-22	2019	377	(234, 625)	0.2	(0.1, 0.3)
2024-11-05	2019	42	(16, 99)	0.0	(0, 0)
2024-12-10	2019	112	(68, 187)	0.1	(0, 0.1)
2025-02-15	2019	532	(304, 1017)	0.3	(0.2, 0.5)
2025-02-28	2019	488	(294, 827)	0.2	(0.1, 0.4)
2025-03-20	2019	1055	(646, 1755)	0.5	(0.3, 0.9)
2025-04-03	2019	430	(260, 711)	0.2	(0.1, 0.4)

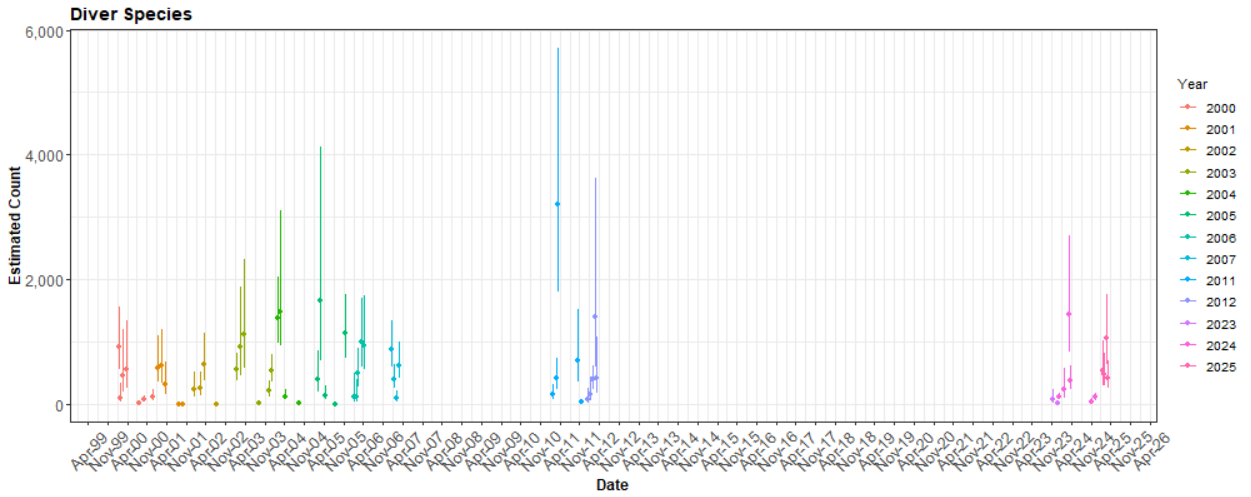

Figure 3-34. The estimated count of diver species for each survey. The 95% CI are percentile-based confidence intervals were derived from a parametric bootstrap with 500 replicates. As the analysis area had the same extension between surveys, the estimated abundances are comparable.

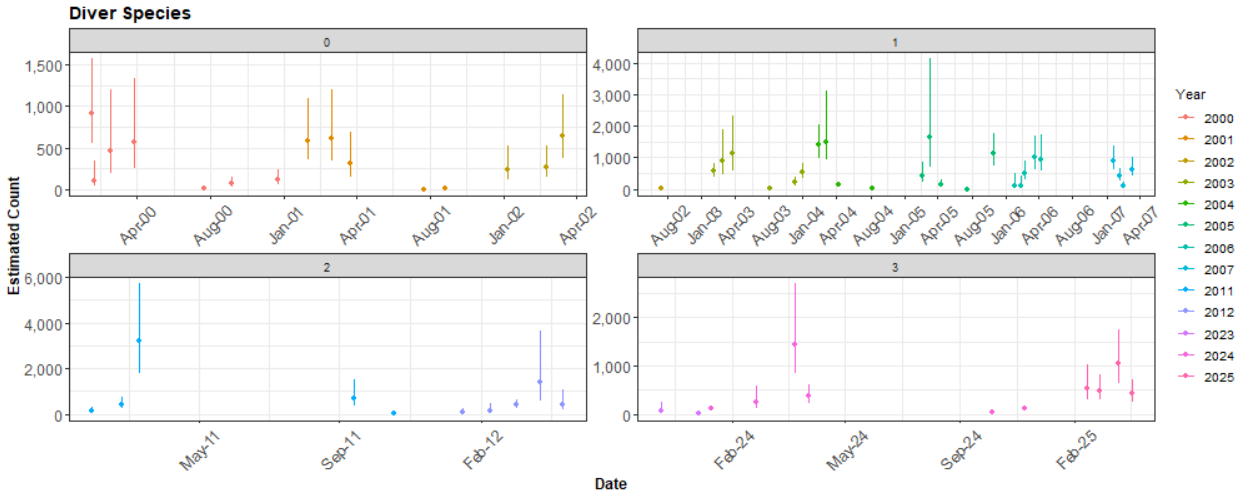

Figure 3-35. The estimated count of diver species for each survey by phase. The 95% CI are percentile-based confidence intervals were derived from a parametric bootstrap with 500 replicates. To show more detail the y-axis is different for each phase.

3.8.3 Density Distributions

Figure 3-36 to Figure 3-39 show the estimated counts of diver species in each 500 m^2 grid cells for each survey in the four phases. Generally, the estimated abundances fitted well to the raw data and there were no notable misalignments. In areas where the estimated counts were systematically higher, the abundances were also relatively high and there were no areas with large, estimated abundances unsupported by the data.

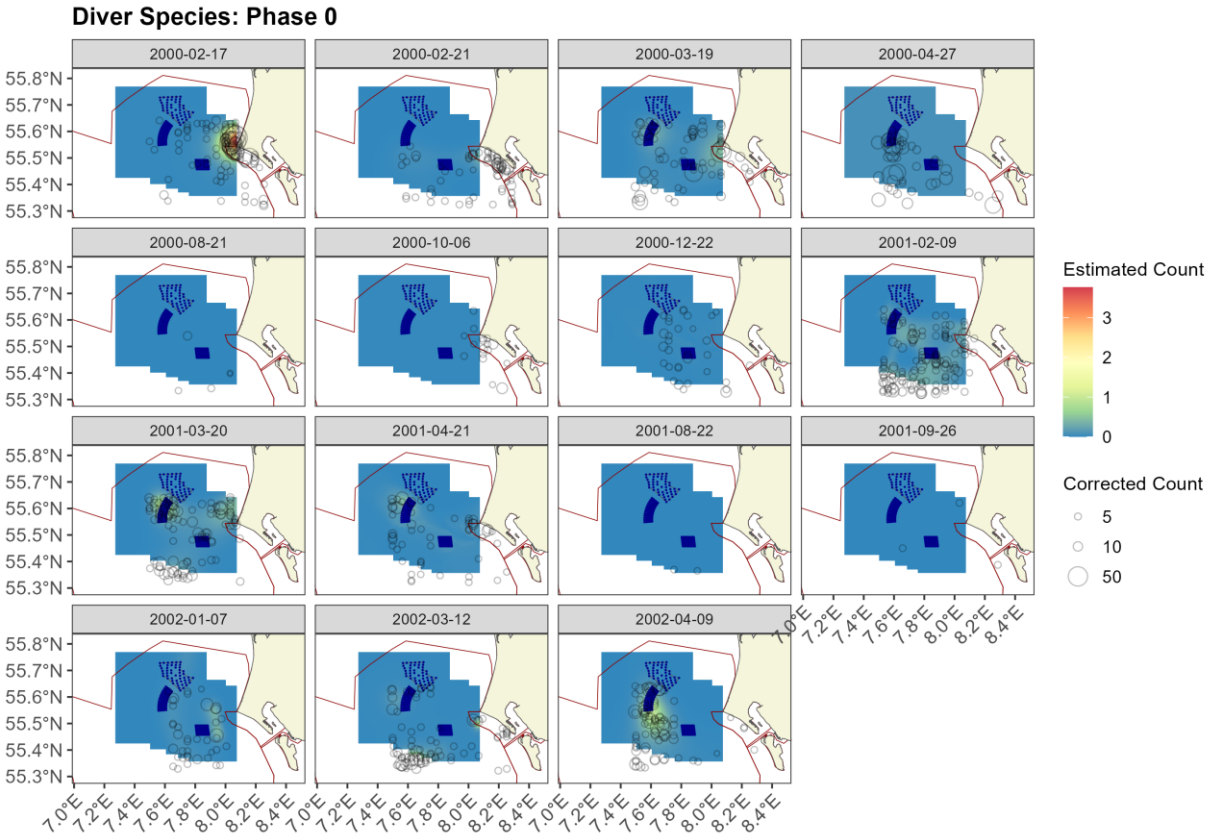

Figure 3-36. Distribution maps showing the estimated diver abundance across the study site for each of the surveys in Phase 0. The estimated counts are per 500 m x 500 m grid cell. The open circles show the distance corrected counts. The coloured graphics represent the predicted counts in each location.

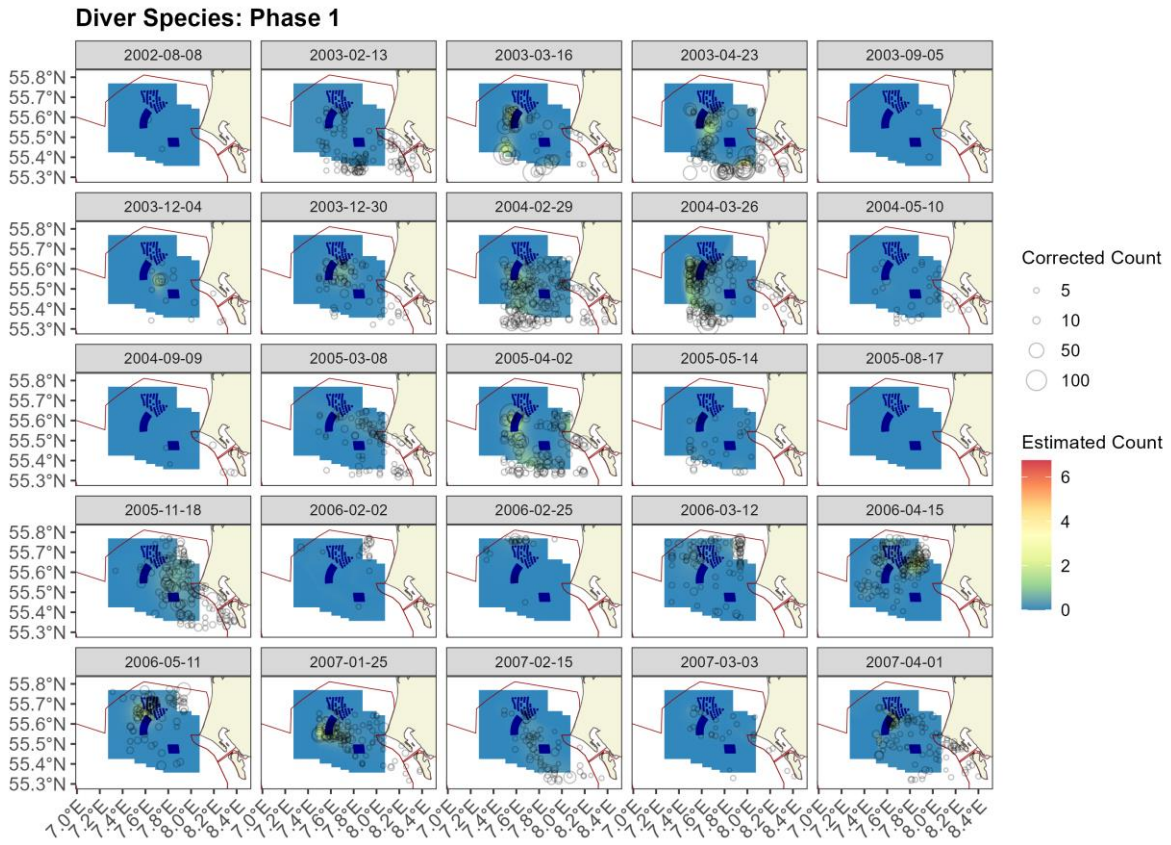

Figure 3-37. Distribution maps showing the estimated diver abundance across the study site for each of the surveys in Phase 1. The estimated counts are per 500 m x 500 m grid cell. The open circles show the distance corrected counts. The coloured graphics represent the predicted counts in each location.

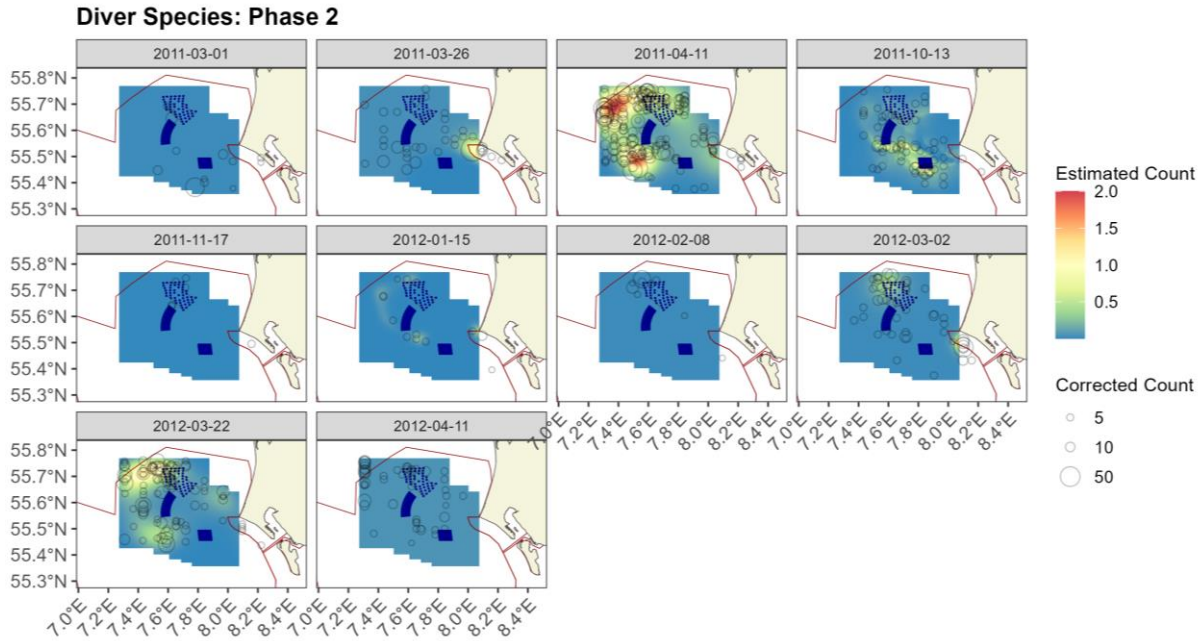

Figure 3-38. Distribution maps showing the estimated diver abundance across the study site for each of the surveys in Phase 2. The estimated counts are per 500 m x 500 m grid cell. The open circles show the distance corrected counts. The coloured graphics represent the predicted counts in each location.

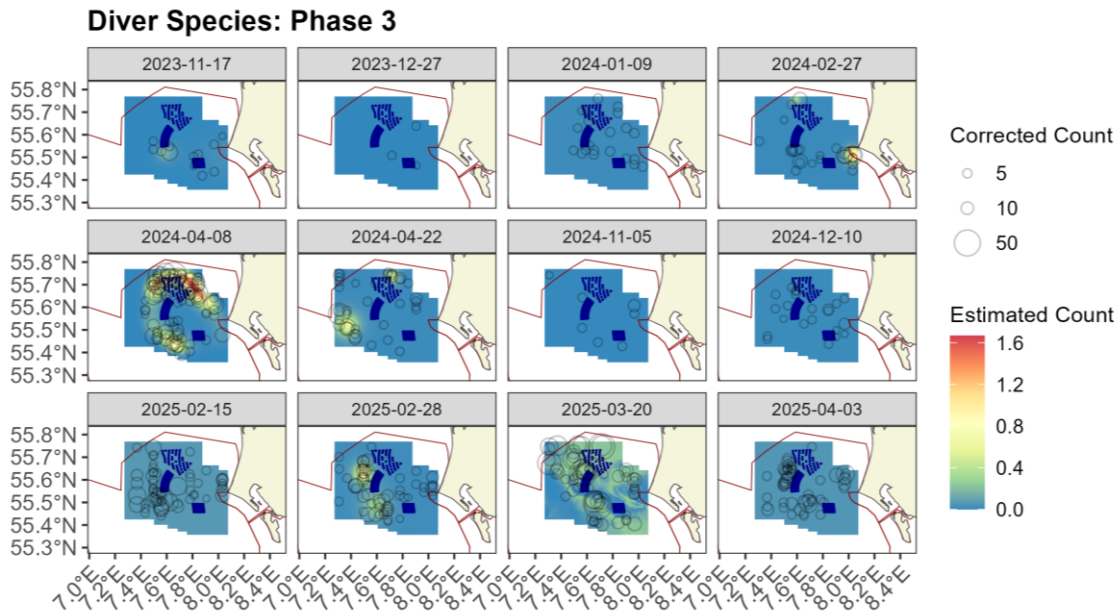

Figure 3-39. Distribution maps showing the estimated diver abundance across the study site for each of the surveys in Phase 3. The estimated counts are per 500 m x 500 m grid cell. The open circles show the distance corrected counts. The coloured graphics represent the predicted counts in each location.

3.8.4 Uncertainty in spatial predictions

Broadly, the highest coefficient of variation (CoV) scores were associated with the `almost zero' predictions and it is known that the CoV metric is highly sensitive to any uncertainty for very small predictions. There was no material overlap between high values of the CoV metric and the transect lines/locations with non-zero counts and therefore results in no concerns in this case (Figure 3-40).

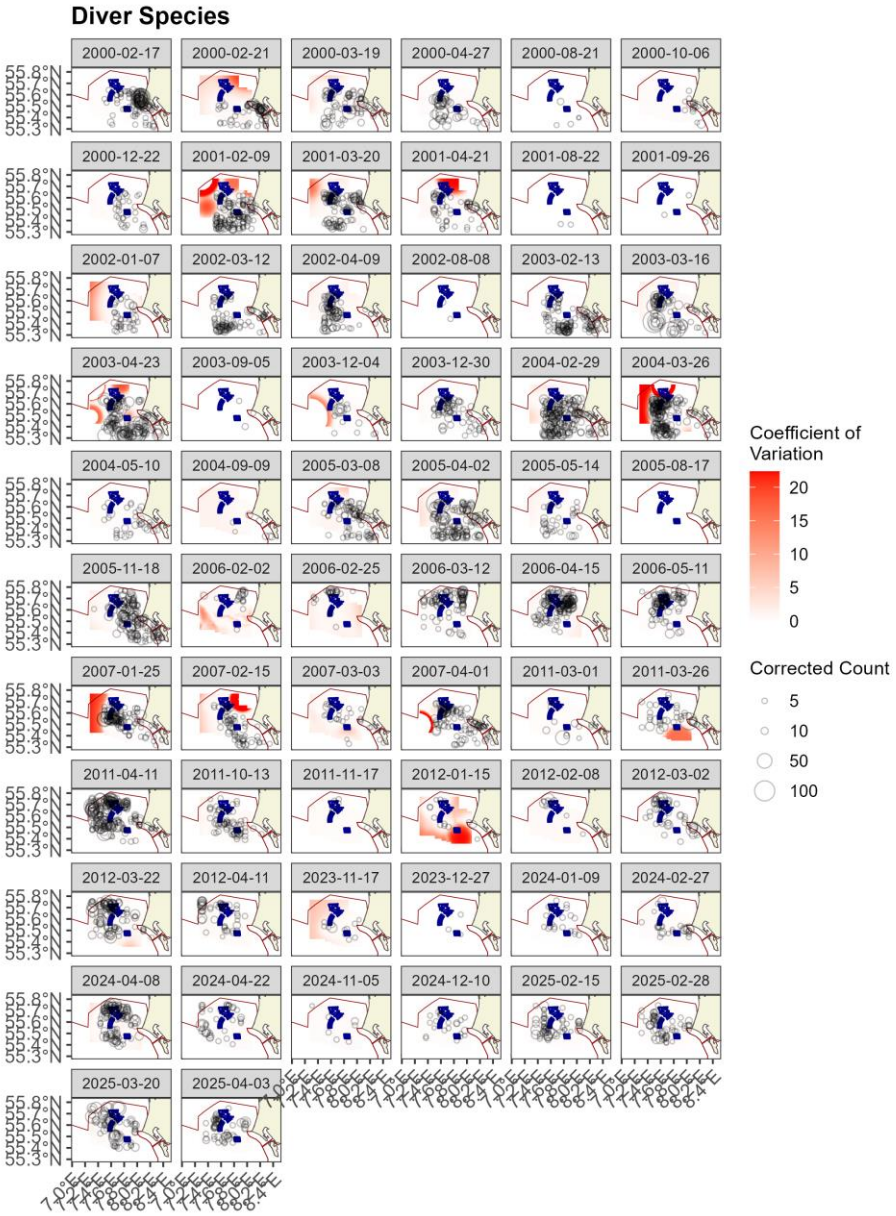

Figure 3-40. Distribution maps showing the coefficient of variation across the study area for each of the surveys of divers. The open circles show the distance corrected counts. The presence of dark red CV scores in areas with virtually zero predictions are an artifact of the very small prediction rather than of any notable concern.

In the case, when the very small, predicted values were excluded (Figure 3-41) there were a few remaining areas of moderately large CoV's. These tended to be in areas where there was little survey effort and so any wide confidence intervals resulting from this are not unwarranted.

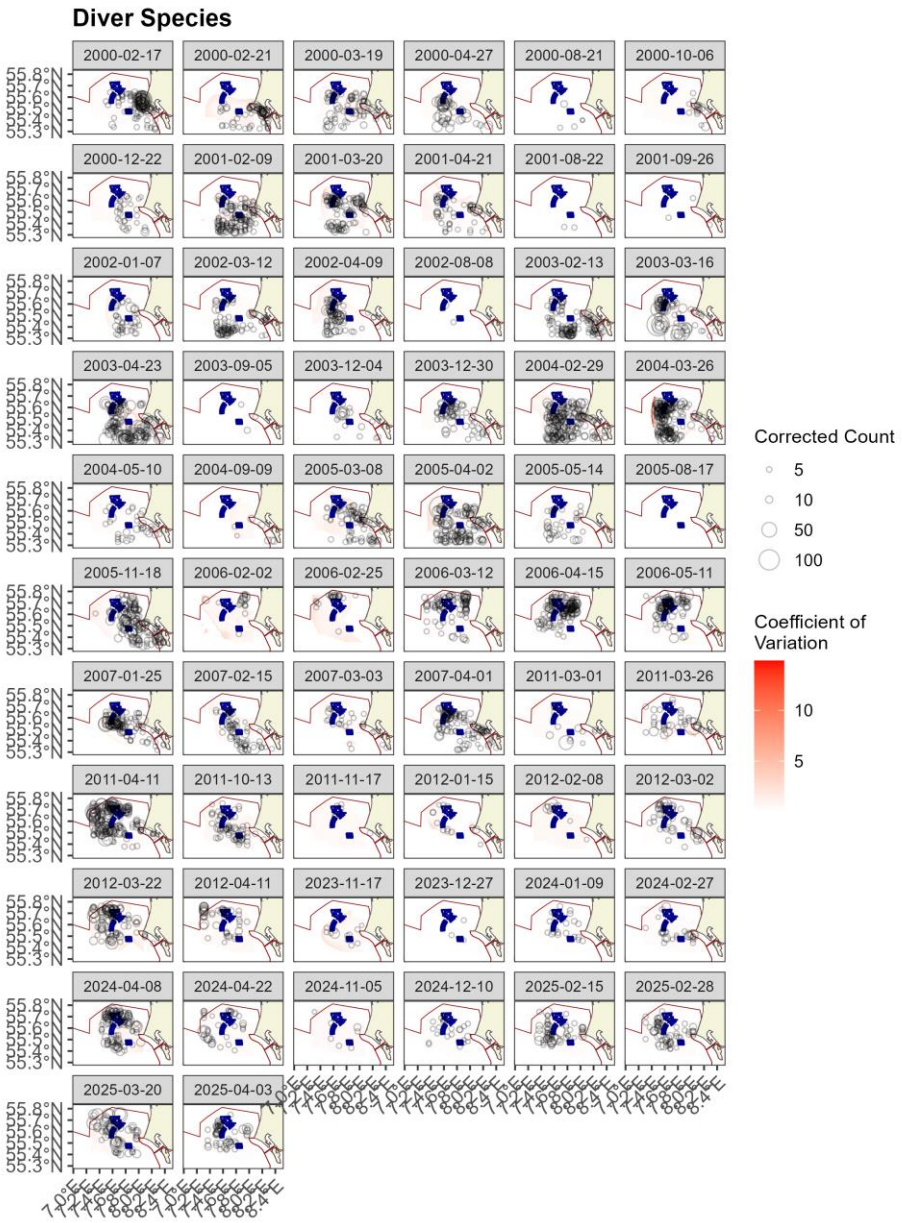

Figure 3-41. Distribution maps showing the coefficient of variation across the study area for each of the surveys of divers after the removal of very small, predicted values. The open circles show the distance corrected counts.

3.9 Diver Spatial Results by Phase

3.9.1 Phase-specific spatial patterns

The distribution of diver species in Phase 0 (Figure 3-42) is concentrated to the east of the study area ca. 4-5 km off Blåvandshuk with a lower density in the area of the future HR II. In Phase 1, the distribution is fairly widespread, but the concentration shifts from the east to settle around the not-yet constructed HR II.

After the construction of HR II there is a general decline in numbers particularly in the area around the now constructed HR II, and the birds are more broadly distributed in the western areas (Phase II, Figure 3-42). In Phase 3, there is a general decrease in the west and south areas with numbers mostly in the north around the constructed HR III farm.

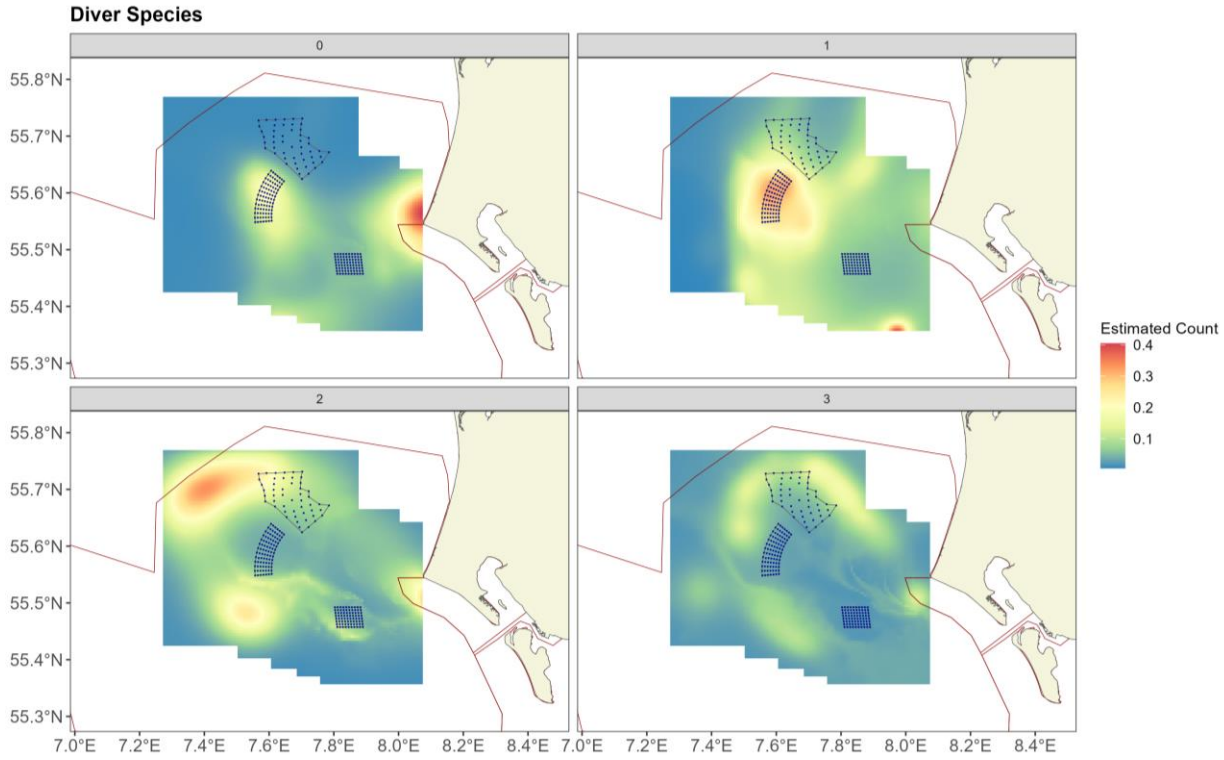

Figure 3-42. Distribution maps showing the estimated diver species abundance across the study site for each of the phases 0 to 3. The estimated counts are per 500 m x 500 m grid cell. The coloured graphics represent the predicted counts in each location.

Divers do not show the expansion of range that common scoters did in the early 2000's but owing to the changing survey coverage for this widespread species and in keeping with the common scoter analysis and the 2014 report (Petersen et al. 2014) we chose to use data from November 2005 for a more detailed assessment of HR II (Phase 1*). Figure 3-43 shows the mean diver density distribution in early Phase 1 surveys concentrate in the yet to be constructed HR II footprint but the late Phase 1 surveys (post November 2005) diver concentrations are to the north of HR II and into the yet to be constructed HR III footprint.

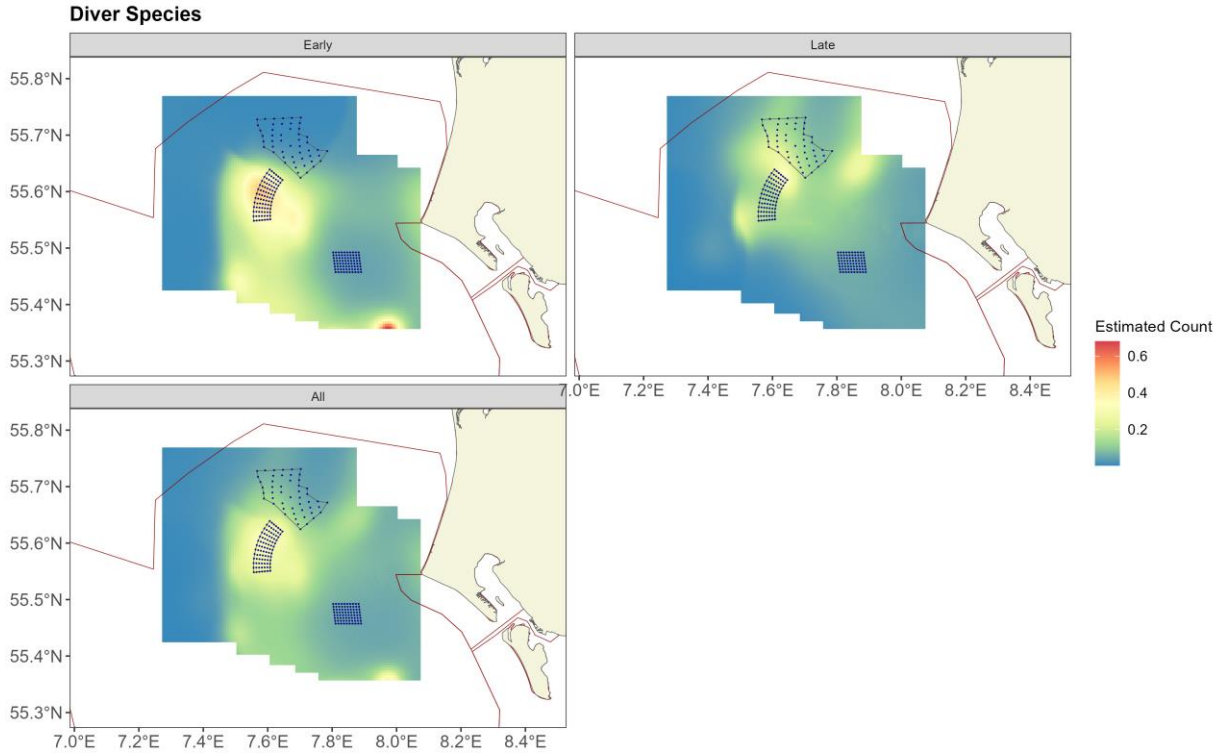

Figure 3-43. Distribution maps showing the estimated diver abundance across the study site within Phase 1 for "Early" surveys (pre November 2005), "Late" surveys (post November 2005) and for all combined. The estimated counts are per 500 m x 500 m grid cell. The coloured graphics represent the predicted counts in each location.

3.9.2 Overall Persistence

In addition to inspecting the mean distribution of divers in each phase, which may be dominated by a few surveys with large numbers of birds, we can assess the persistence of birds in each grid cell overall and by phase. The persistence analysis describes, at a fine geographical scale, areas of higher or lower usage by the species, evaluated over many surveys.

Across the 62 surveys (spanning 25 years) there was moderate to low persistence across much of the predicted area (Figure 3-44). The highest persistence (~ 50%) occurred in the central parts of the study area, with some reduction in this metric towards the western edge of the area of interest.

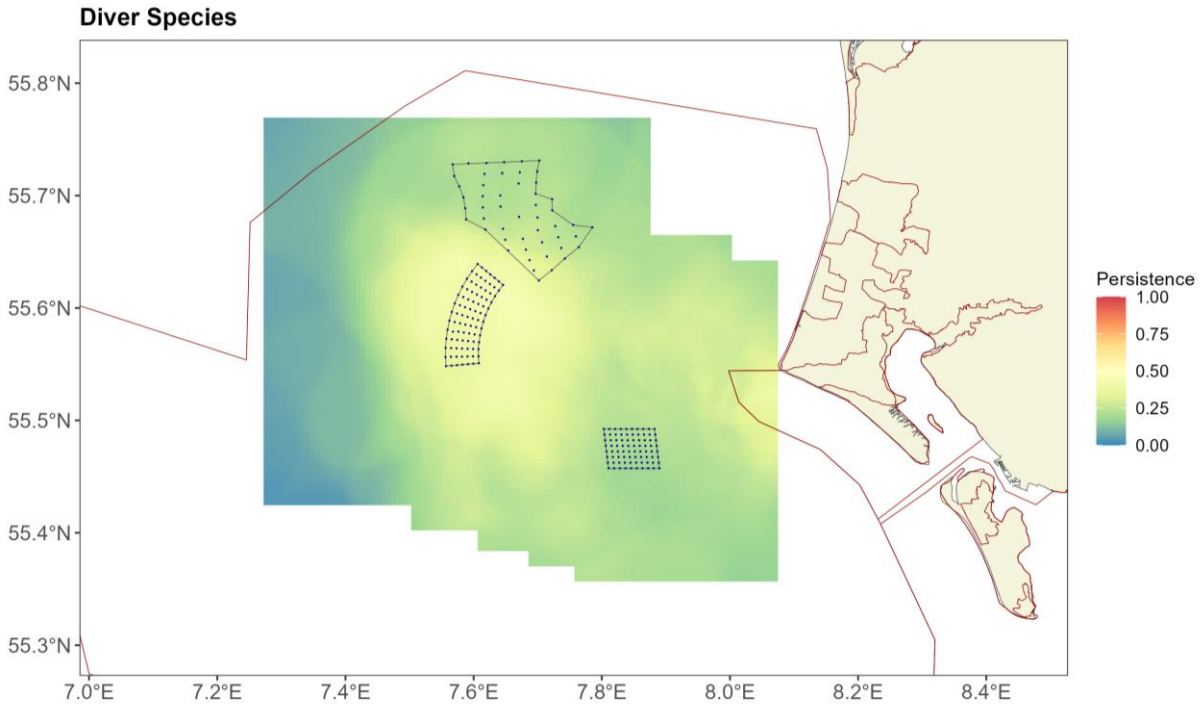

Figure 3-44. Persistence scores for divers across the 62 surveys. The polygons represent the windfarms Horns Rev I, II and III (black line) with turbine locations indicated by the black dots.

Figure 3-45 to Figure 3-48 show the persistence of birds within each phase. In Phase 0, prior to any construction, the birds were distributed across the area with some concentrations to the central area and southern and eastern edges, indicating that the birds, across multiple surveys, consistently preferred those areas to other parts of the area. Notably, there was moderate persistence in the footprint of soon-to-be constructed HR I, while high persistence scores in the to-be footprints of HR II and low persistence scores in the to-be footprints of the HR III area (Figure 3-45).

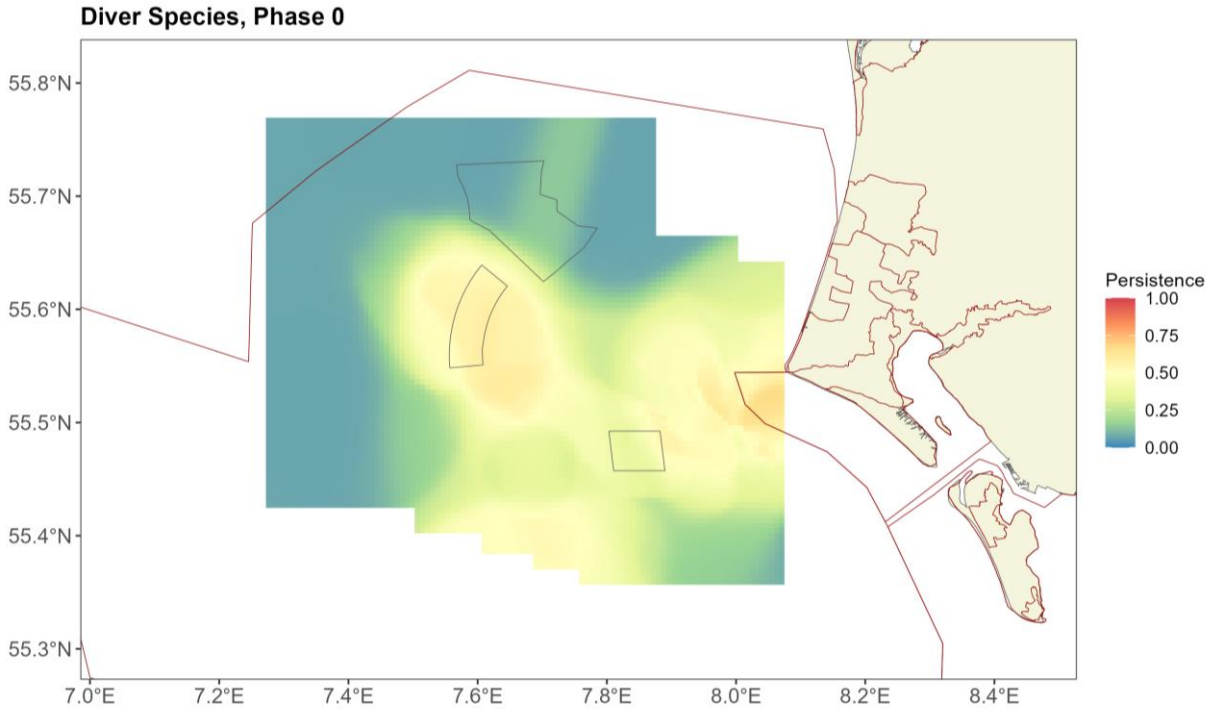

Figure 3-45. Persistence scores for diver species across the 15 surveys in Phase 0. The polygons represent the wind-farms Horns Rev I, II and III (black line).

In Phase 1 however, there is a shift into the centre of the area from the southern parts of the survey area and from the area close to Blåvandshuk (western tip of Jutland). The highest persistence scores was found in the area just northeast of the HR II and south of HR III wind farms, none of which were constructed at this point in time (Figure 3-46).

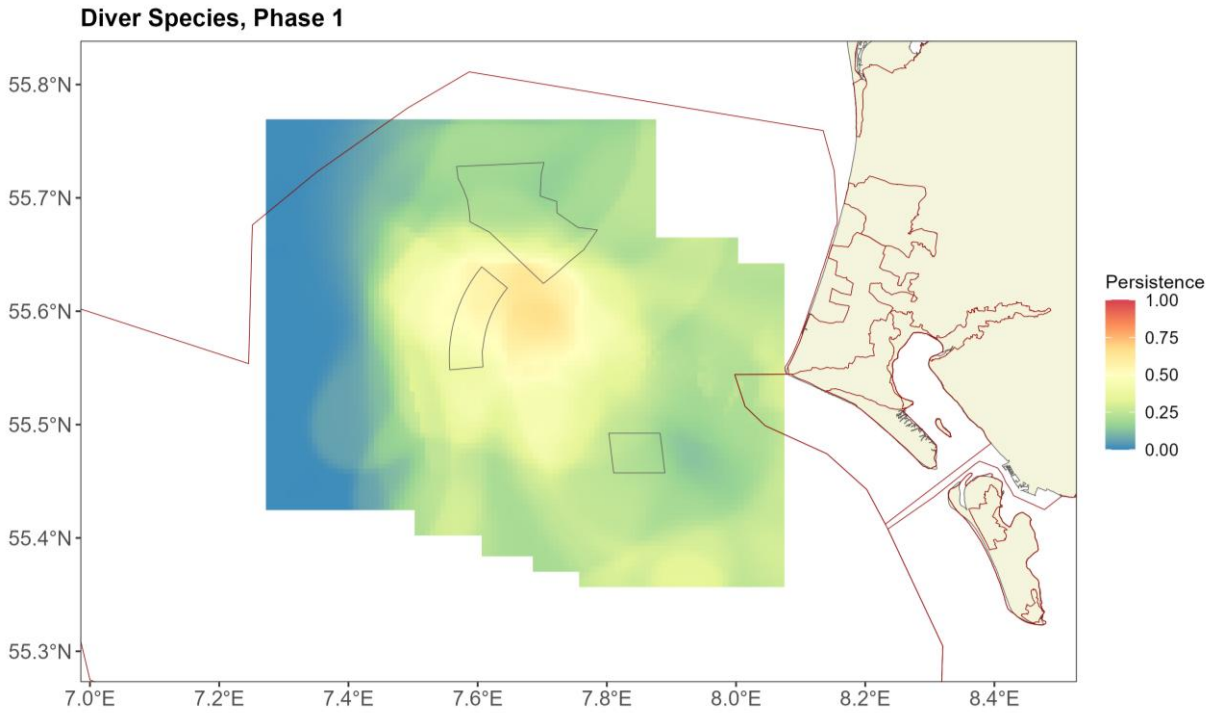

Figure 3-46. Persistence scores for diver species across the 25 surveys in Phase 1. The polygons represent the wind-farms Horns Rev I, II and III (black line).

Phase 2 is 2-5 years post-construction HR II and 9-10 years post-construction HR I. In this phase, the divers have a much more broadly distributed pattern and are largely evenly spread, except where persistence is lower in the south-eastern edge of the area (Figure 3-47). Persistence in the HR I footprint is relatively low and lower than in Phases 0 and 1.

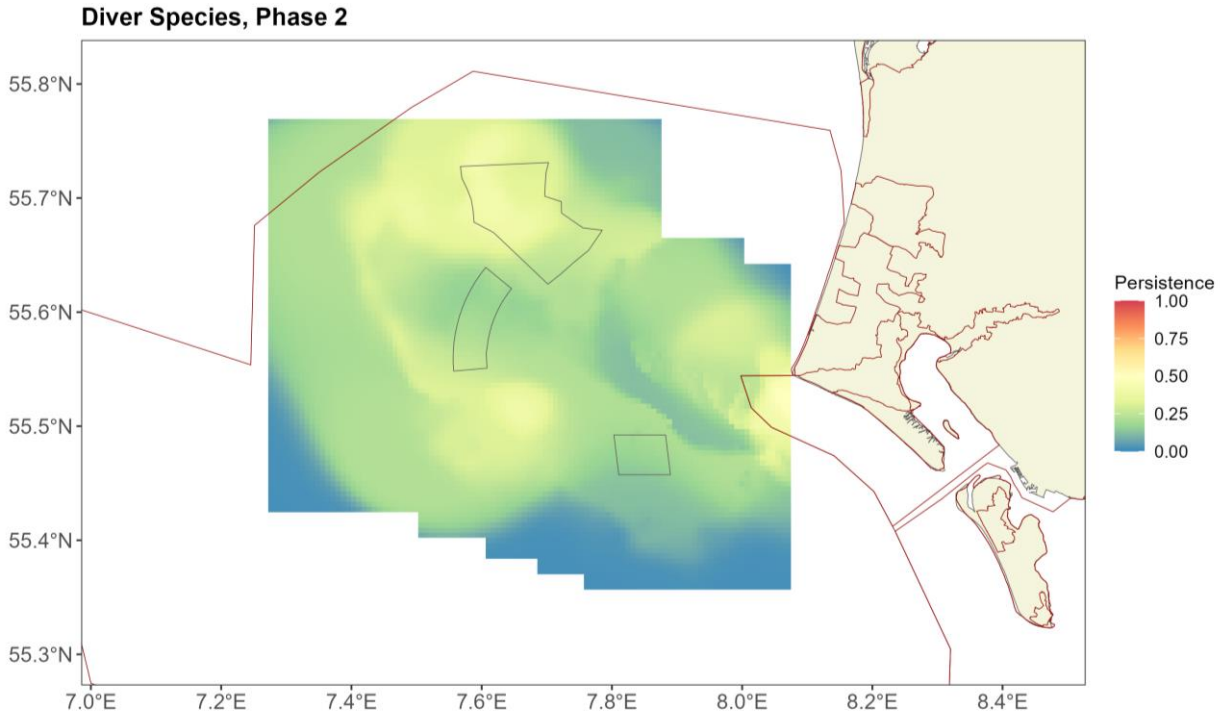

Figure 3-47. Persistence scores across the 10 surveys in Phase 2. The polygons represent the windfarms Horns Rev I, II and III (black line).

The most recent surveys, Phase 3, are 5-7 years post-construction of HR III, 11-13 years post-construction HR II and 21-23 years post-construction of HR I. During these surveys, the birds were still relatively widely distributed and showed relatively low persistence overall (Figure 3-48).

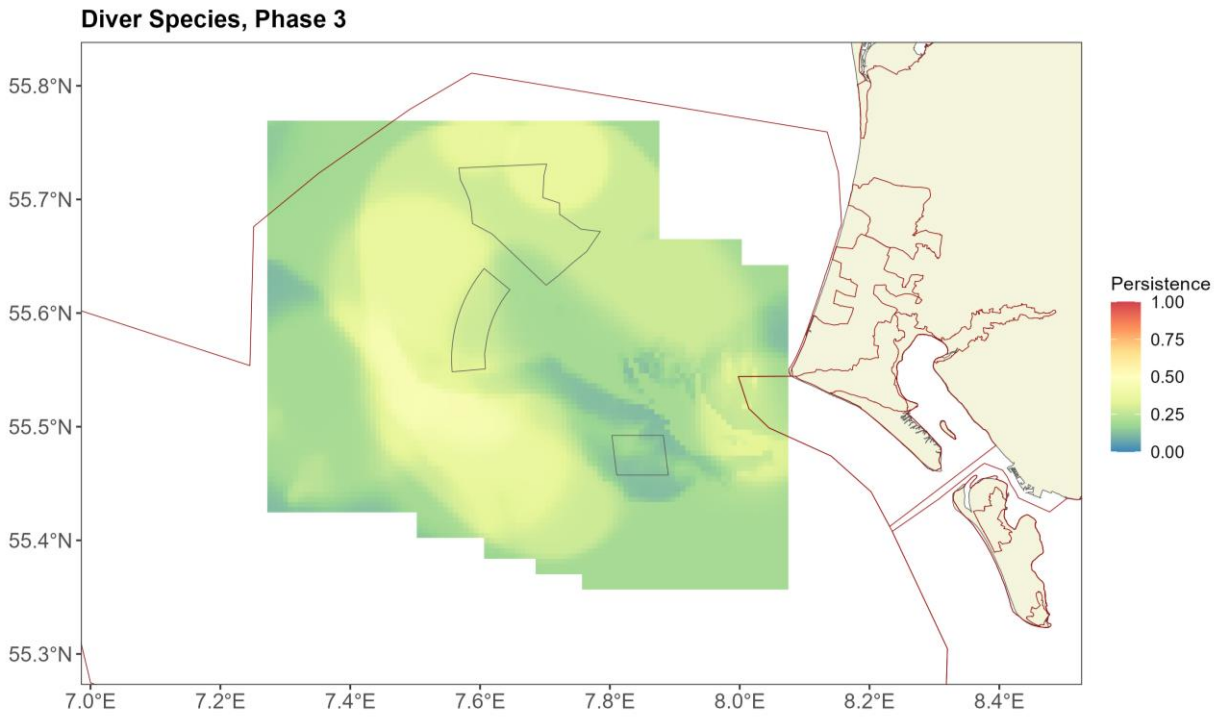

Figure 3-48. Persistence scores across the six surveys in Phase 3. The polygons represent the windfarms Horns Rev I, II and III (black line).

3.9.3 Phase-specific windfarm footprint densities

Closer inspection of the estimated density of diver species within and around windfarm footprints at various spatial scales was carried out to better understand any windfarm related changes (Figure 3-49 and Table 3-7). For instance, if there were no changes in diver species density across the 25 years in this figure: either inside the footprint or up to one or two kilometers from the footprint then we would expect to see horizontal lines for all four colours in Figure 3-49. However, the likelihood of changes in bird density across this time frame is incredibly high, regardless of windfarm construction, and so any changes must be examined from several perspectives.

In the study area as a whole, there has been an increase in density of diver species between Phases 1* and 2 and a decline in Phase 3 (indicated by the black lines in Figure 3-49), providing a backdrop of variable densities during the 25 years across the survey area.

Inside the footprint of each of the three windfarms (HR I, HR II and HR III) we see different patterns as each windfarm is constructed. For HR I, the density was constant from Phase 1*-2 with a decline after Phase 2 that reflects the pattern throughout the study area.

Within the HR II footprint, there was a very sharp decrease in density from Phase 1* to 2 followed by a levelling off in density in Phase 3. The density of birds in Phase 3 in both the HR I and II footprints was lower than the mean density of the study area as a whole.

Regarding HR III, there is quite large uncertainty in Phases 1* and 2 indicating that the densities in the two phases were likely very similar. In Phase 3, there was a marked decline in density, in keeping with the decreased density in the study area as a whole.

Within one and two kilometers of each windfarm footprint we also saw very similar patterns to those observed inside the footprint in each case.

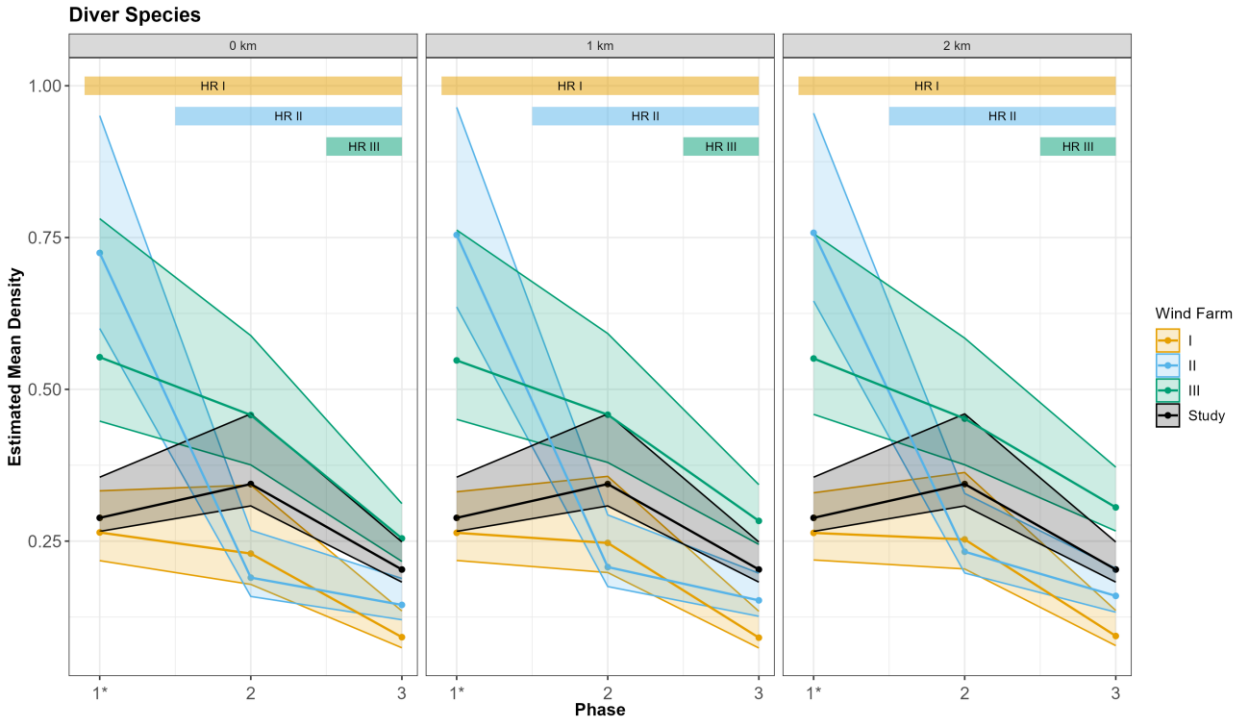

Figure 3-49. Graphs showing the estimated mean diver density inside the footprint (indicated by 0 km from the footprint), footprint including a 1 km buffer (indicated by 1 km from the footprint) and footprint including a 2 km buffer (indicated by 2 km) of each windfarm for Phases 1 to 3. The bars at the top show the post-construction periods for each wind farm.*

In the HR II area there was a 75% decrease in diver density between Phase 1* and Phase 2, followed by a further decrease of 24% between Phase 2 and Phase 3, resulting in an overall 80% decline between Phase 1* and Phase 3 (Table 3-7).

Table 3-7. Table of diver abundance estimates and 95 percentile-based confidence intervals for each wind farm footprint and phase.

Phase	I	II	III
1*	5.36 (4.41, 6.74	22.1 (18.3, 29)	47.3 (38.3, 66.8)
2	4.65 (3.62, 6.94)	5.79 (4.85, 8.17)	39.2 (32.1, 50.4)
3	1.86 (1.51, 2.73)	4.42 (3.68, 5.75)	21.8 (18.5, 26.7)

3.9.4 Phase-specific differences

Having looked at general trends in density across the three footprints and three phases we can also assess changing spatial patterns using spatial difference plots. Between Phases 0 and 1 there was a widespread significant increase in numbers with the largest appearing centrally around the future HR II footprint (Figure 3-50). There was also a large significant decrease off Blåvandshuk. Notably, there is no significant change in the HR I footprint.

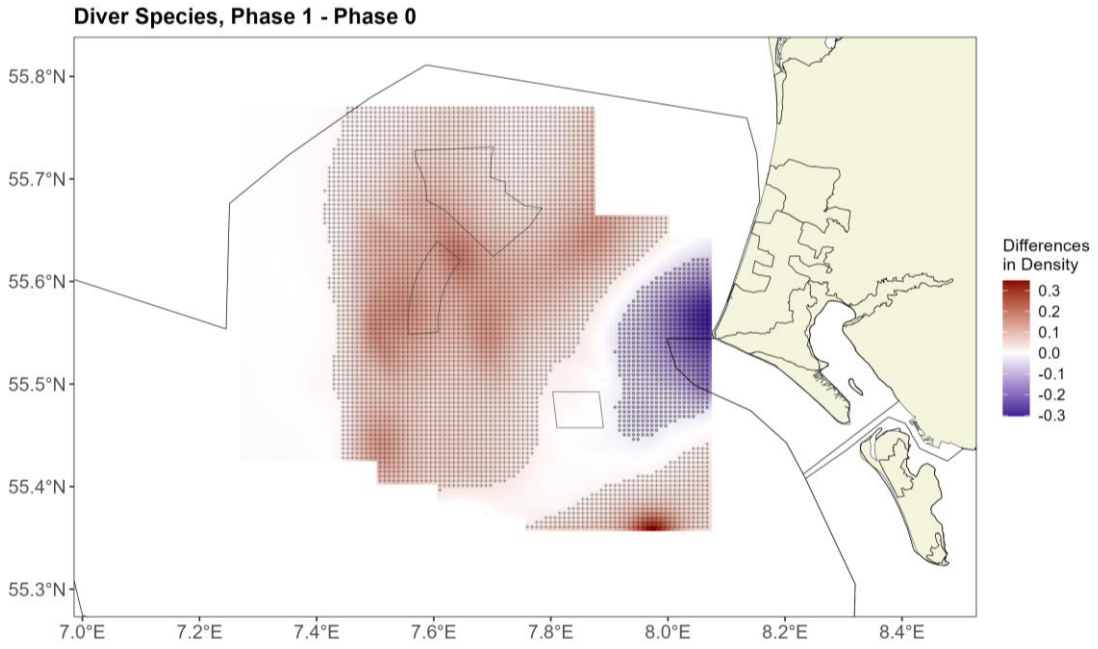

Figure 3-50. Map showing the estimated differences in diver distribution between Phase 1 and Phase 0. Positive differences indicate more birds in Phase 1. A "+" sign in the reddish background colours indicates a significant positive difference and a "o" in bluish background colours a significant negative difference.

The statistically significant, and substantial, decreases in density in and around the HR II footprint subsequent to its construction (Phase 1* to 2) is clear in Figure 3-51. At the same time significantly higher densities of divers was seen in the northwestern, the southwestern parts of the study area, with smaller areas of increased densities seen off coastal Blåvandshuk and an area just south of the HR I footprint.

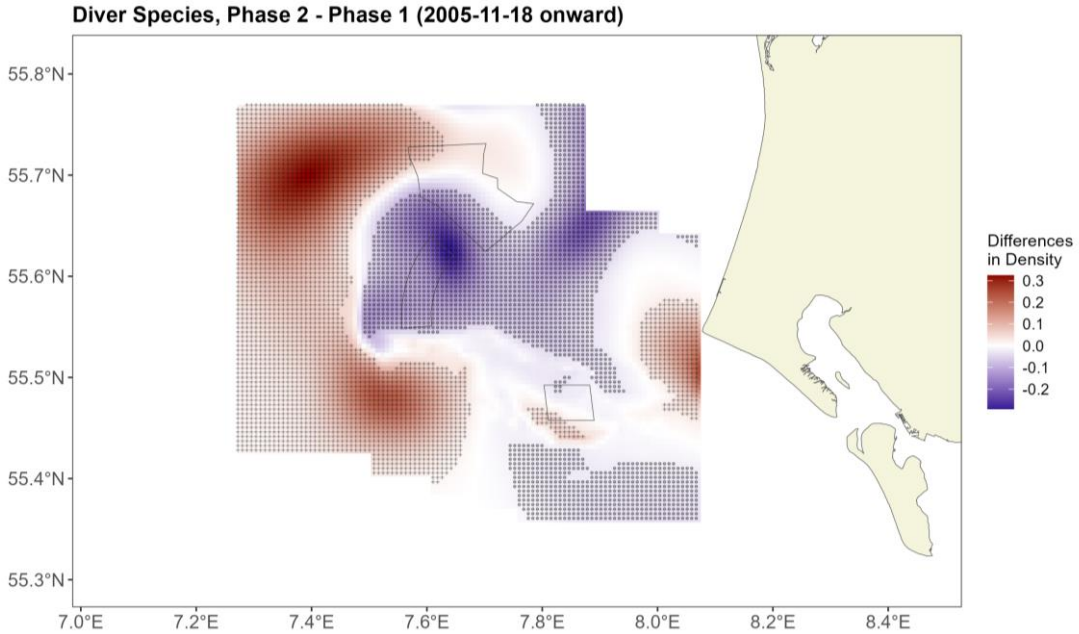

Figure 3-51. Map showing the estimated differences in diver distribution between Phase 2 and Phase 1. Positive differences indicate more birds in Phase 2. A "+" sign in the reddish background colours indicates a significant positive difference and a "o" in bluish background colours a significant negative difference.*

Eleven to thirteen years post-construction of HR II there were significant decreases in the centre and western parts of the survey area compared with two to three years post-construction (Phase 3 to 2), particularly focused in the area to the west and south of the HR II footprint. A smaller area ca. 4-5 km west northwest of the western side of HR II showed significant increases in diver abundance between these two phases (Figure 3-52). The

concentration of divers has shifted from the west in Phase 2 to increase, in Phase 3, northeast and inshore from the now constructed HR III windfarm. There was also a small but significant increase in numbers in the far south of the study area.

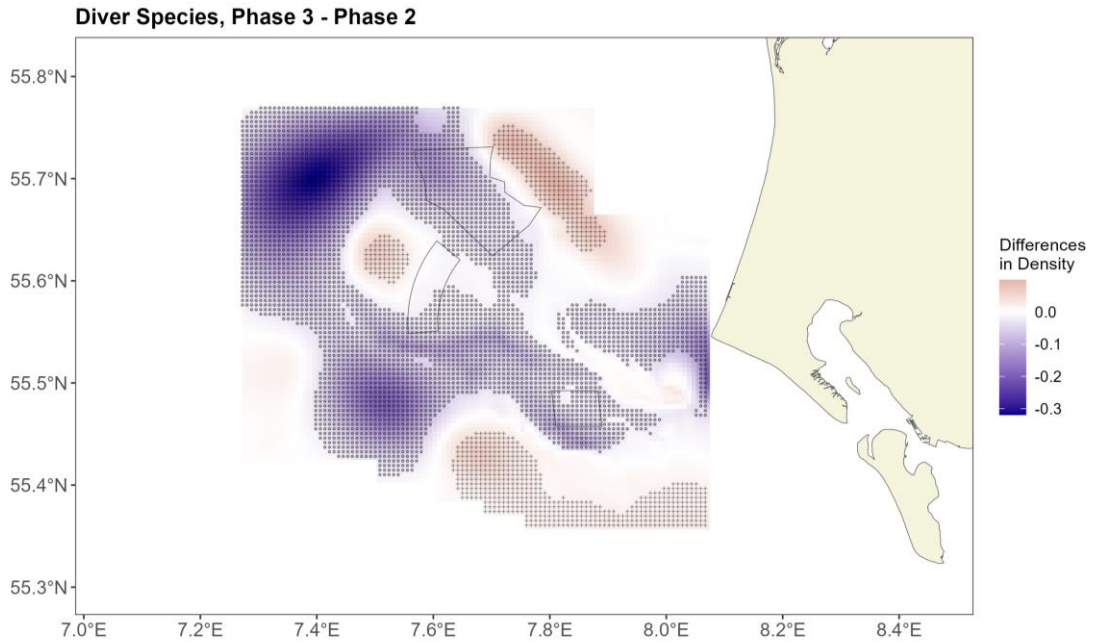

Figure 3-52. Map showing the estimated differences in diver distribution between Phase 3 and Phase 2. Positive differences indicate more birds in Phase 3. A "+" sign in the reddish background colours indicates a significant positive difference and a "o" in bluish background colours a significant negative difference.

Although overall there were significant decreases (Phase 1* to 3), the largest significant decreases are centred over and close to the footprint of HR II (Figure 3-53) in the areas of highest density in Phase 1* (Figure 3-25). There was evidence of declines in density across most of the HR III footprint. There were significant increases in density found to the northeast of the HR III footprint and in the western and southwestern parts of the study area.

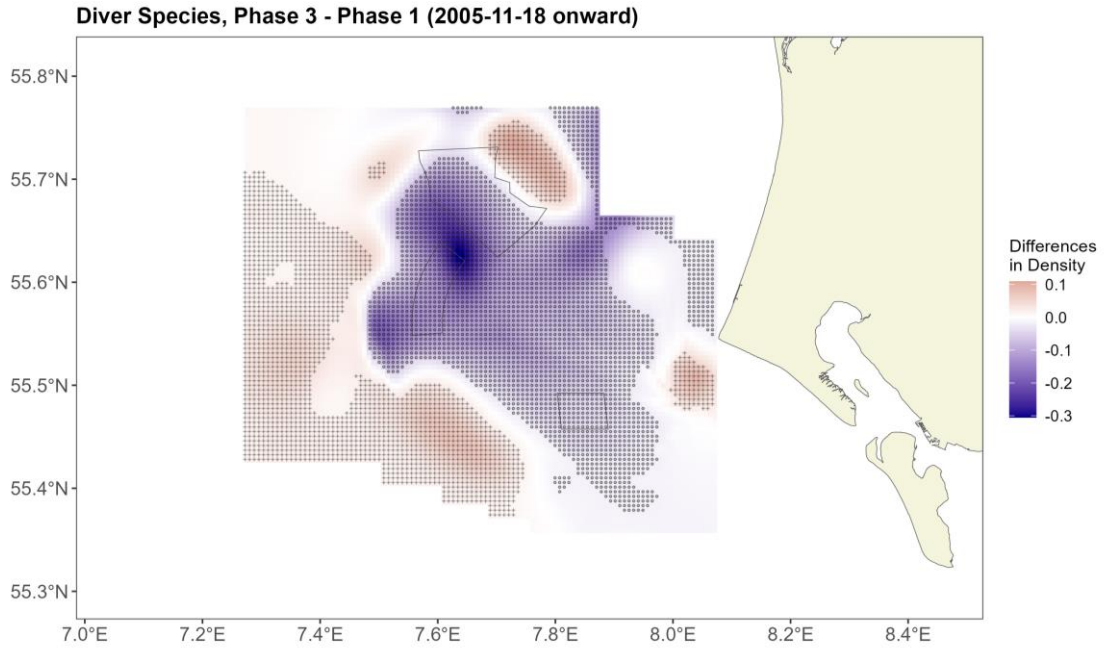

Figure 3-53. Map showing the estimated differences in diver distribution between Phase 3 and Phase 1. Positive differences indicate more birds in Phase 3. A "+" sign in the reddish background colours indicates a significant positive difference and a "o" in bluish background colours a significant negative difference.*

In general, across Phase 1* to 3 there were significant reductions in diver densities around all three windfarms and in the central parts of the survey area. In particular, there was compelling evidence of a larger decline in densities in and around the footprint of HR II once operational (Phase 1* to 2). For HR I there were no significant changes in densities between Phase 0 and 1 or minor changes between Phase 1* and 2.

3.10 Diver Horns Rev II (HR II) specific results

In addition to the difference plots, we can look in more detail at the HR II footprint. Table 3-8 shows that 100% of the cells in the HR II are estimated to have significantly decreased density post-construction (Phases 1* to 2 and 1*-3). Between Phases 2 and 3 there was a significant decrease in 30% of the footprint. No cells in the footprint were estimated to have increased in any of the Phases 1*, 2, or 3.

*Table 3-8. Table showing the percentage of cells in the Horns Rev II wind farm footprint that estimate an increase or a decrease in abundance of divers and also the percentage of cells that significantly increase or decrease (calculated from the bootstrap predictions). The * for Phase 1 indicates the shortened Phase 1.*

Horns Rev II	Pre-con. to 2-3 yrs post-con.	2-3yrs post-con. to 11-13 yrs post-con.	Pre-con. to 11-13 yrs post con.
	(Phase 1*-2)	**(Phase 2-3)**	**Phase (1*-3)**
% of cells in footprint increasing	0	0	0
% of those cells significantly increasing	0	0	0
% of cells in footprint decreasing	100	100	100
% of those cells significantly decreasing	100	30.3	100

3.10.1 HR II related changes across phases in all directions

We can also assess how the density changes between phases varies with distance from the footprint. To do this we collapse the spatial patterns down into one dimension using concentric rings of increasing distance from the footprint. Figure 3-54 illustrates a displacement effect (reduction in density) post-construction (Phase 2–1*) within approximately 6 km from the footprint (where the upper 95% confidence interval rises to zero (no difference)).

The Phase 2-3 comparison does not show compelling impact of the construction of the HR II windfarm on the density of divers. However, there is evidence of an overall decline in density regardless of distance from the footprint.

Comparing Phase 1* to Phase 3, 11-13 years post-construction, we see the combination of these effect giving compelling evidence for a displacement effect within about 9.5 km from the HR II footprint (Figure 3-54). Beyond this, the densities return to pre-construction levels.

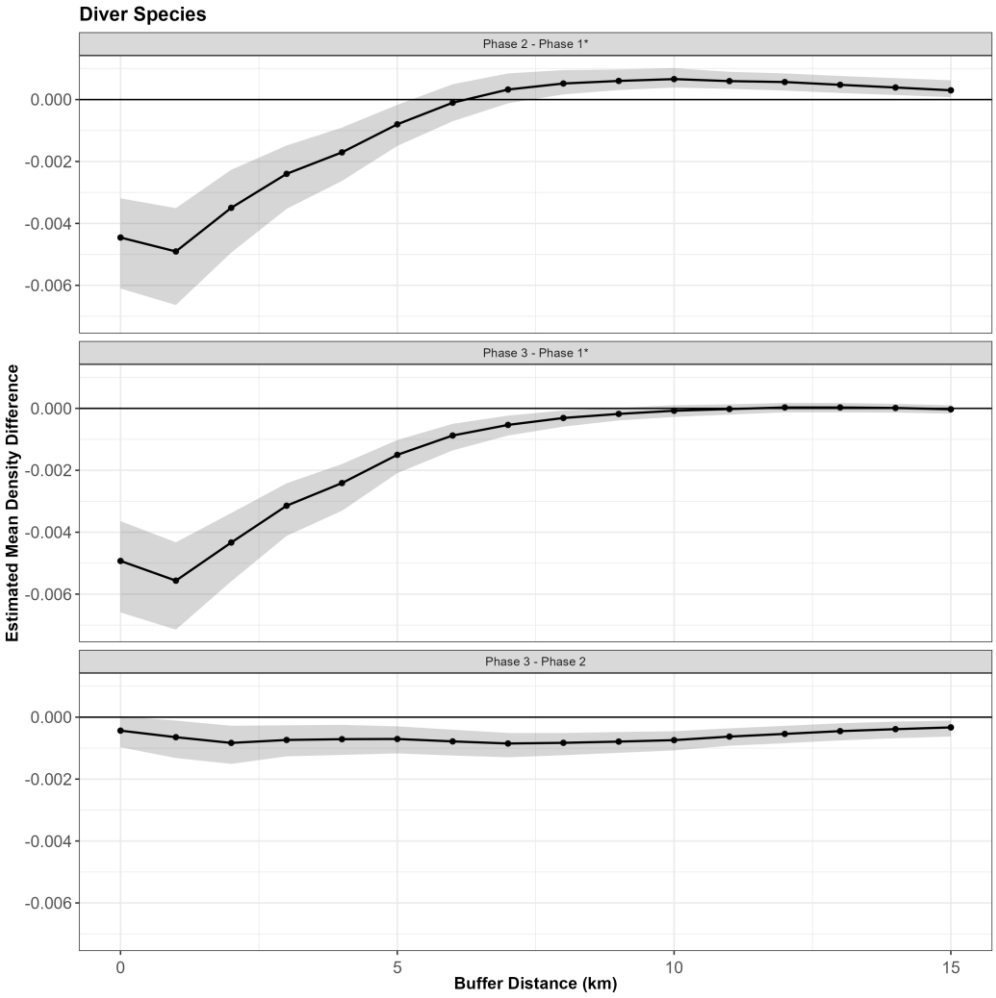

Figure 3-54. Graphs showing the change in the estimated mean density difference between Phases 1-2, 1*-3 and 2-3, with increasing distance to the HR II footprint.*

3.10.2 HR II related changes across Phases, direction specific

In contrast to Figure 3-54 which aggregates any distance related changes in and around the HR II footprint in all directions, the results were also examined by selected 'sectors', because of the presence of other OWF and generally differing environments. Using the same approach as for the common scoter, we selected the same three sectors: North-East (NE) which includes the HR III footprint, South-East (SE), and West (W) (see Figure 3-27).

Figure 3-55 illustrates post construction of HR II, we see displacement of Diver species evident to 6.5 km of the footprint in the NE, 5 km in the SE and 4.5 km in the W sectors. Beyond these displacement distances, in the NE and SE sectors, there is no evidence of a change from pre-construction levels but in the W sector the density significantly increases compared with pre-construction.

Over the longer time span (pre to post construction of HR II and III; Phase 3-1*), the displacement distances increase to 9.5 km in the NE, all the way to the maximum 15 km for the SE sector and to 5.5 km in the W sector. There is still evidence of a significant increase beyond this in the W sector, but the magnitude is much reduced.

Comparing Phase 2 and 3, all sectors show a general trend of decreasing density, regardless of distance from the footprint. The greatest decreases in density occur 6-8 km from the HR II footprint for both the SE and NE sectors and beyond 8 km for the W sector.

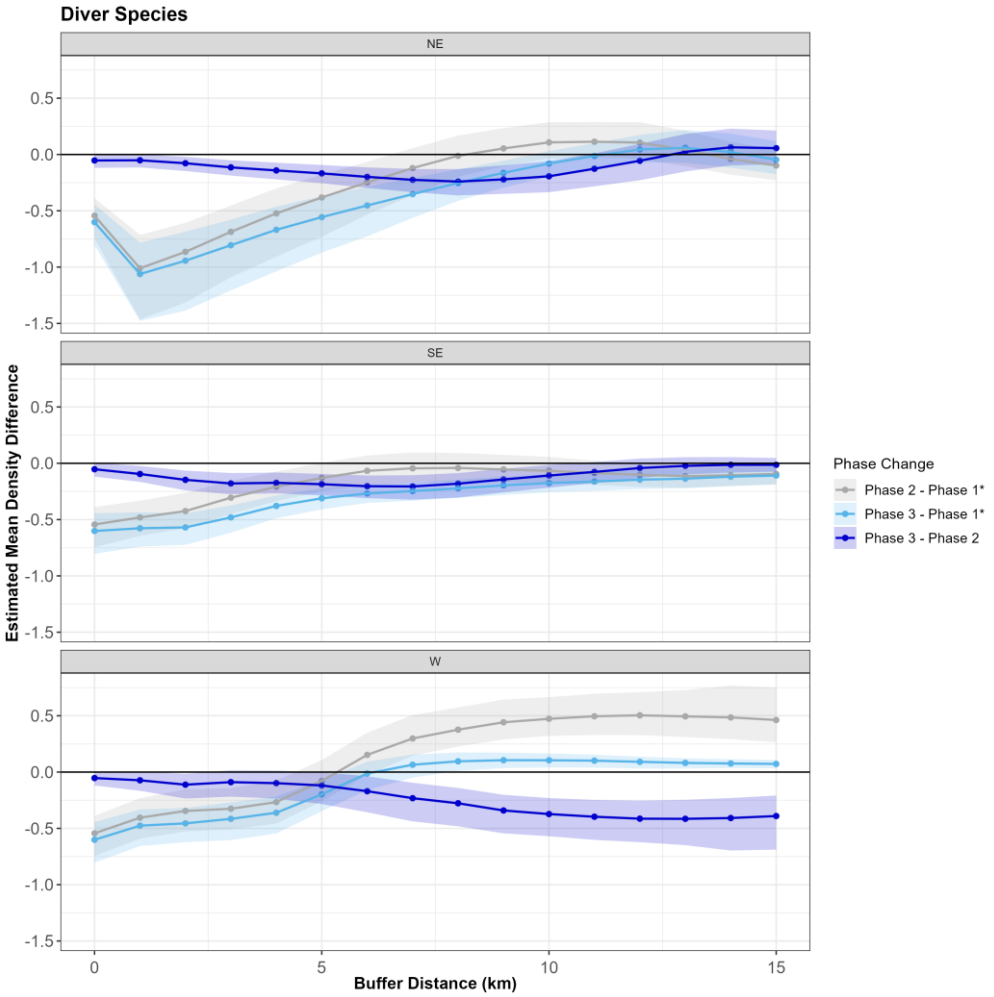

Figure 3-55. Figure showing the differences with distance to footprint by phase change and by sector.

4 Discussion

Over the 25 years that of surveys have been carried out within the greater Horns Rev area, the area covered by these surveys has gradually extended (see Figure 1-2). The gradual extension of the survey area happened in response to the changing needs associated with new and existing wind farm investigations. In general, the surveyed area extended from an initially southeastern area to extend increasingly into more northern and offshore areas to encompass assessing the effects of HR II and HR III. The most dramatic changes in survey areas occurred in the autumn of 2005, in the Phase 1 period (for a description of the different phases see "List of key terms" on page 6). This also coincided with the expansion in range for common scoters. Since both the survey coverage and the distribution of diver species, and particularly common scoters, differed markedly between early (pre-November 2002) and late (November 2002-2005) periods, the ability to detect significant changes in distributions of both species over time during Phase 1 were challenging. As a result, we chose to use the latter period (from November 2005 onwards, denoted Phase 1*), as also undertaken by Petersen et al. (2014), for comparisons to Phases 2 and 3.

Despite the changes in both survey area coverage and distribution of especially common scoter, we were still able to derive abundance estimates in the survey area for every survey. This was possible, regardless of coverage, by using pseudo-absences to fill in the gaps between the area of interest and the covered area of a particular survey. For common scoters this was a reasonable assumption given that there were very few birds in the offshore parts of Horns Rev prior to their range expansion and the survey coverage expansion. However, diver species were more widely distributed during these early survey years and it is likely that abundances for the surveys performed under Phase 0 and the early Phase 1 are underestimated, particularly in the area of the yet to be constructed HR III OWF – another reason to restrict our Phase comparisons to 1* onwards.

HR I did not offer a platform for robust comparisons pre- and post-construction due to the above-mentioned large-scale changes in bird abundances and distributions. Diver densities in the HR I footprint remained relatively constant between Phase 1* and 2 but showed a significant decrease between Phase 2 and 3, a decline that was in line with an area-wide decline. For common scoter a significant decrease in density was observed in much of the HR I footprint across Phases 1* to 2 and to a lesser extent between Phases 2 and 3. Due to the above-mentioned large-scale changes in common scoter distribution, it is difficult to associate these changes with the construction of the wind farm.

There is strong evidence for divers being significantly displaced around the footprint of HR II within 5.5 km between Phase 1* and 2 and within 8.5 km between Phase 1* and 3. The largest displacement distances were observed in the northeast (6.5 km) and southeast (15 km) for these two different periods. From Phase 1* to 3 diver densities declined by 80% within the footprint of the HR II wind farm. These significant declines in diver density were observed in 100% of the cells within the footprint of HR II during Phases 1* to 2 and Phase 1* to 3, and in 30% of the cells between Phase 2 to 3. These results are in accordance with another study from the German North Sea area that combined digital aerial survey data on diver distribution and satellite telemetry data from red-throated divers. Data was collected in April and May from 2015 to 2017 from four aerial digital surveys and Argos PPT satellite telemetry data from 33 birds. The results showed a 90% reduction in red-throated diver density within the footprint of the OWF's and out to a distance of 5 km from their periphery, and significant displacement could be shown out to a distance of 10-15 km (Heinänen et al. 2020).

Common scoters showed significant displacement at HR II out to 3 km between Phase 1* and 2 and 6 km between Phase 1* and 3. The greatest displacement distances occur in the western sector in both Phase difference periods (5 km and 8 km respectively). Within the HR II footprint common scoter densities declined by 80% between Phase 1* and 3.

After the construction of HR III declines in densities of both common scoter and diver species were observed in that area. This decline was in line with the general density decline for both species in the survey area and was furthermore less pronounced than was the case for HR II. Common scoter densities increased in the HR III area between the Phase 1* and 2, i.e. pre-construction of HR III. From Phase 2 to 3, i.e. after the construction

of HR III, significant decreases of common scoters were observed, which was in line with a density decline in the general survey area.

Despite the declines in density seen in both the HR II and III footprints, when scoters are present they still persistently use both footprints, even after construction. The same cannot be said for diver species, which more persistently used the HR II footprint in Phases 0 and 1 (pre-construction) compared to Phases 2 and 3 (post-construction). Their persistence in HR I also decreased post-construction (Phase 0 and 1) and remained low in Phases 2 and 3. The trend is less clear for HR III.

We can only speculate what the mechanisms behind these observed displacement effects might be. It seems highly likely that large scale complicating factors such as the abundance and distribution of the food supply for both species have driven the major changes witnessed in the distribution and abundance of both species across the entire study area over the years for which we have data. However, in relation to the responses associated with the construction of the OWFs, there are four likely major factors that could form the stimuli responsible for the displacement responses shown by common scoter and divers at smaller spatial scales. These are displacement from (i) physical disruption to their favoured spatial distribution caused by maintenance ship-traffic associated with the servicing of the wind turbines, (ii) constant visual disturbance caused by the turning turbine blades or (iii) the lighting of the turbines at night or (iv) the noise caused by the turbines. Ultimately, displacements of the birds could be caused by negative prey-species responses to the presence of the OWFs. Because of lack of data to evaluate, this hypothesis remains very speculative.

We infer that (but lack any data for) the levels of shipping traffic associated with the turbines is likely constant and more or less of equal intensity across all of the three HR windfarms. We might also expect that much of the shipping traffic would be to the east of all three OWF and therefore affect the densities more in the SE/NE sectors. The largest displacements of common scoter post-construction of HR II has occurred in the western sector, rather than the eastern sector, and significant increases in density from a distance of 1 km (from HR II) in both the SE and NE sectors. The diver displacement distances are generally larger than for scoters, and post construction of HR II the largest displacement is seen in the NE sector, which could indicate some vessel disturbance. However, post construction of HR III there were significant increases in diver density on the eastern side of the footprint of this OWF. Even in the absence of shipping data, the evidence suggests that ship-traffic is an unlikely factor driving displacement for these species.

In the case of factors (ii), (iii) and (iv) above, the responses of birds to these visual and auditory stimuli would be predicted to diminish with increasing distance, and if both divers and common scoters avoid adverse stimuli by remaining at a certain distance from such stimuli, it might be expected that displacement is a threshold distance-related response to point-stimulus. If the birds prefer to keep a certain distance away from a turbine because of its visual (rotating blades or lighting at night) or auditory impact, and that that distance is less than half the distance between adjacent turbines, the birds will be reticent to swim between consecutive lines of turbines. If this is the case, we may hypothesise that the more irregular distribution of turbines and the far greater inter-turbine distances associated with HR III could potentially contribute to a reduced displacement response of common scoter and red-throated diver compared with that seen following the construction of HR II. After one year of post construction data for HR III, there was some evidence that there was indeed a reduced displacement response compared to HR II. However, the addition of the second year of Phase 3 data, where very few birds were observed, has masked any evidence of this owing to the overall declines seen for both species.

Results from the 2024/2025 survey season revealed a very marked overall decline of common scoter densities in the study area as compared to previous years, with estimated abundances comprising only ca. 14% of the numbers estimated for the season 2023/2024. This sudden change occurred during a time with no changes in the wind farms and therefore cannot be associated with the presence of the wind farms. We hypothesise that

there was a sudden change in prey availability, however there are no data available on the status of the bivalve community in the survey area, so it is not possible to establish a potential relationship between common scoter numbers and food availability in this area.

5 Conclusions

Environmental impact assessments of OWF's evaluate the potential impact on birds, but very few studies have ever attempted to empirically study the actual effects of construction by comparing pre- and post-construction studies on bird distributions. We have been able to undertake such a unique study at Horns Rev to assess the displacement effects of two critical bird species following the construction of three OWF's during 2002 to 2019. The study is based on 62 aerial surveys of birds conducted in that area between 2000 and 2025. Although complicated by long-term and large-scale changes in abundance and distributions of the two species probably caused by other, unknown factors, we found equivocal evidence for displacement of divers and common scoter following the construction of the wind farms.

HR I did not offer a platform for robust comparisons pre- and post-construction due to the above-mentioned large-scale changes in bird abundances and distributions. Divers increased in the area between Phase 1* and 2, but decreased between Phase 2 and 3, a decline that was in line with an aera-wide decline. For common scoter, a sharp decline was observed in the HR I area across Phases 1* to 2. Due to the above-mentioned large-scale changes in common scoter distribution, this decline could not be associated with the construction of the wind farm.

There was strong evidence for divers being significant displaced around the footprint of HR II, within a distance of 6 km between Phase 1* and 2 and within a distance of 9.5 km between Phase 1* and 3. Over that same period diver densities declined by 80% within the footprint of the wind farm. During Phases 1* to 2 and Phase 1* to 3 significant declines in diver density was observed in 100% of the cells within the footprint of the wind farm, whereas significant declines was observed in 30% of the cells between Phase 2 to 3. Common scoters showed significant displacement from HR II out to 6 km between Phase 1* and 3. Within the HR II footprint common scoter densities decline by 80% between Phase 1* and 3.

After the construction of HR III, declines in densities of both species were observed in that area, a decline that was less pronounced than was the case for HR II and a decline that was in line with the general diver density decline in the general survey area. Common scoter densities increased in the HR III area between the Phase 1* and 2, i.e. pre-construction of HR III. Between Phase 2 and 3, i.e. post- construction of HR III, sharp declines of common scoters were observed, which was in line with a density decline in the general survey area.

6 Recommendations for future studies

The results of this report emphasize the importance of compiling long term data series on bird distributions within and around wind farm sites, both pre- and post-construction of OWF's. We recommend such studies to be conducted in and around existing and upcoming wind farm sites. The Rødsand II/Nysted OWF's offer an opportunity to investigate long-term changes in the distribution of long-tailed duck *Clangula hyemalis*, which could potentially provide valuable information on the long-term effect from OWF's on this species. A project to provide data for such analysis has been scheduled by the Danish Energy Agency for 2026. The German OWF's Wikinger and Arkona on Adler Grund in the Baltic Sea may provide additional options for investigating this. Similarly, the Anholt OWF in Kattegat offers an opportunity to compare pre- and post-construction effects on divers.

We urge immediate investigation to describe the displacements effects of increasing inter-turbine distances at other European offshore windfarm developments on these two (and other) species, to find support for the hypothesis that the density and size of turbines may affect the degree of displacement of certain bird species (as potentially suggested by the HR III results presented here). Kriegers Flak and neighbouring wind farms in Swedish and German waters also have wind farms of varying turbine size and densities. Unfortunately, there are no available pre-construction bird distribution data from Kriegers Flak to support such analyses. Data from various OWF's in the German Bight, Germany, in the Thames Estuary and the Wash, UK could also potentially provide data for such comparisons.

7 References

Berman, Mark, and T. Rolf Turner. 1992. "Approximating Point Process Likelihoods with GLIM." *Journal of the Royal Statistical Society. Series C (Applied Statistics)* 41 (1): 31–38. http://www.jstor.org/stable/2347614.

Buckland, S. T., DR Anderson, KP Burnham, JL Laake, D. L. Borchers, and L. Thomas. 2001. *Introduction to Distance Sampling: Estimating Abundance of Biological Populations*. United Kingdom: Oxford University Press.

Buckland, S. T., Rexstad, E.A., Marques, T.A, & Oedekoven, C.S. 2015. Distance Sampling: Methods and Applications. – Springer, DOI 10.1007/978-3-319-19219-2.

Heinänen, S. Zydelis, R., Kleinschmidt, B., Dorsch, M., Burger, C., Markunas, J., Quillfeldt, P. & Nehls, G. 2020. Satellite telemetry and digital aerial surveys show strong displacement of red-throated divers (Gavia stellata) from offshore wind farms. - Marine Environmental Research 160, 104989.

Fliessbach, K.L., Borkenhagen, K., Guse, N., Markones, N, Schwemmer, P. & Garthe, S. 2019. A Ship Traffic Disturbance Vulnerability Index for Northwest European Seabirds as a Tool for Marine Spatial Planning. – Front.Mar.Sci. 6:192. https://doi.org/10.3389/fmars.2019.00192

Lamb, J., Gulka, J., Adams, E., Aonghais, C. & Williams, K. 2024. A synthetic analysis of post-construction displacement and attraction of marine birds at offshore wind energy installations. - Environmental Impact Assessment Review 108, 107611.

Leys, Christophe, Christophe Ley, Olivier Klein, Philippe Bernard, and Laurent Licata. 2013. "Detecting Outliers: Do Not Use Standard Deviation Around the Mean, Use Absolute Deviation Around the Median." *Journal of Experimental Social Psychology* 49 (4): 764–66.
https://doi.org/https://doi.org/10.1016/j.jesp.2013.03.013.

Marques, F. F. C., and S T Buckland. 2004. "Covariate Models for the Detection Function." In *Advanced Distance Sampling*, edited by ST Buckland, DR Anderson, KP Burnham, JL Laake, DL Borchers, and L Thomas, pp31–47. United Kingdom: Oxford University Press.

Marques, T. A., L. Thomas, S. G. Fancy, and S. T. Buckland. 2007. "Improving Estimates of Bird Density Using Multiple- Covariate Distance Sampling." *The Auk* 124 (4): 1229–43.
https://doi.org/10.1093/auk/124.4.1229.
R Core Team. 2022. *R: A Language and Environment for Statistical Computing*. Vienna, Austria: R Foundation for Statistical Computing. https://www.R-project.org/.

Petersen, I.K., Christensen, T.K, Kahlert, J., Desholm, M. & Fox, A.D 2006. Final results of bird studies at the offshore wind farms at Nysted and Horns Rev, Denmark. – Report request, Commissioned by DONG energy and Vattenfall A/S. NERI, National Environmental Research Institute, Ministry of the Environment, 161 pp.

Petersen, I.K. & Fox, A.D. 2007. Changes in bird habitat utilisation around the Horns Rev 1 offshore wind farm, with particular emphasis on Common Scoter. Report request, Commissioned by Vattenfall A/S. NERI, National Environmental Research Institute, Ministry of the Environment, 36 pp.

Petersen, I.K. & Nielsen, R.D. 2011. Number and distribution of birds in and around the Horns Rev 2 Offshore Wind Farm. Spring 2011. Report commissioned by DONG Energy A/S. Aarhus University, DCE - Danish Centre for Environment and Energy. 22 pp.

Petersen, I.K., Nielsen, R.D. & Mackenzie, M.L. 2014. Post-construction evaluation of bird abundances and distributions in the Horns Rev 2 offshore wind farm area, 2011 and 2012. Report commissioned by DONG Energy. Aarhus University, DCE – Danish Centre for Environment and Energy. 51 pp.

Petersen, I.K., Nielsen, R.D., Therkildsen, O.R. & Balsby, T.J.S. 2017. Fældende havdykænders antal og fordeling i Sejerøbugten i relation til menneskelige forstyrrelser. Aarhus Universitet, DCE – Nationalt Center for Miljø og Energi, 38 s. - Videnskabelig rapport fra DCE - Nationalt Center for Miljø og Energi nr. 239. http://dce2.au.dk/pub/SR239.pdf

Petersen, I.K. & Sterup, J. 2019. Number and distribution of birds in and around two potential offshore wind farm areas in the Danish North Sea and Kattegat. Aarhus University, DCE – Danish Centre for Environment and Energy, 40 pp. Scientific Report. No. 327. http://dce2.au.dk/pub/SR327.pdf

Schwemmer, P., Mendel, B., Sonntag, N., Dierschke, V. & Garthe, S. 2011. Effects of ship traffic on seabirds in offshore waters: implications for marine conservation and spatial planning. - Ecological Applications, 21(5), 2011, pp. 1851-1860

Scott-Hayward, L. A. S., M. L. Mackenzie, C. R. Donovan, C. G. Walker, and E. Ashe. 2014. "Complex Region Spatial Smoother (CReSS)." *Journal of Computational and Graphical Statistics* 23 (2): 340–60.

Scott-Hayward, L. A. S., M. L. Mackenzie, and C. G. Walker. 2023. "MRSea R Package (V1.5.0): Spatially Adaptive Uni and Bi-Variate Regression Splines Using SALSA." University of St Andrews.

Scott-Hayward, L. A. S., M. L. Mackenzie, C. G. Walker, G. Shatumbu, W. Kilian, and P. du Preez. 2023. "Automated Surface Feature Selection Using SALSA2D: Assessing Distribution of Elephant Carcasses in Etosha National Park." https://arxiv.org/abs/2202.07977.

Scott-Hayward, L. A. S., C. S. Oedekoven, M. L. Mackenzie, and C. G. Walker. 2014. "MRSea R Package: Statistical Modelling of Bird and Cetacean Distributions in Offshore Renewables Development Areas. University of St. Andrews: Contract with Marine Scotland: SB9 (CR/2012/05)." University of St Andrews.

Walker, C. G., M. L. Mackenzie, C. R. Donovan, and M. J. O'Sullivan. 2010. "SALSA - a Spatially Adaptive Local Smoothing Algorithm." *Journal of Statistical Computation and Simulation* 81 (2): 179–91.

8 APPENDICES

Appendix 1

Survey overview with distribution maps for common scoter and divers by survey

8.1 Survey overview

The 62 aerial surveys of bird in the Horns Rev area were conducted between February 2000 and April 2025. The transect coverage in kilometers by survey was between 516 and 1.612 Km (*Table **8-1***).

Table 8-1. Table detailing the survey effort (number kilometers covered transect line by survey) for each of the 62 surveys conducted between 2000 and 2024. Note that survey numbers 27 and 31 (marked with asterisks) were conducted over two days.

Survey number	Survey date	Km of transect	Survey number	Survey date	Km of transect	Survey number	Survey date	Km of transect
1	2000-02-17	826.9	21	2003-12-04	698.4	39	2007-03-03	1368.8
2	2000-02-21	574.3	22	2003-12-30	634.9	40	2007-04-01	1612.1
3	2000-03-19	823.4	23	2004-02-29	870.8	41	2011-03-01	599.6
4	2000-04-27	738.0	24	2004-03-26	867.6	42	2011-03-26	645.0
5	2000-08-21	755.6	25	2004-05-10	865.5	43	2011-04-11	643.6
6	2000-10-06	724.0	26	2004-09-09	794.3	44	2011-10-13	642.3
7	2000-12-22	612.3	27*	2005-03-08	296.0	45	2011-11-17	619.5
8	2001-02-09	754.7	27*	2005-03-09	580.7	46	2012-01-15	658.8
9	2001-03-20	826.1	28	2005-04-02	868.3	47	2012-02-08	637.4
10	2001-04-21	826.2	29	2005-05-14	871.5	48	2012-03-02	604.1
11	2001-08-22	818.9	30	2005-08-17	868.2	49	2012-03-22	627.2
12	2001-09-26	761.7	31*	2005-11-18	634.4	50	2012-04-11	630.9
13	2002-01-07	685.1	31*	2005-11-19	577.4	51	2023-11-17	599.3
14	2002-03-12	728.3	32	2006-02-02	847.8	52	2023-12-27	531.8
15	2002-04-09	681.4	33	2006-02-25	848.3	53	2024-01-09	589.7
16	2002-08-08	685.2	34	2006-03-12	850.2	54	2024-02-27	587.4
17	2003-02-13	699.1	35	2006-04-15	845.4	55	2024-04-08	586.0
18	2003-03-16	850.8	36	2006-05-11	852.7	56	2024-04-22	592.0
19	2003-04-23	859.6	37	2007-01-25	1441.0			
20	2003-09-05	840.0	38	2007-02-15	1357.7			

The transect coverage and the distribution of the observed common scoters by survey is given in Figure 8-1 to Figure 8-10.

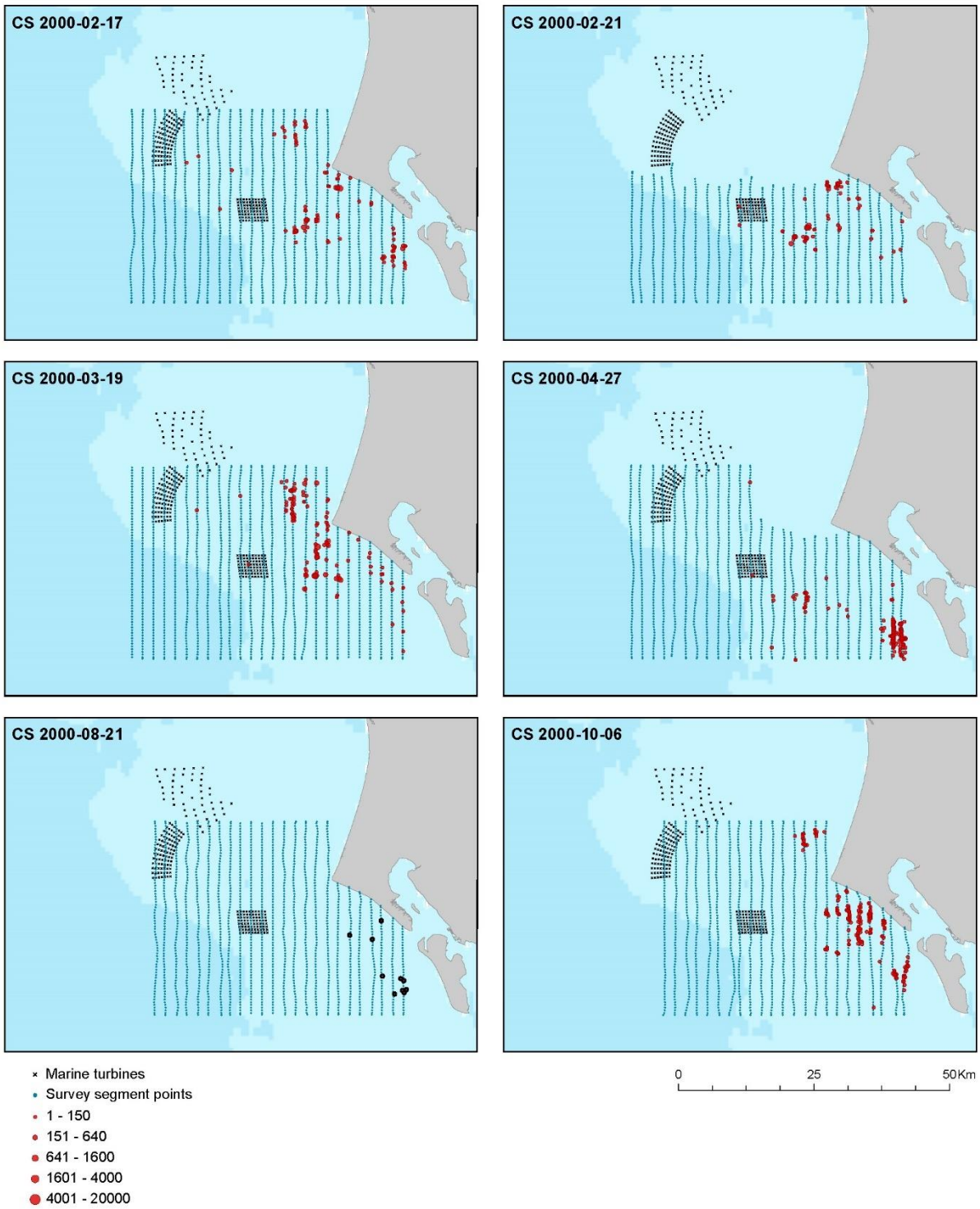

Figure 8-1. The distribution of observed common scoter during six surveys from February 2000 to October 2000.

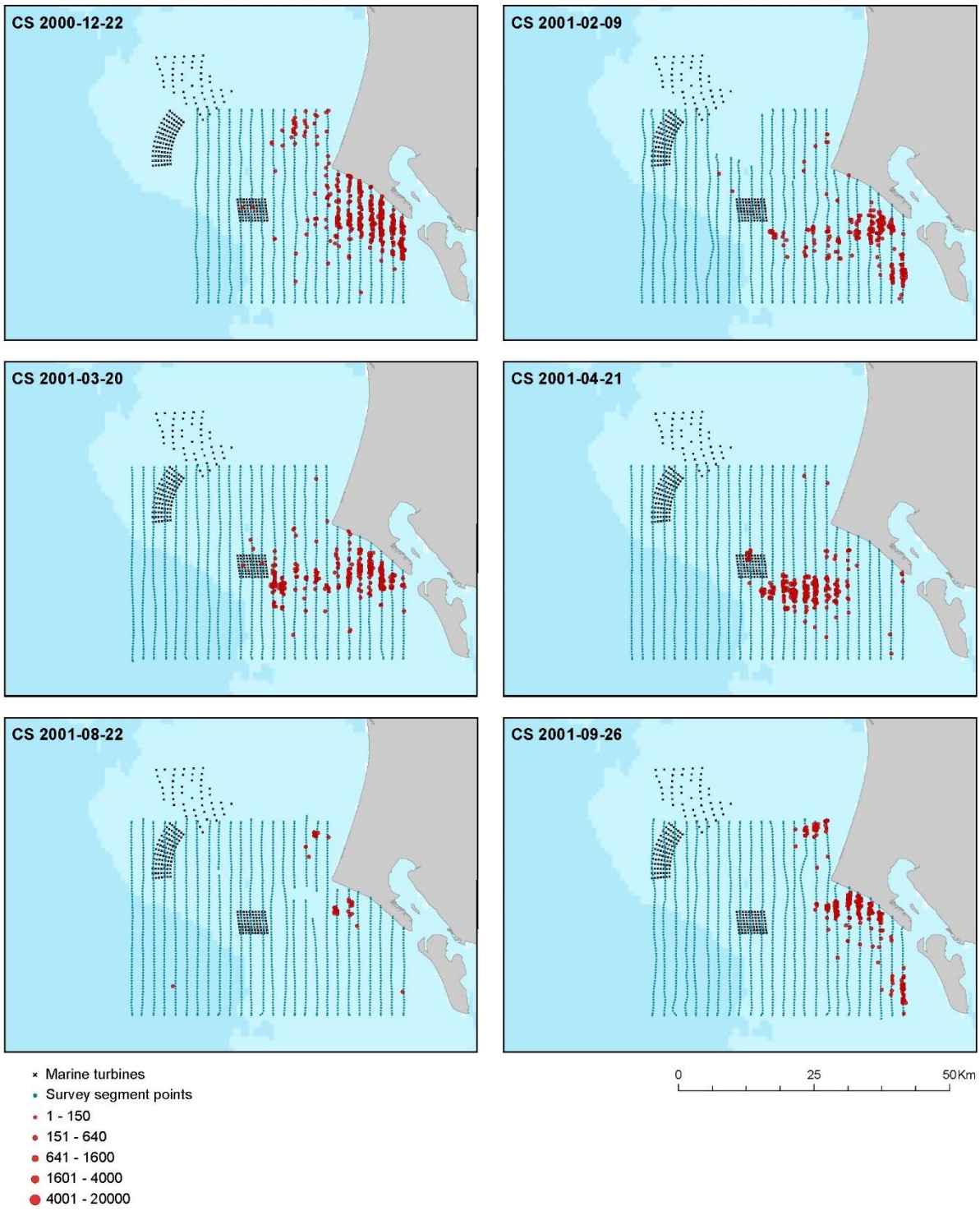

Figure 8-2. The distribution of observed common scoter during six surveys from December 2000 to September 2001.

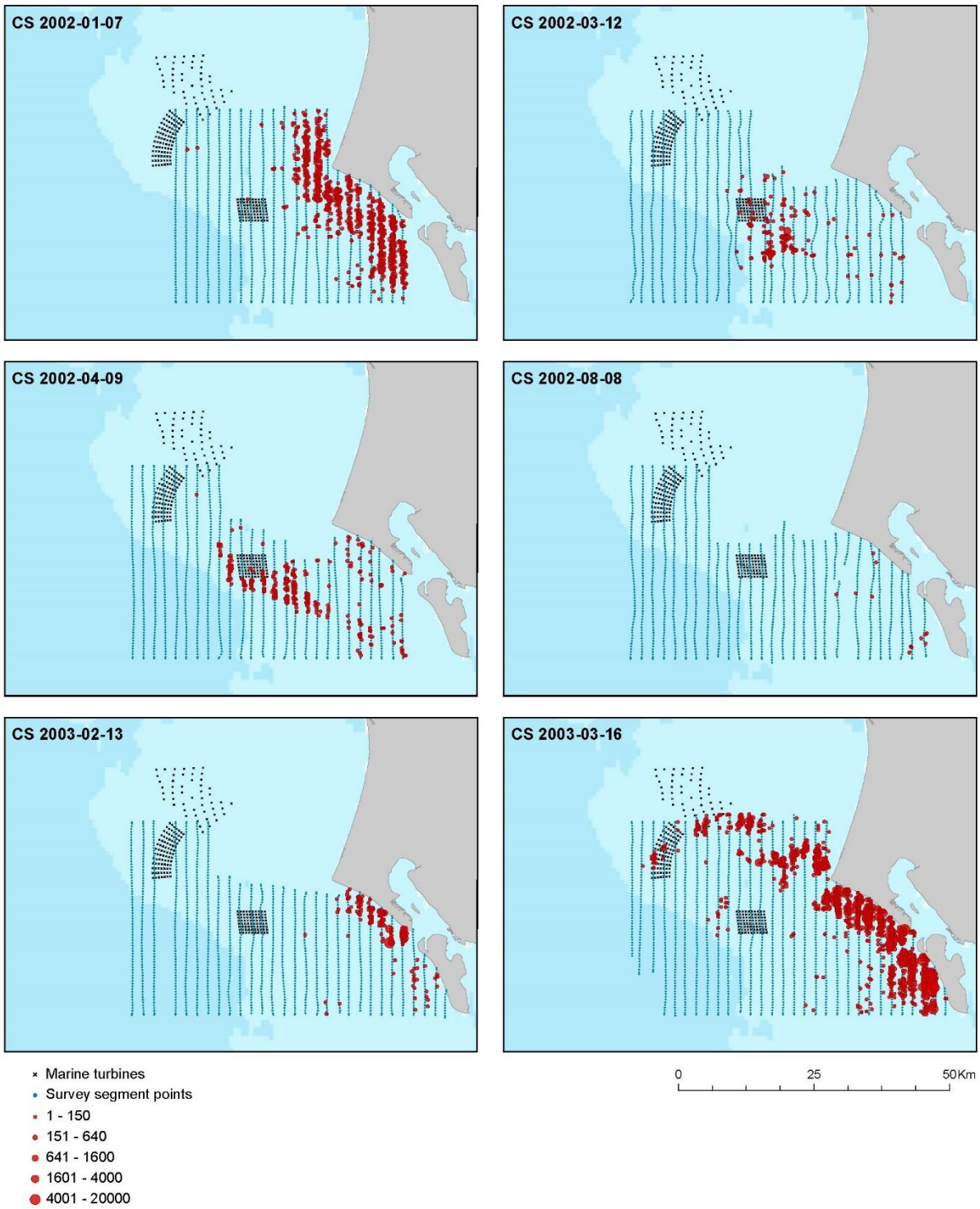

Figure 8-3. The distribution of observed common scoter during six surveys from January 2002 to March 2003.

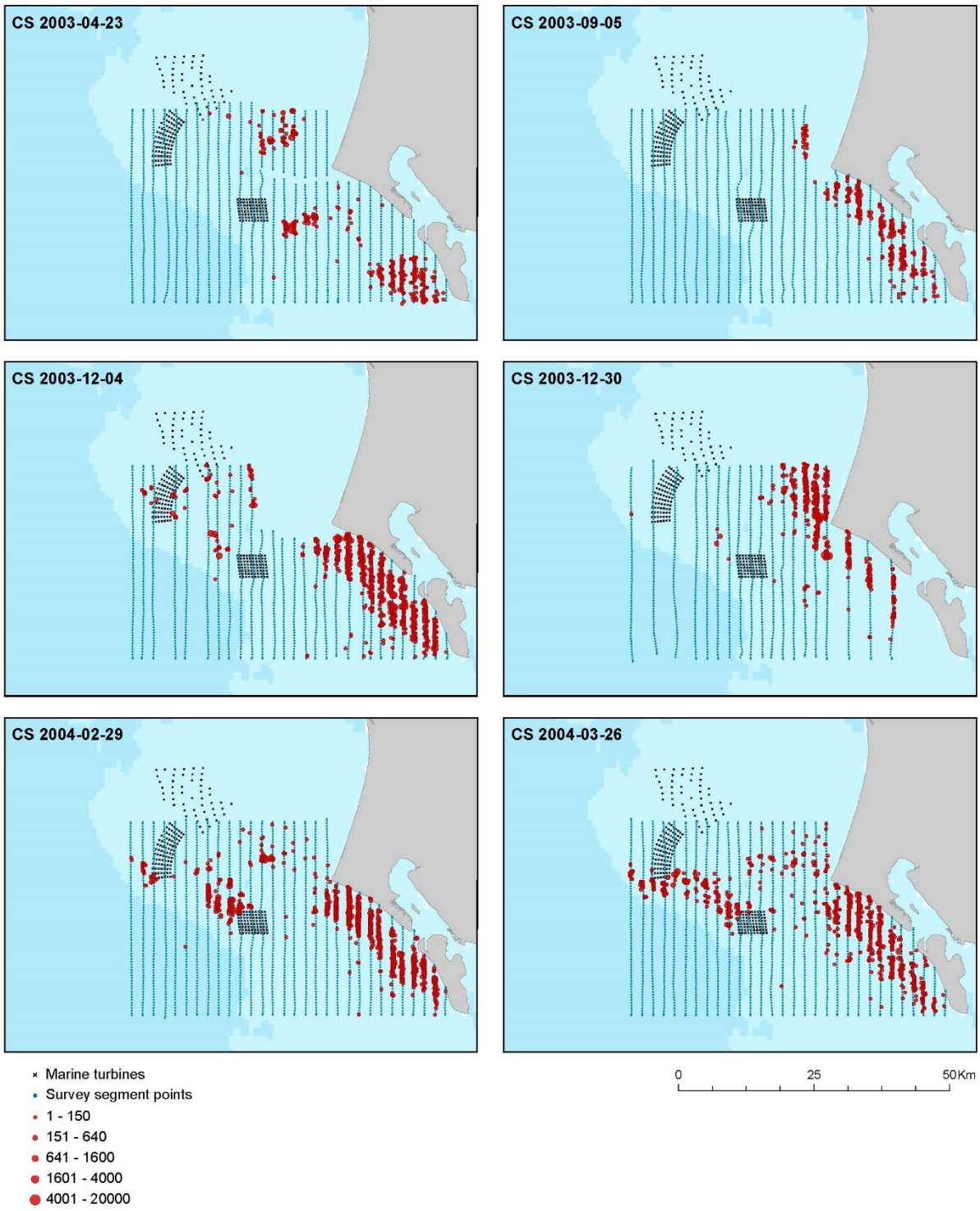

Figure 8-4. The distribution of observed common scoter during six surveys from April 2003 to March 2004.

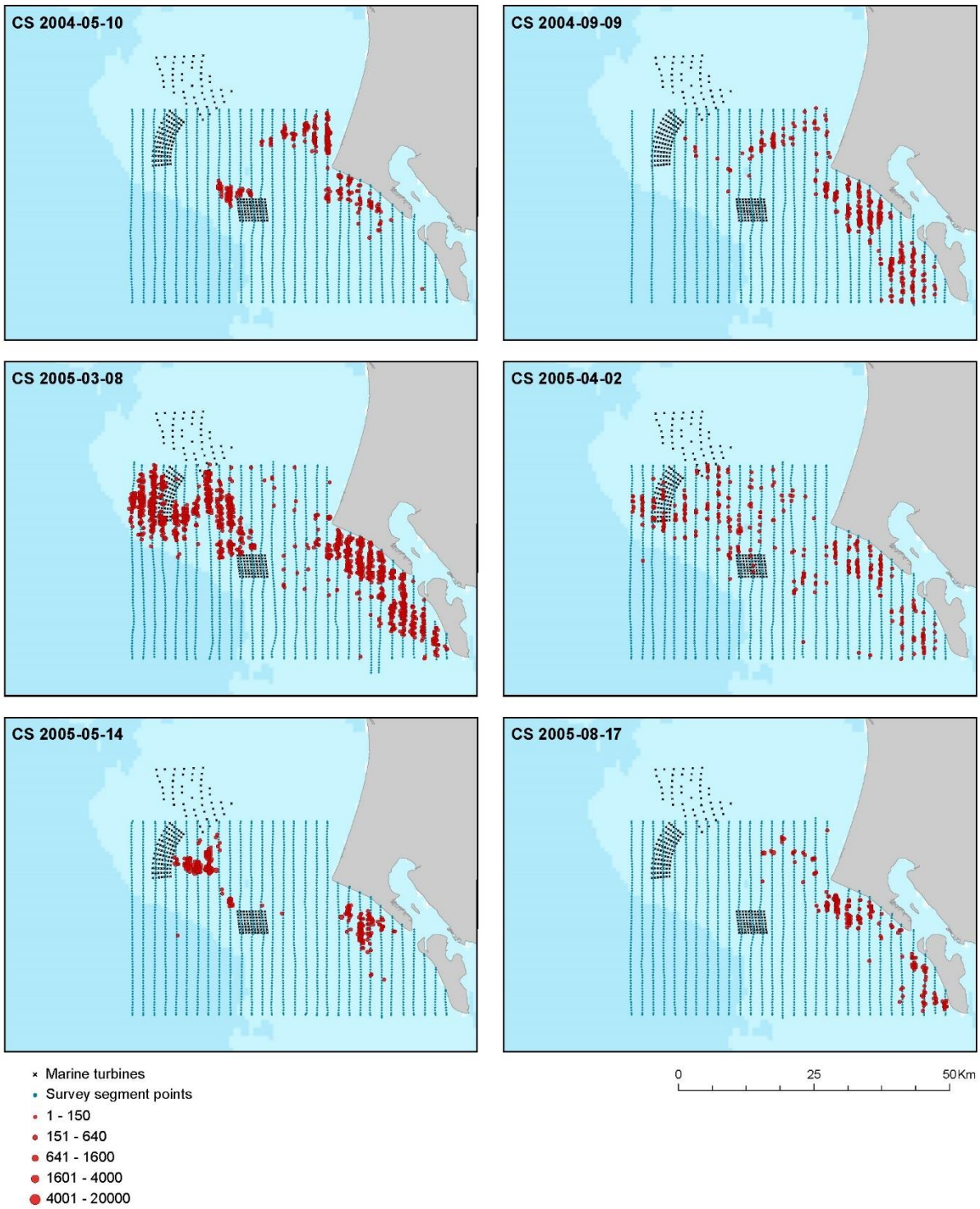

Figure 8-5. The distribution of observed common scoter during six surveys from May 2004 to August 2005.

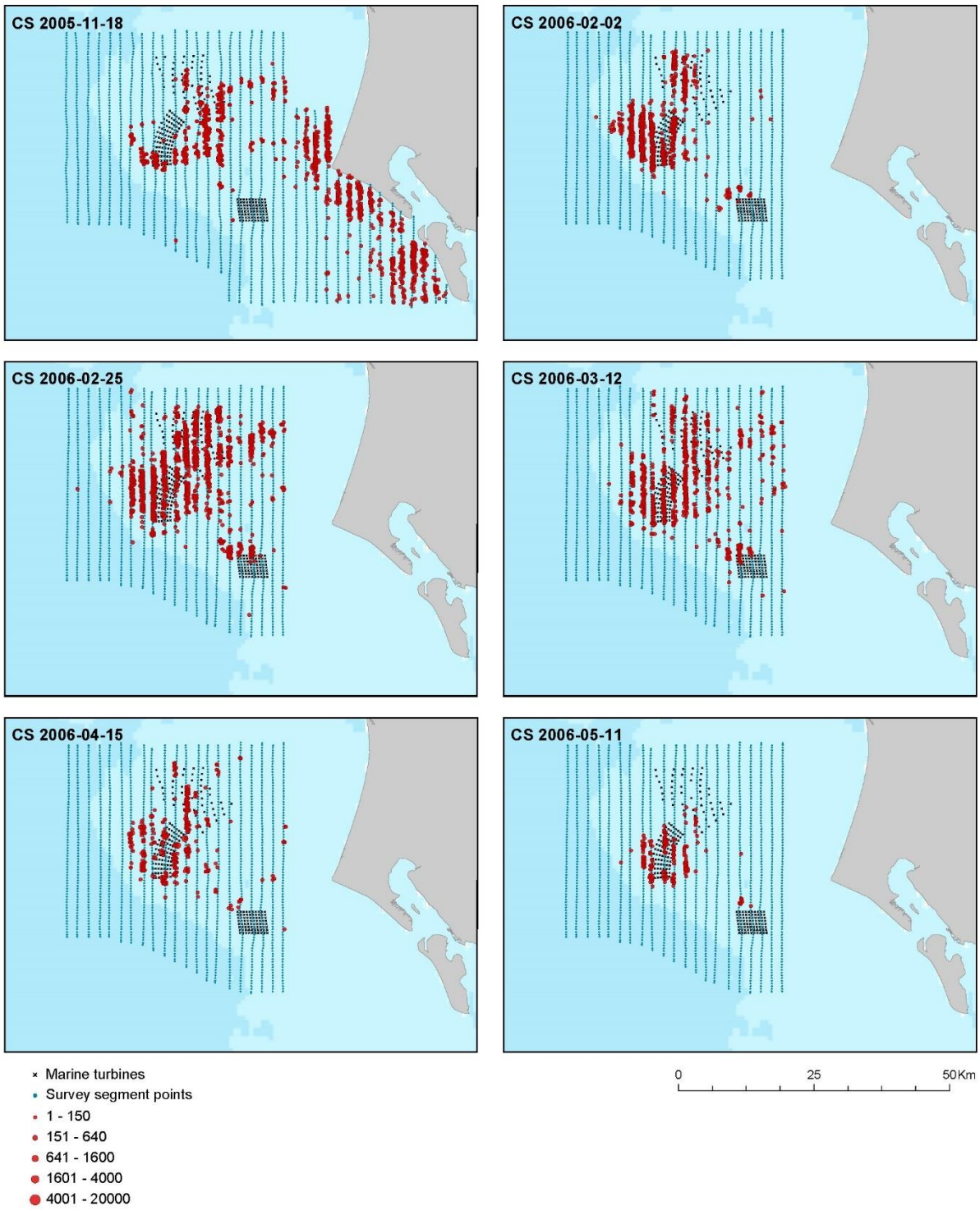

Figure 8-6. The distribution of observed common scoter during six surveys from November 2005 to May 2006.

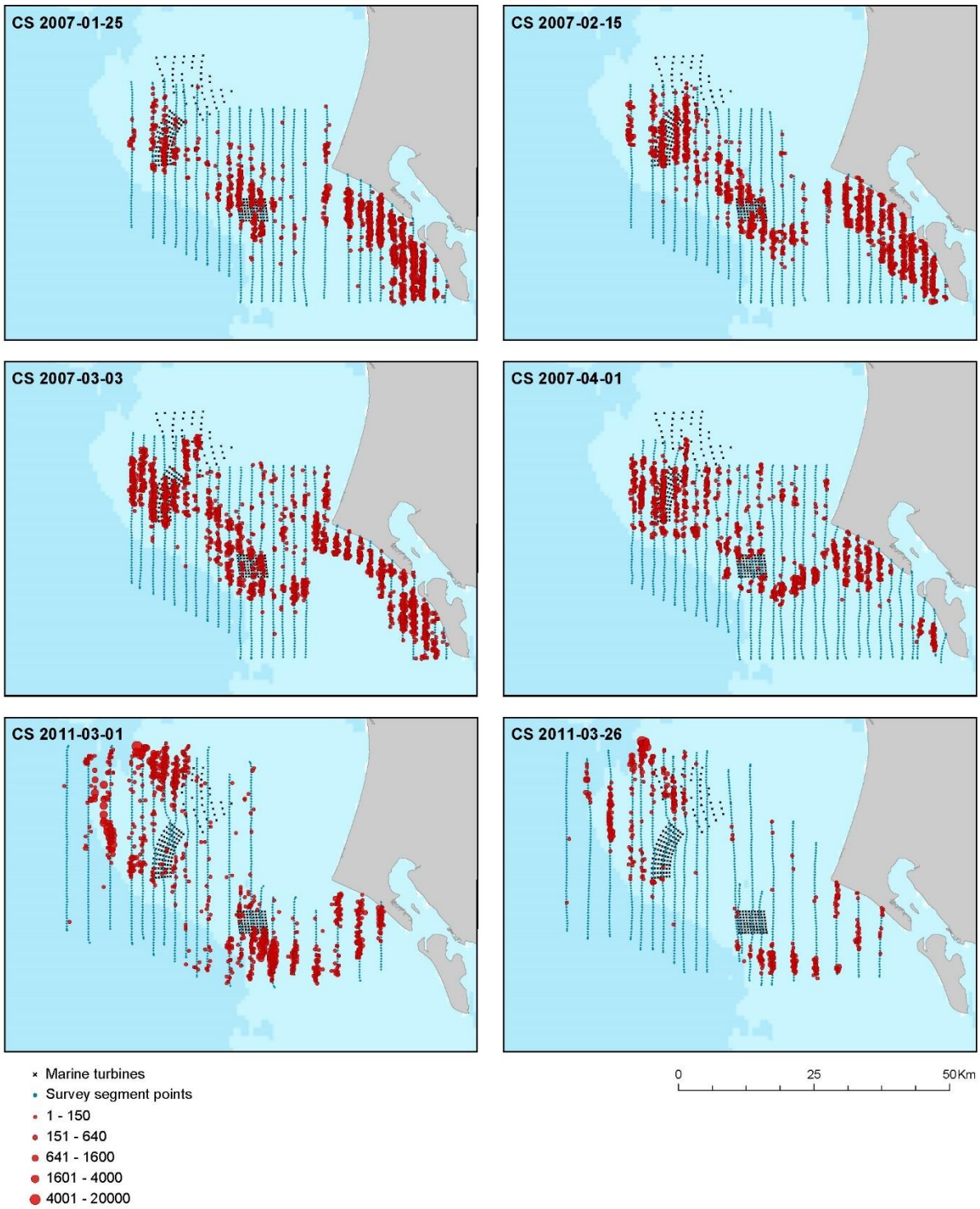

Figure 8-7. The distribution of observed common scoter during six surveys from January 2007 to March 2011.

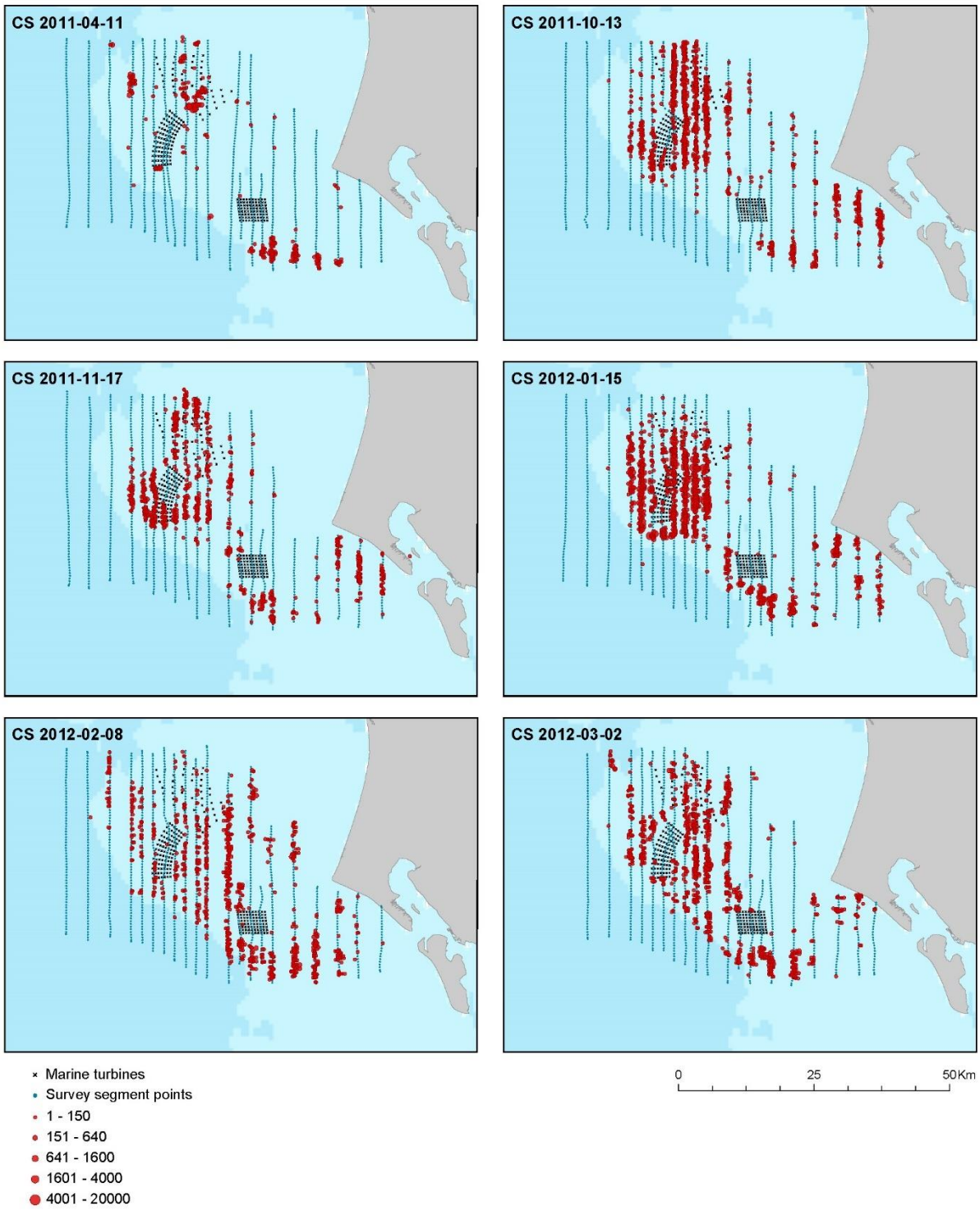

Figure 8-8. The distribution of observed common scoter during six surveys from April 2011 to March 2012.

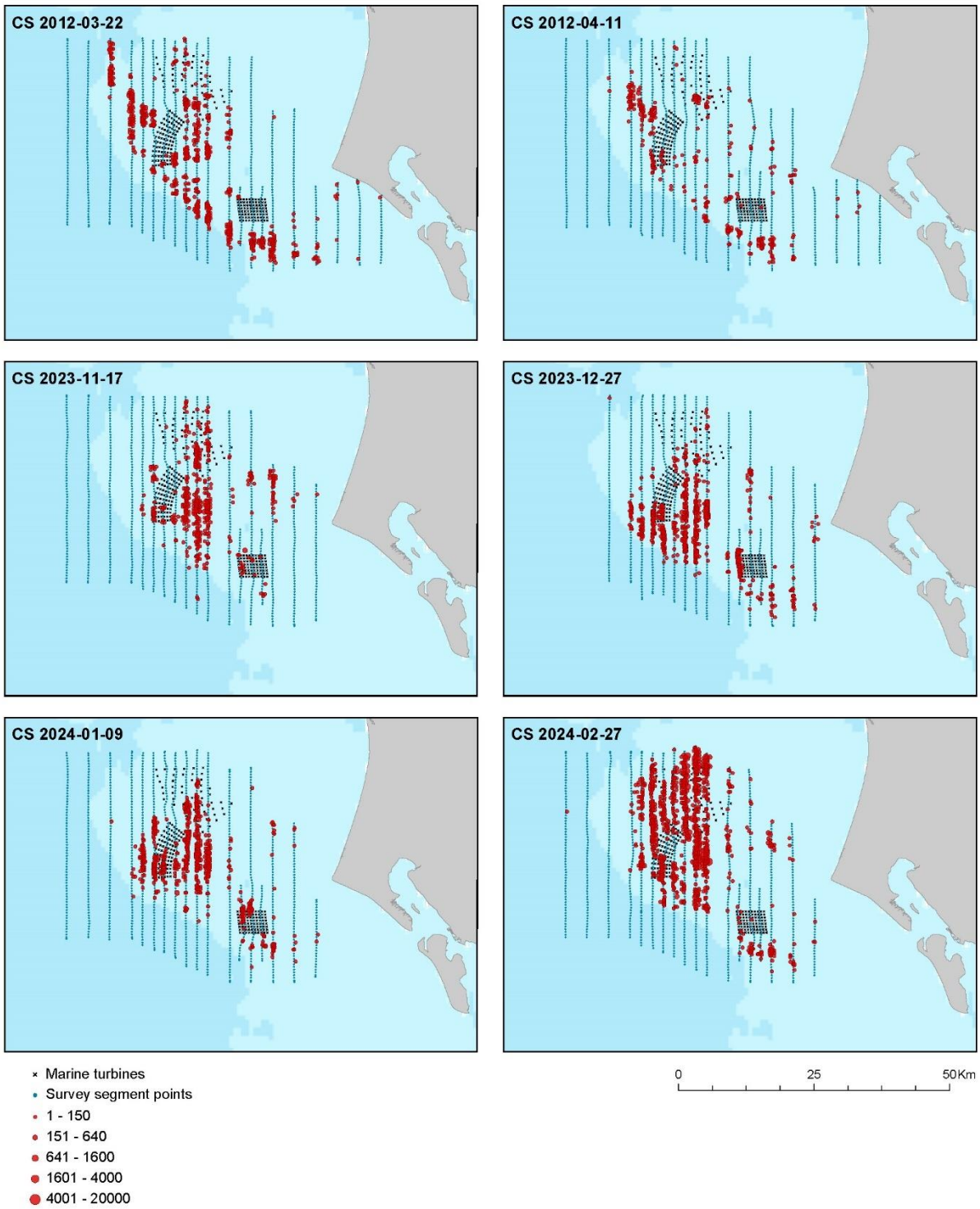

Figure 8-9. The distribution of observed common scoter during six surveys from March 2012 to February 2024.

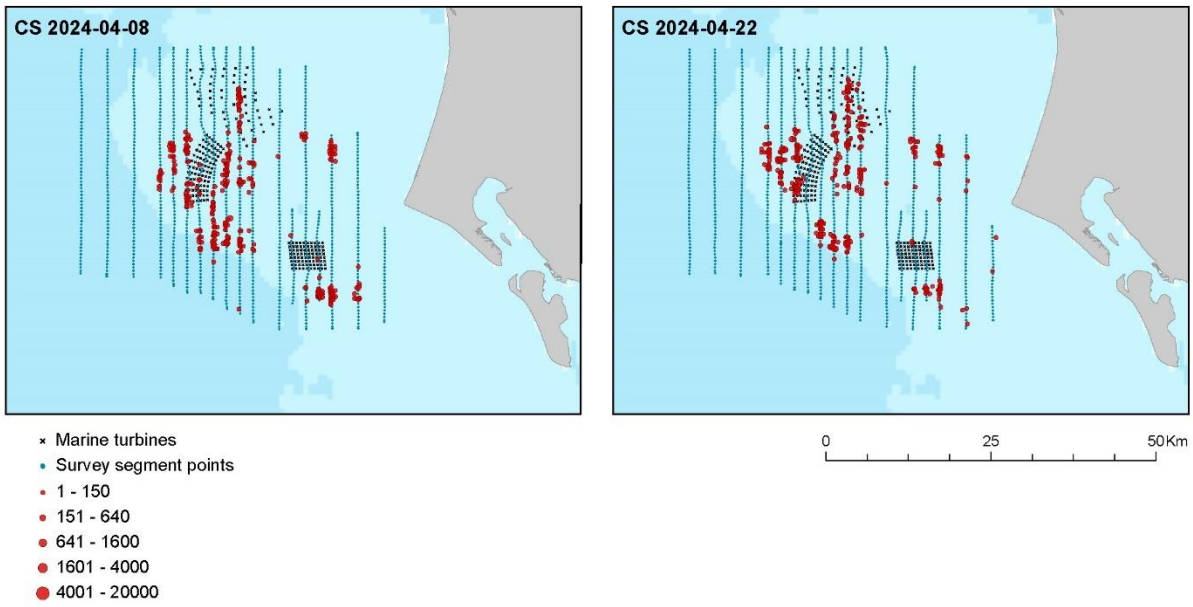

Figure 8-10. The distribution of observed common scoter during two surveys in April 2024.

The transect coverage and the distribution of the observed red-throated divers/black-throated divers by survey is given in Figure 8-11 to Figure 8-20.

Figure 8-11. The distribution of observed red-throated diver/black-throated diver during six surveys from February 2000 to October 2000.

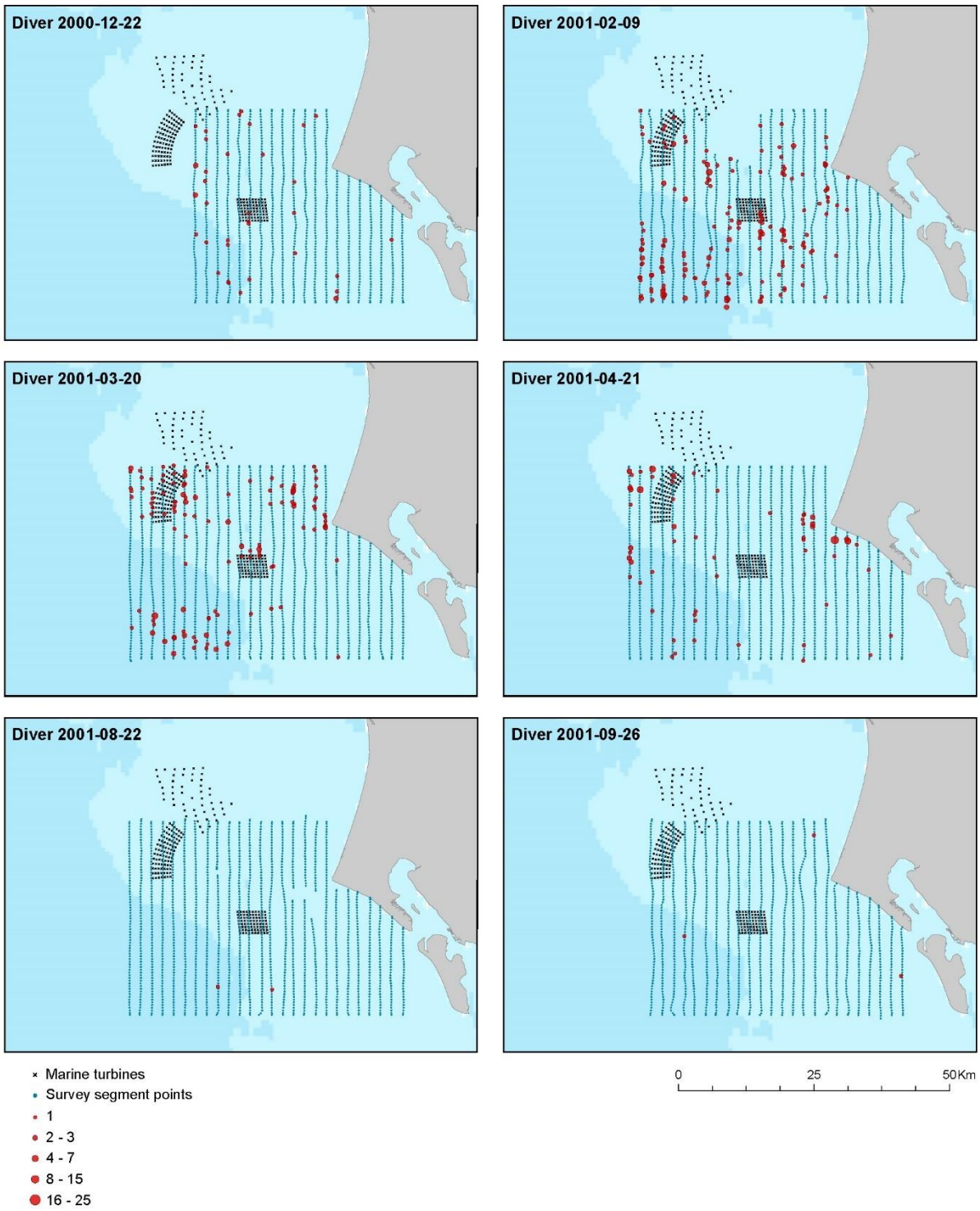

Figure 8-12. The distribution of observed red-throated diver/black-throated diver during six surveys from December 2000 to September 2001.

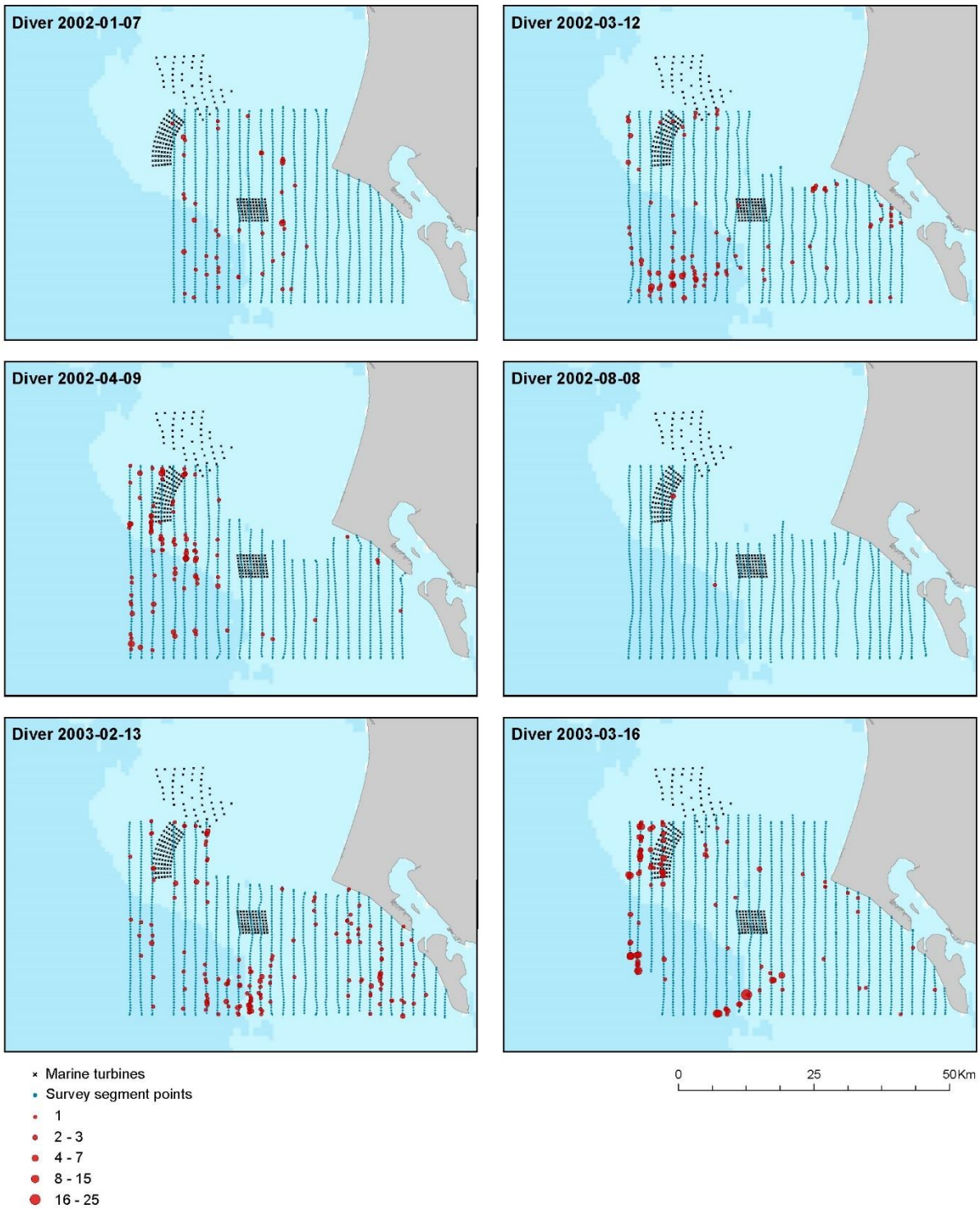

Figure 8-13. The distribution of observed red-throated diver/black-throated diver during six surveys from January 2002 to March 2003.

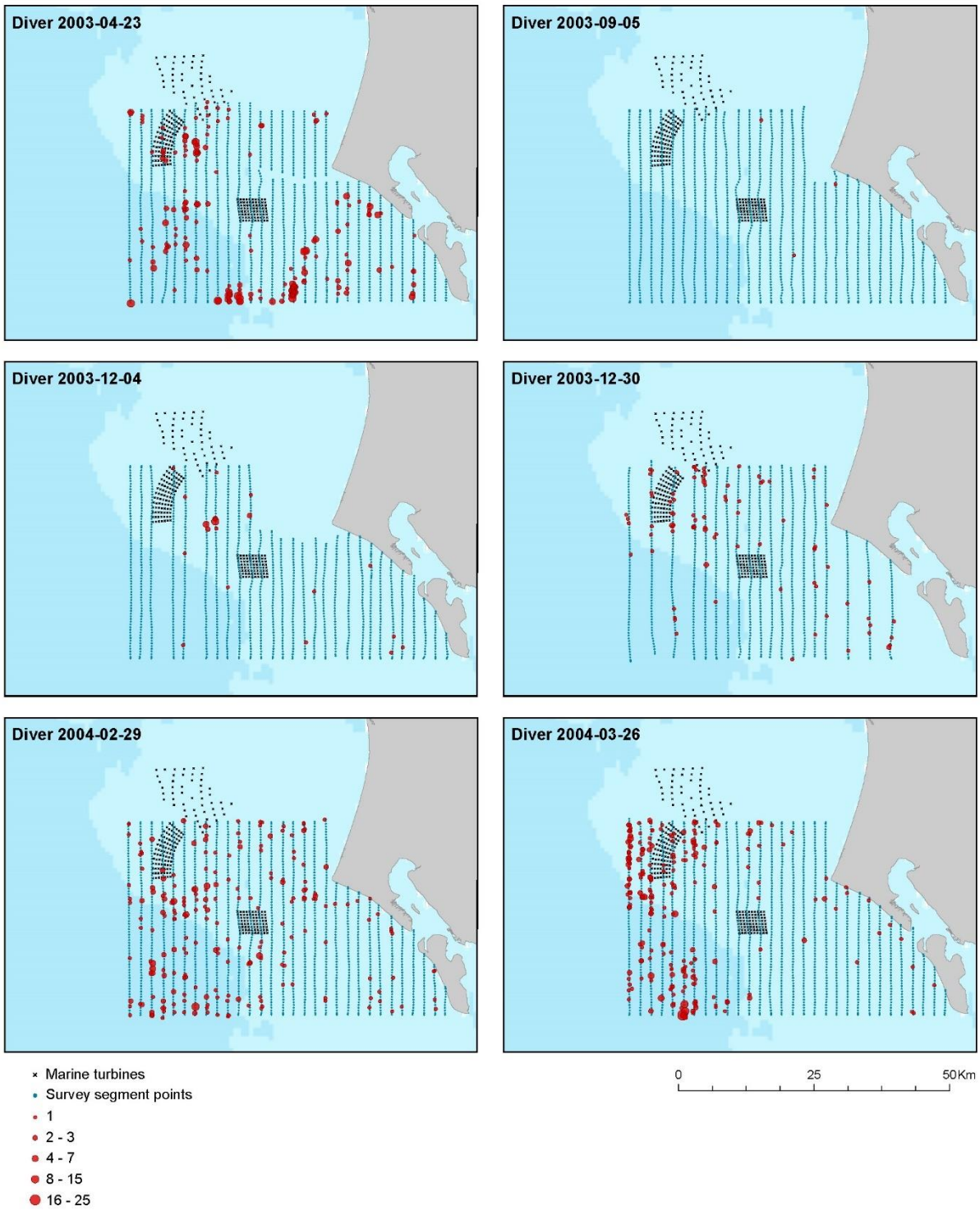

Figure 8-14. The distribution of observed red-throated diver/black-throated diver during six surveys from April 2003 to March 2004.

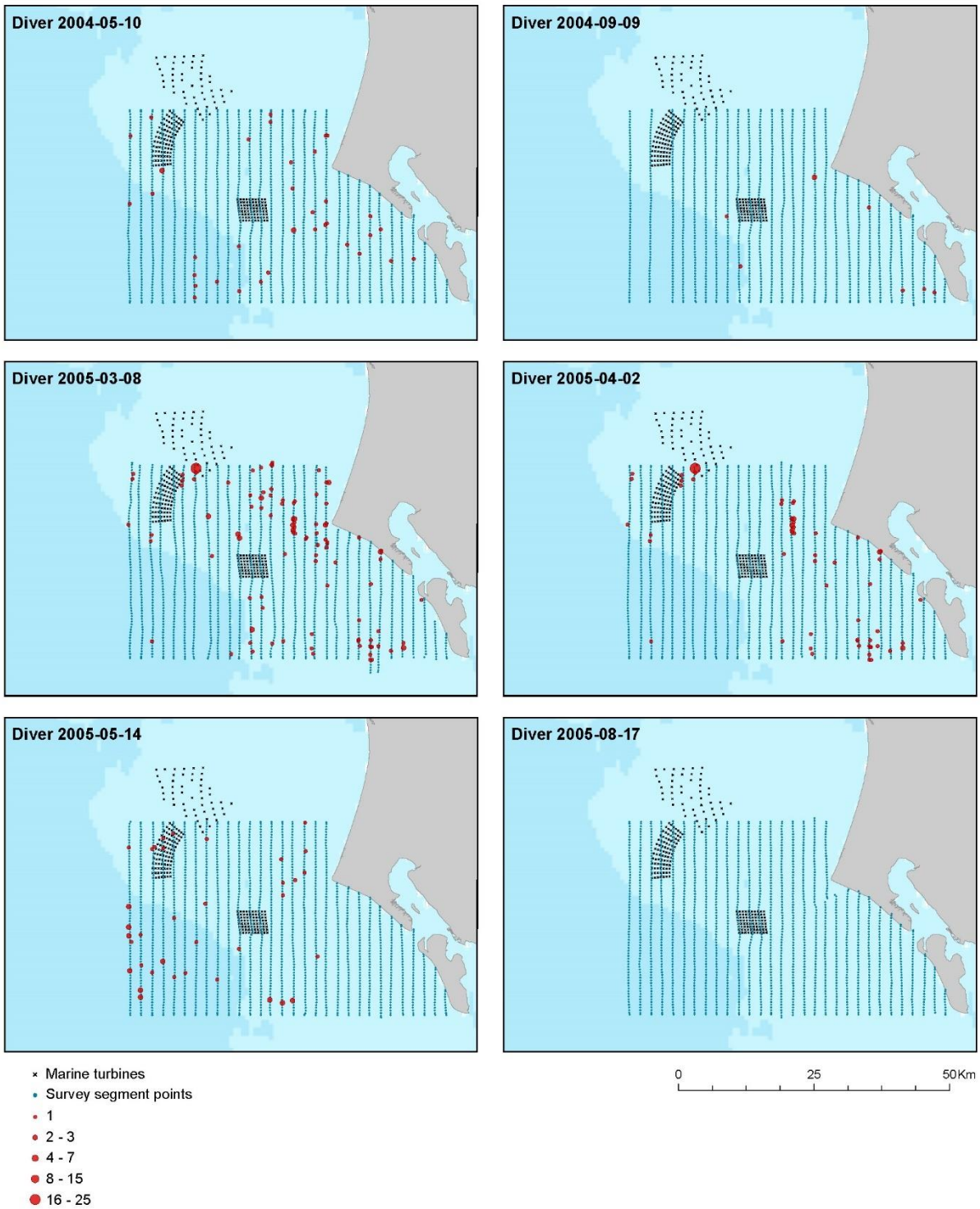

Figure 8-15. The distribution of observed red-throated diver/black-throated diver during six surveys from May 2004 to August 2005.

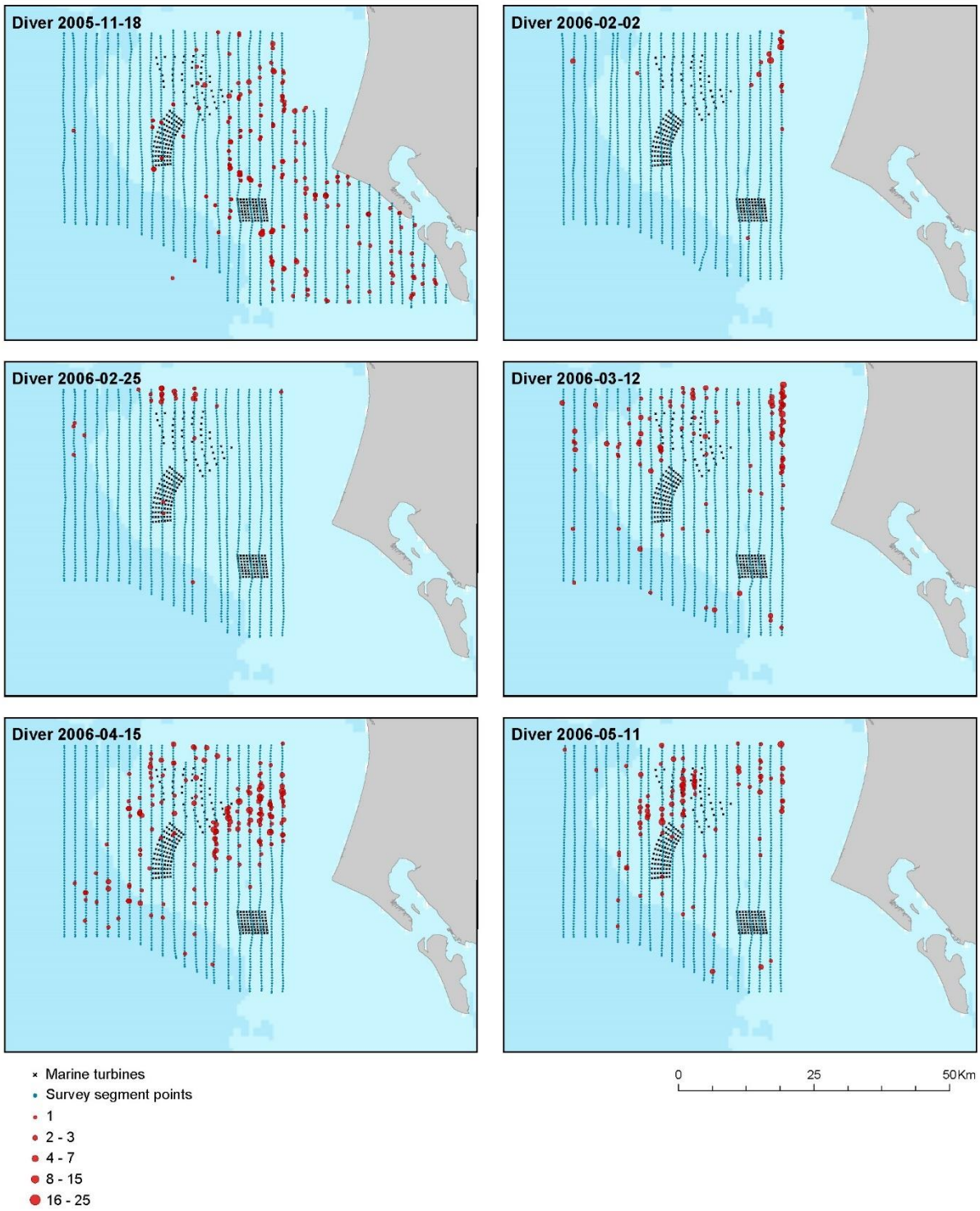

Figure 8-16. The distribution of observed red-throated diver/black-throated diver during six surveys from November 2005 to May 2006.

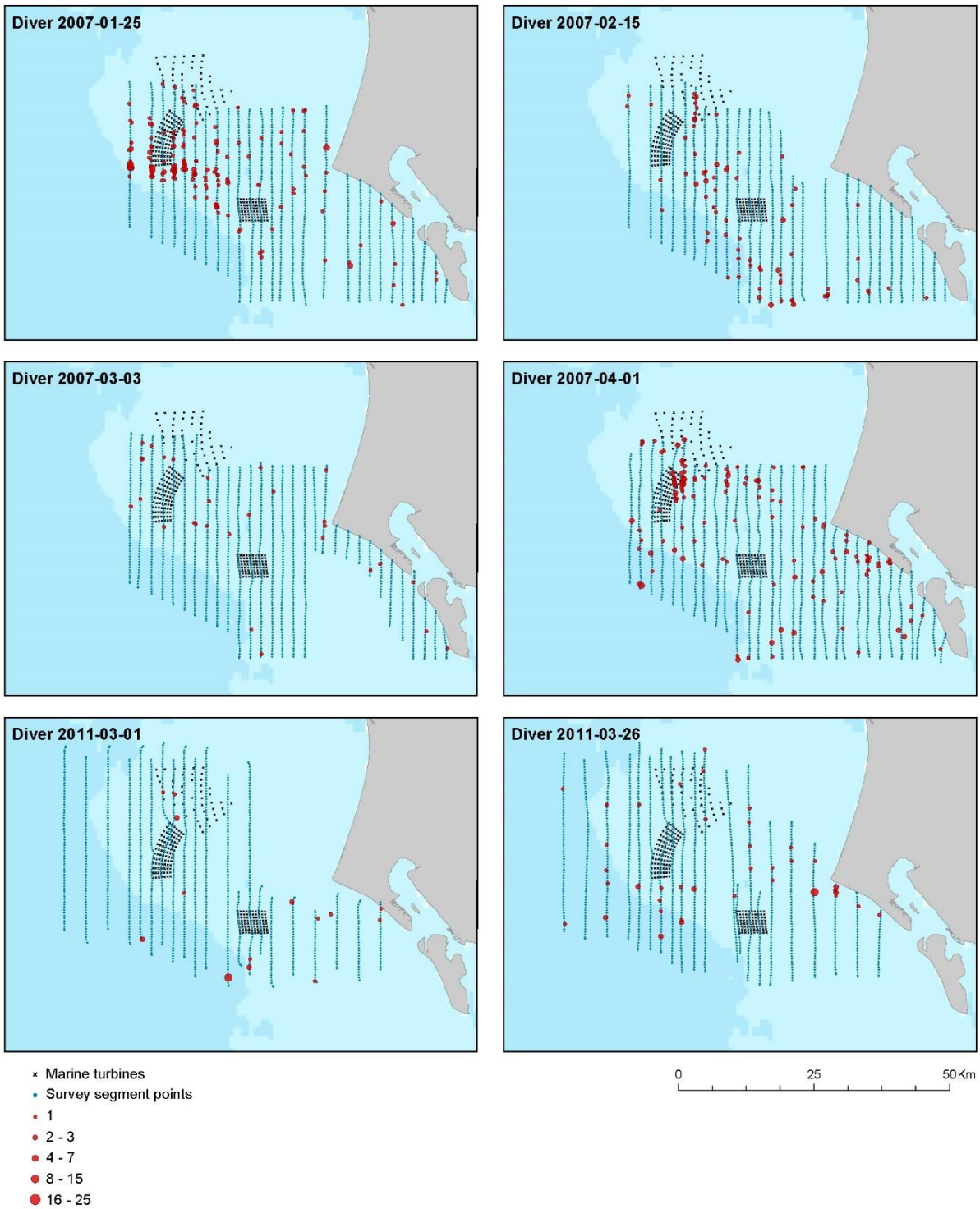

Figure 8-17. The distribution of observed red-throated diver/black-throated diver during six surveys from January 2007 to March 2011.

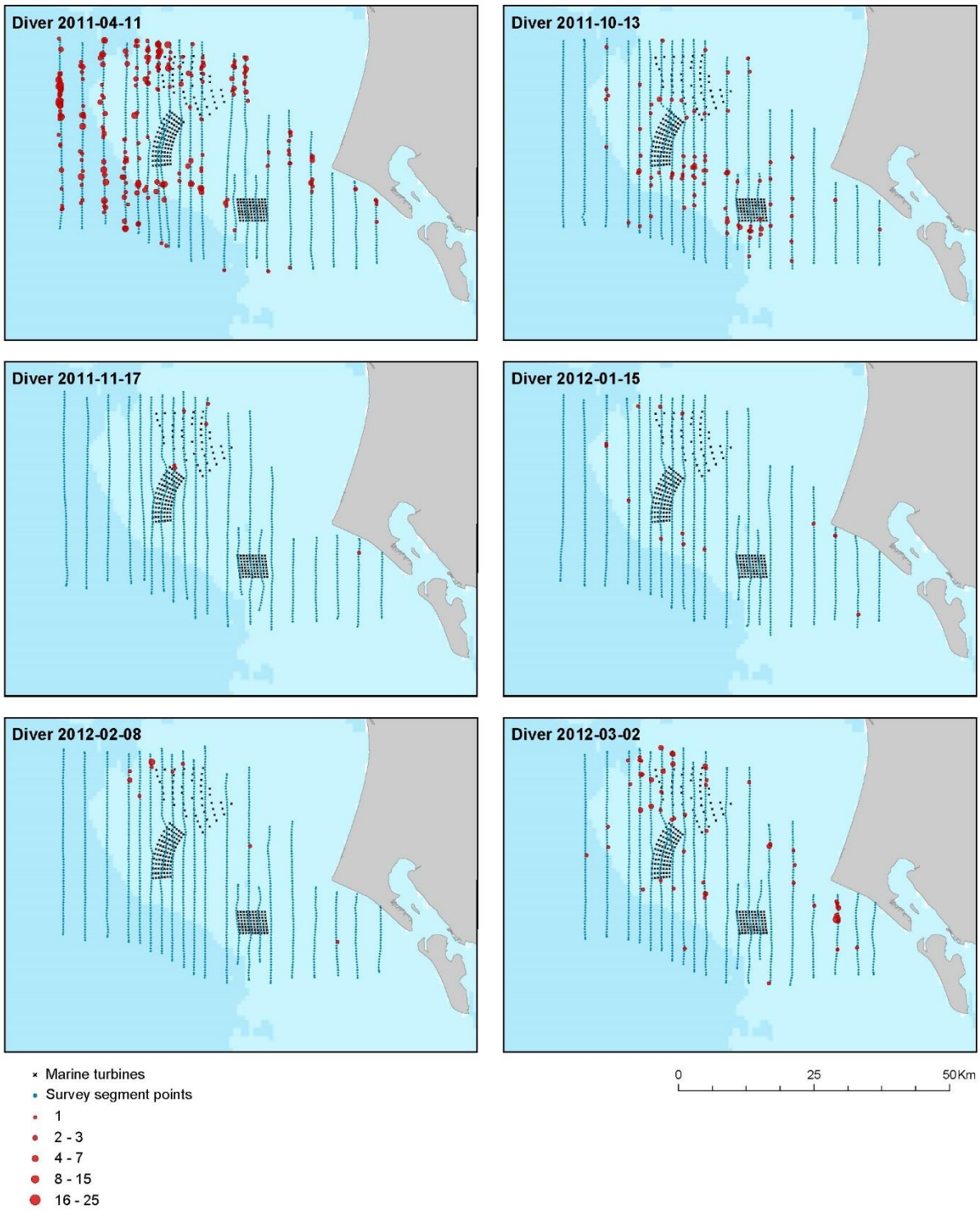

Figure 8-18. The distribution of observed red-throated diver/black-throated diver during six surveys from April 2011 to March 2012.

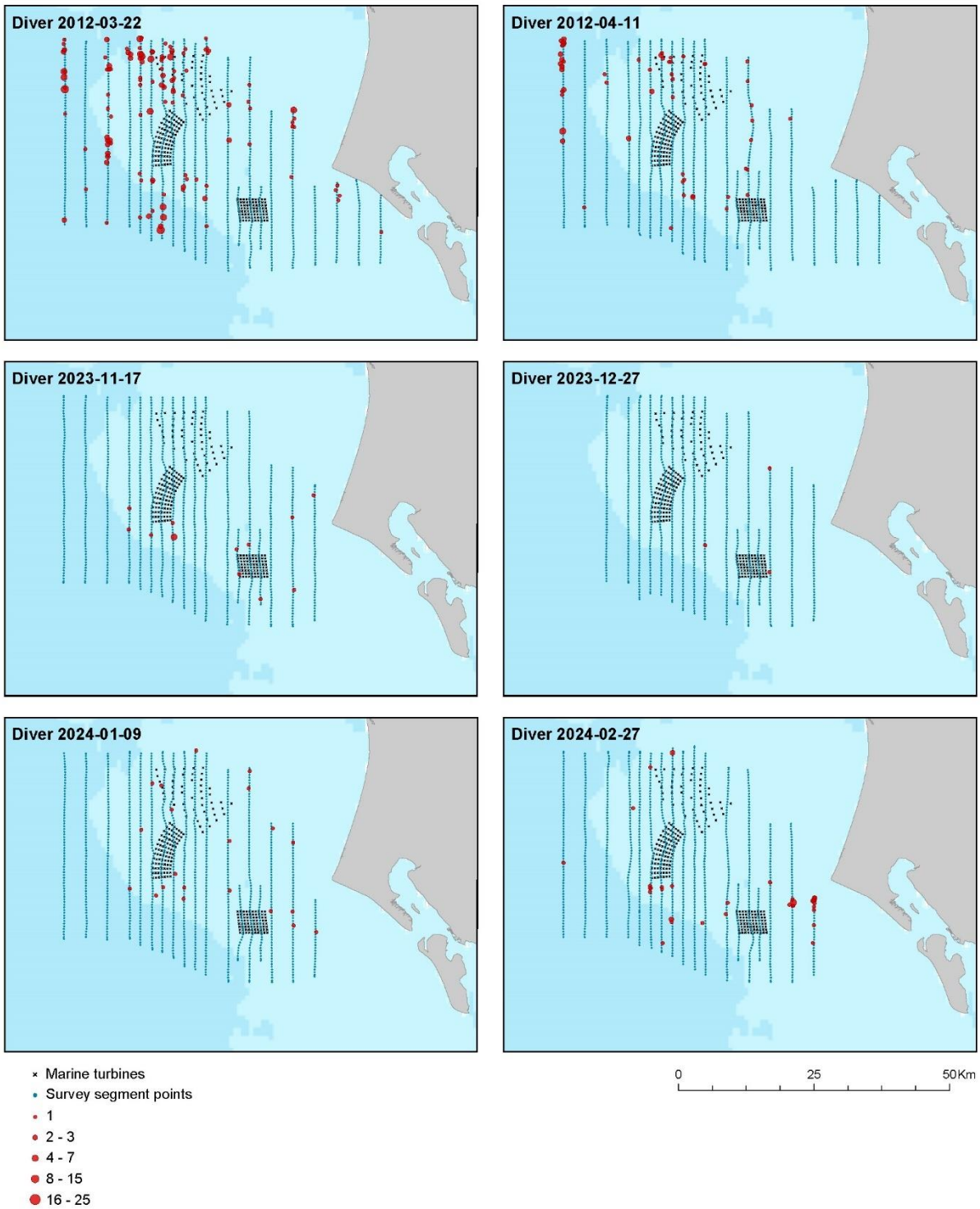

Figure 8-19. The distribution of observed red-throated diver/black-throated diver during six surveys from March 2012 to February 2024.

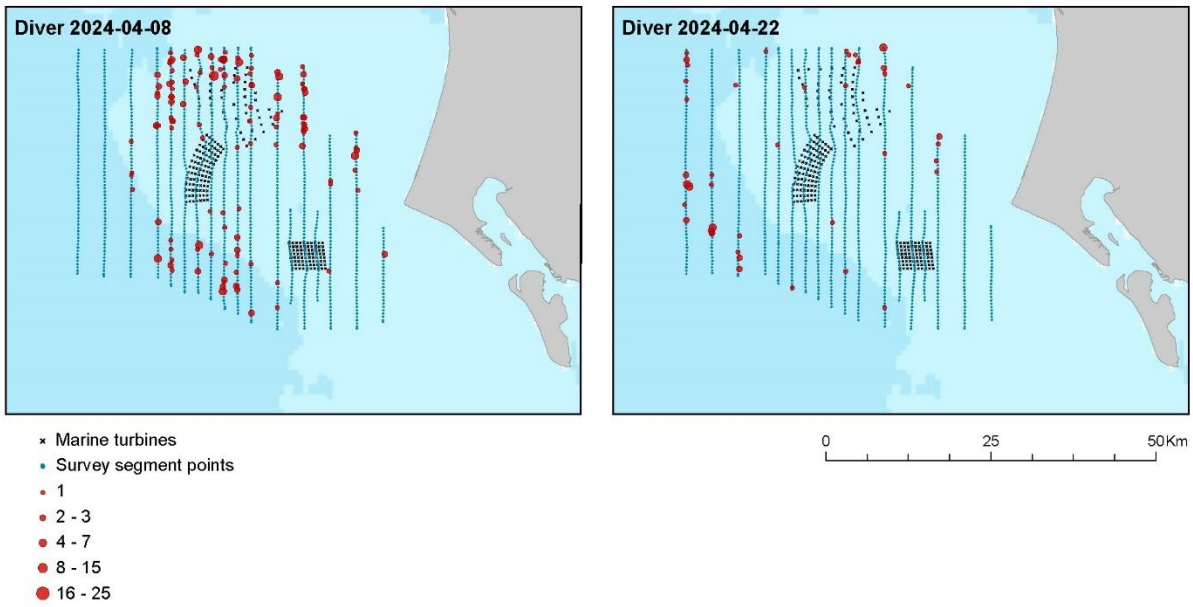

Figure 8-20. The distribution of observed red-throated diver/black-throated diver during two surveys in April 2024.

Appendix 2

Details of the Modelling Methods

8.2 Distance Sampling

Distance sampling analyses were conducted for each of the species/species groups by pooling the information across all surveys.

When fitting detection functions, the effects of covariates, other than perpendicular distance, are incorporated into the detection function model directly (Multiple Covariate Distance Sampling, MCDS) (F. F. C. Marques and Buckland 2004; T. A. Marques et al. 2007; Buckland et al. 2001). In these cases, the probability of detection becomes a multivariate function, which represents the probability of detection at perpendicular distance and covariates, where Q is the number of covariates). In this study, using a half-normal detection function $e^{-\left(\frac{y^2}{\sigma^2}\right)}$ the covariates were incorporated via the scale term, σ, where for sighting j, σ has the form:

$$\sigma_j = \exp\left(\beta_0 + \sum_{q=1}^{Q}(\beta_q v_{jq}\right)$$

where β_0 and β_q $(q = 1, \dots, Q)$ are parameters to be estimated (Buckland et al. 2001). Both half-normal and hazard rate detection functions were fitted with BIC used to choose between the two models. The candidate variables trialled were bird group size, behaviour, observer and sea state (see Table 2-2). For some observers there were too few observations so in those cases, the observers' observations were combined with the next smallest. Observations with sea states greater than four were removed. For scoters, which were occasionally seen in very large numbers (up to 20,000), any observations with ≥ 2000 birds were assumed to have perfect detection and omitted from the detection analysis. These observations were included in the segmentation in preparation for the spatial analysis.

Table 12: Table detailing the covariates used in the detection function fitting.

Covariates	***Values***
Behaviour	S (sitting or diving) and F (flying or flushing)
Observer	17 Observers
Sea State	0, 0.5, 1, 1.5, 2, 2.5, 3, 3.5 (calm to rough)

8.2.1 Mitigating the effects of Glare

Detection of sea birds from aerial surveys can be influenced by sighting conditions, such as sun glare and sea state. Data to describe sighting conditions is usually collected in-situ, however when this is absent, alternative methods are required to identify (and adjust for) heterogeneity in the detection probability. Accounting for such heterogeneity is particularly important for distance sampling where near-perfect detection at the track line is an often-required assumption.

We used detection information from band A for the left-hand and right-hand sides of the aircraft to identify transect lines with likely poor sighting conditions. For both species, the identified transects had observations from the affected side removed and the coverage reduced to one side (i.e. returning a one-sided transect).

The effects of glare, and any mitigations as a result, was approached using a dedicated analysis. The analysis was designed to quantify the extent that directional sun glare can lead to left/right hand side bias in counts within a single transect line with the same direction of travel. Specifically, we assumed that the proportion of left or right sightings in band A should be 0.5 and follow a Binomial distribution. We compared the proportions for each transect to a critical value calculated as the quantile of the Binomial $(n, p = 0.5)$ distribution at three standard errors greater than the mean and where n is equal to the number of observations on the transect. Three standard errors is a common measure in extreme value theory (Leys et al. 2013). Any transects whose values were greater than the critical value had the observations from the smaller side removed and the coverage reduced to a single side.

8.2.2 Spatial Modelling

Model Framework

The response variable for the spatial models under analysis here, are bird counts in a small area (segment) which have been corrected for detectability. This response was modelled using a Tweedie framework, which includes an estimated dispersion parameter (ϕ) and Poisson-Gamma mixing parameter (ξ) to return an appropriate mean-variance relationship in each case. The mixing parameter takes on values from 1 (equivalent to quasi-Poisson) and 2 (equivalent to Gamma). If the estimated parameter was close to one, the models were considered quasi-Poisson. A set of candidate explanatory variables were associated with each segment to model the signal, and in this study each of the 62 surveys was analysed separately, including covariate selection, for each species. The candidate environmental covariate was water depth (bathymetry) while distance from coast (as a one-dimensional term) was also considered in each model, in the unlikely case there was compelling evidence for consistent spatial patterns with distance from coast which were the same in all directions. Additionally, to account for more realistic (and localised) surface patterns (due to perhaps unmeasured covariates) a spatial surface was also fitted to each model. Specifically, a two-dimensional CReSS-based surface using a Gaussian radial basis function was included in the model (Scott-Hayward, Oedekoven, et al. 2014).

As an illustration, the following equation represents an example of a Tweedie model with log link function and fitted with a one-dimensional smooth term (e.g., bathymetry) alongside a two-dimensional spatial smooth:

$$y_{ij} \sim Tw(\mu_{ij}, \phi, \xi)$$

$$\mu_{ij} = e^{\left(\beta_0 + s_1\left(\text{Bathymetry}_{ij}\right) + s_2\left(\text{XPos}_{ij}, \text{YPos}_{ij}\right)\right)}$$

where y_{ij} is the estimated count for transect i segment j and s_1 represents either a quadratic B-spline or natural cubic spline smooth of depth. Here, s_2 is a two dimensional smooth of space (with coordinates XPos and YPos in UTMs). Implicit in this model are also coefficients for the intercept (β_0) and any spline based coefficients associated with the smooth terms. The effort associated with each observation varied depending on the associated segment area and so segment area was included as an offset term (on the log scale).

A globally applicable depth or distance to coast term and a more flexible spatial term were trialled for inclusion in each model, to indicate how best to model spatial patterns in each case. In particular, this quantifies if any spatial patterns are sufficiently described by the one-dimensional covariates (which applies the same across the surface) or if a more considered approach to spatial patterns was required for each survey and for each species. For example, if depth was selected and a two-dimensional spatial element was not deemed necessary (as determined by the model selection procedure governed by objective fit criteria) then this signals that any spatial patterns are primarily a function of the depth, regardless of the geographical location of this depth in the survey area.

If the two-dimensional spatial term was selected for inclusion in a model, then the spatial density patterns (over and above any environment-related terms) were accommodated using a spatially adaptive term which permits different amounts of flexibility across the surface in a targeted and yet parsimonious way (hence, relatively complex spatial patterns can be accommodated with very few parameters).

Selection between competing models was undertaken using an information criterion metric, BIC, which has a penalty related to the extent of the data supporting the model.

Model specification, selection and fitting

CReSS-SALSA based spatially adaptive generalized additive models, with targeted flexibility, were fitted to data from each survey to allow for non-linear relationships between the one-dimensional and two-dimensional covariates and the response (Scott-Hayward, Mackenzie, et al. 2014, 2014; Scott-Hayward et al. 2023; Walker et al. 2010).

All covariates were permitted to have a linear or nonlinear relationship with the response, and when a smooth term was included in a model it was specified to be either a quadratic (degree 2) *B*-spline (df=3,4,5) or a natural cubic spline (df=2,3,4). In cases where these degrees of freedom boundaries were reached however, a broader range of parameters were trialled instead. The degrees of freedom for these terms determine the flexibility of these smooth (and nonlinear) relationships - the more degrees of freedom, the more flexible the relationship can be.

The location of this flexibility (along the x-axis) in these terms (e.g., depth) was also determined as part of the model selection process. This permitted the relationship in some areas of the covariate range to be relatively complex (e.g., in shallow waters) and the relationship in other areas (e.g., in deep waters) to be relatively simple. In both smooth types, a maximum of three internal knots was permitted along with the spline specific number of boundary knots. The number and location of knots was determined by an objective fit criterion.

The spatial patterns in each analysis were based on a two-dimensional spatial term (of variable complexity). The flexibility of the spatial element constituted part of the model selection procedure and for each survey was determined using a Spatially Adaptive Local Smoothing Algorithm (SALSA). While this model selection element technically occurred between limits (df=[2,100]), the flexibility chosen in each case was not bounded in practice by those values since the selection procedure occurred well within the bounds of the specified range.

The `MRSeaPP` `R` package, designed to fit both CReSS and SALSA type models when quadrature points are included, was used for model fitting. For computational reasons, BIC was used to determine the flexibility of the smooth terms (knot number and placement) while, the more computationally intensive 5-fold cross-validation (CV) was used to govern the inclusion/exclusion of covariates (R Core Team 2022; Scott-Hayward, Mackenzie, and Walker 2023). The CV procedure attempts to balance the fit to data unseen by the model while minimising the number of parameters (parsimony). Note, this cross validation was predicated on preserving correlated blocks of survey data (transect lines) so that any residual autocorrelation present was not disrupted when choosing folds. This was considered necessary to ensure independent sampling units under the scheme.

Parameter inference

The response data were collected along survey lines in sequence, and so consecutive observations are likely to be correlated in space and time (i.e., points close together in space and/or time are likely to be more similar that points distance in time and/or space). Further, the covariates included in the model are unlikely to explain these patterns in full and so some element of these patterns are likely to remain in model residuals. These patterns are a violation of residual independence (which underpin traditional model approaches such as Generalized Additive Models), and thus robust standard errors were routinely used as part of the **MRSeaPP** modelling framework to account for residual auto-correlation.

Uncertainty about model parameter estimates proceeded via robust standard errors due to the nature of the survey procedure. These essentially work by inflating the standard errors (which would normally be obtained under traditional approaches) in relation to the positive correlation observed within pre-specified blocks of residuals. In cases, where this residual correlation is minimal, the adjustments are small, and when the correlation is more extreme, the inflation is larger.

A transect-based blocking structure was used to reflect potential correlation within blocks while independence (i.e., no correlation) between blocks was assumed. To ensure this assumption was realistic, the decay of any residual correlation to zero (i.e., independence) with the distance between points (within blocks along transects) was assessed visually. Specifically, transects in each survey were used as the blocking structure and an Auto Correlation Function (ACF) plot on this basis was used to check the suitability of this blocking structure, via a 'decay to zero' trend within blocks.

Modelling diagnostics

To assess the adequacy of model fit in each case, a range of diagnostic measures were used.

The assumed mean-variance relationship under the model was assessed visually using plots of the fitted values from the model against the variance of the residuals. In this analysis, Tweedie models were employed which assume a nonlinear mean-variance relationship:

$$Var(y) = V(\mu)\phi = \mu^{\xi}\phi$$

ϕ is the dispersion parameter. The dispersion parameter was estimated for each model and this estimate was used in the visual assessment of this mean-variance relationship assumed to hold under the model. ξ is the power parameter and is estimated prior to model fitting using a maximum likelihood profile approach. Based on the nature of the response data, values of ξ were permitted between 1 (Quasi-Poisson) and 2 (Gamma).

QQ plots and residuals against predicted values plots were assessed to ascertain the level of agreement between the data and the model. These plots were created using the **DHARMa** **R** package and using simulated residuals.

Regarding interpretation the left panel is a uniform QQ plot, and the right panel shows residuals against predicted values, with outliers highlighted in red. Given these outputs, we would expect that a correctly specified model shows:

a) a straight 1-1 line, as well as no compelling evidence against the null hypothesis of a correct overall residual distribution, as indicated by the *p*-values for the associated tests in the QQ-plot.

b) visual homogeneity of residuals in both the vertical and horizontal directions, in the residuals against predictor plot.

Pearson residuals for each model were also visualised spatially to ensure there were no areas of consistent bias across the survey area. This would be indicated by clusters of negative or positive residuals in spatially similar locations.

Residual independence was not assumed to hold under the model and instead model inference proceeded under robust standard errors. As described, Auto Correlation Function (ACF) plots were instead used to check the suitability of this blocking structure, via a 'decay to zero' trend within blocks.

8.2.3 Model Predictions and estimates of uncertainty

Based on each selected model, predictions of counts were made to a grid of points (each point representing 500x500 meter grid cell) across the study region. Additionally, abundances within the survey-based prediction region were obtained by summing the grid cell counts across the relevant areas.

The uncertainty in the detection function was reflected using a parametric bootstrap ($n = 500$) of the fitted distance sampling model. This generated new estimated counts for each segment. The selected spatial model was then re-fitted to each of the new datasets to obtain a new set of parameter estimates for the model. The final output of this process was a parametric bootstrap procedure using the robust variance-covariance matrix from each parametric bootstrap model. These were used to calculate 500 sets of model predictions which generated 95% percentile-based intervals and allowed a coefficient of variation for each grid cell to be calculated. If it was not possible to fit a spatial model to the data, the abundance estimates for the survey were calculated from the distance analysis parametric bootstraps.

A calculation of 'persistence' was also undertaken across surveys within phases, and across all surveys considered together, within species using the geo-referenced estimates of density (abundance/associated area)

across the survey area. Persistence scores were calculated for every grid cell in the following way: Each bootstrap replicate was allocated a binary value based on whether, or not, the estimate in each location was above the mean estimated density (1) throughout the survey area or below this mean estimated density (0). This was performed for all sets of plausible predictions in each grid cell (based on the bootstrap replicates) and the proportion of these bootstrap predictions in excess of the mean (indicated by the value of 1) was calculated for each grid cell to give a persistence score for that location. A persistence score of 1 indicates that the density in that grid cell was estimated to be above average in every bootstrap replicate in every survey (so uniformly above the mean; high persistence) while a value of 0.1 indicates that just 10% of the estimates were above the estimated mean, and thus indicates low persistence in that location.

Distributional changes over time were evaluated by comparing the estimated distributions from the four phases. Additionally, any changes during this time in and around the three wind farm footprints could also be observed. Difference plots were used to visualise any spatially explicit changes in the distribution of animals. The bootstraps from the modelling process described above were used to generate a 95- percentile interval for the difference in abundance in each grid cell. If the interval contained zero it was deemed not to indicate a statistically significant difference in abundance between the two comparison years. If the range of plausible values for the difference (indicated by the 95% confidence interval) did not include zero, then the change was deemed to be significantly positive or negative. These bootstrap based cell-wise differences between phases were also viewed in concentric rings with distance from the Horns Rev II footprint.

8.2.4 Observed number of birds observed by species and survey, 2023 to 2025

Table 8-2. The number of observed birds by species and survey during the 2023/2024 Horns Rev surveys

Species	Sum	17 NOV 2023	27 DEC 2023	09 JAN 2024	27 FEB 2024	04 APR 2024	22 APR 2024
Diver sp.	49	11	3	12	2	21	
Red-throated diver	317	4		9	42	196	66
Gannet	526	11	7			192	316
Cormorant	6	1		3	1	1	
Shag	1		1				
Brent goose	4	4					
Tufted duck	2				2		
Common scoter	151,400	11,404	17,370	26,594	80,503	5,924	9,605
Velvet scoter	173	1	9	3	13	26	121
Arctic skua	1					1	
Common gull	314		4	60	188	62	
Herring gull	1,921	251	165	238	1,042	220	5
Lesser black-backed gull	11				1	10	
Great black-backed gull	43	1	9		5	25	3
Little gull	103	55	4	19	19	4	2
Kittiwake	382	178	135	37		31	1
Gull sp.	645	3	3	502		87	50
Arctic/common tern	209						209
Sandwich tern	148						148
Tern sp.	39						39
Razorbill	22		18			4	
Razorbill/common guillemot	1,795	306	25	11	121	1,277	55
Common guillemot	86	12	3		2	65	4

Table 8-3. The number of observed birds by species and survey during the 2024/2025 Horns Rev surveys.

Species	Sum	05 NOV 2024	10 DEC 2024	15 FEB 2025	28 FEB 2025	20 MAR 2025	03 APR 2025
Diver sp.	42		4	12	3	22	1
Red-throated diver	476	9	21	98	87	182	79
Black-throated diver	1				1		
Grebe sp.	10					10	
Gannet	35	16		2	1	13	3
Cormorant	4	1	1	2			
Grey heron	1						1
Greylag goose	19						19
Teal	8					8	
Wigeon	6					6	
Common eider	2			2			
Common scoter	18,052	3,573	6,353	3,701	1,082	2,257	1,086
Velvet scoter	66	1	13	24	8	2	18
Diving duck sp.	4				4		
Common gull	1,960	246	160	67	175	1,004	308
Herring gull	390	240	51	4	13	37	45
Common gull/herring gull	274				103	127	44
Lesser black-backed Gull	18	1			2	4	11
Great black-backed gull	16	11	1	2	1	1	
Black-headed gull	18					17	1
Little gull	477	141	127	75	27	107	
Kittiwake	826	673	29	19	32	73	
Gull sp.	254	101		37	16	25	75
Razorbill	8		3		4		1
Razorbill/common guillemot	742	217	40	45	21	411	8
Common guillemot	61	19	3			36	3